Analysis and Modelling of Financial Logarithmic Return Data using Multifractal and Agent-Based Techniques

Elena Green

B.Sc.

Thesis presented for the degree of

Doctor of Philosophy

to the

National University of Ireland Maynooth

Department of Mathematical Physics

October 2014

Research Supervisor

Professor Daniel M. Heffernan

DECLARATION

This thesis has not been submitted in whole or in part to this or any other university for any other degree and is, except where otherwise stated, the original work of the author.

Elena Green

Abstract

In recent years physicists have become involved in studying the financial market and the vast data it generates. The constantly-updated streams of information are a perfect testing ground for the hypothesis that the laws of statistical physics might apply to human behaviour.

In this thesis, I study two empirical log return time series for the stylised facts of financial data. I then use Multifractal Detrended Fluctuation Analysis to study the empirical log returns for multifractal scaling. I find that extreme events are inimical to the scaling in highly leptokurtic data. I also find that the temporal correlations in the data are crucial to the scaling whereas the shape of its distribution is not as important.

I then develop my own agent-based model of the market. With just a few different types of traders operating according to some simple rules, my model generates log returns with many of the statistical properties found in empirical data. The option for traders to opt out of trading is the source of the thin-peaked distribution of the simulated log returns. The distribution of log returns becomes more closely described by a Gaussian at longer lags. This is a consequence of basing the fundamental value of the stock on geometric Brownian motion. Since transition to Gaussianity at long lags is also a feature of empirical log returns, this implies that real traders are also influenced by some geometric Brownian process. Log returns generated by the model also have volatility clustering, are uncorrelated and asymmetrically distributed.

I test the log returns generated by my model for their scaling properties and find that they do not have multifractal scaling. This is an interesting result since the simulated log returns do feature other properties of empirical data. I then extend the model in some basic ways to include more heterogeneity. Some limited multifractal scaling is found in the simulated log returns of the extended model. Because the model produces stochastic output, it is extremely difficult to exactly determine the scaling properties. However the results hint at the possibility that the multifractality found in empirical log returns is a consequence of the heterogeneity in both the investment horizons and beliefs of traders in the market.

When inhomogeneities are considered (if at all) they are treated as unimportant fluctuations amenable to first order variational treatment. Mathematical complexity is certainly an understandable justification, and economy or simplicity of hypotheses is a valid principle of scientific methodology; but submission of all assumptions to the test of empirical evidence is an even more compelling law of science.

- Gerard de Vaucouleurs (1970)

Contents

List of Acronyms

ABM	Agent-Based Model
ACF	Autocorrelation Function
ADF	Augmented Dickey-Fuller
ARCH	Autoregressive Conditional Heteroscedasticity
BM	Brownian Motion
CLT	Central Limit Theorem
DFA	Detrended Fluctuation Analysis
DJIA	Dow Jones Industrial Average
EMA	Exponential Moving Average
EMH	Efficient Market Hypothesis
fBM	fractional Brownian Motion
FTSE	Financial Times Stock Exchange
GARCH	Generalised ARCH
GBM	Geometric BM
iid	independent and identically distributed
MACD	Moving Average Convergence Divergence
MDH	Mixture of Distributions Hypothesis
MF-DFA	Multifractal DFA
MMAR	Multifractal Model of Asset Returns
MRW	Multifractal Random Walk
MSM	Markov Switching Multifractal
NASDAQ	National Association of Securities Dealers Automated Quotations
PMM	Poisson Multifractal Model
SEMF	Self-Excited Multifractal
SPH	Stable Paretian Hypothesis
TAQ	Trades And Quotes
WTMM	Wavelet Transform Modulus Maxima

Chapter 1

Modelling the Market: An Evolution of Understanding

1.1 Introduction

This chapter presents an introduction to the financial market and financial data. It describes the basic mechanism of the market. It also discusses some points which need to be considered before we can begin to study the data, such as the units and scales which will be used. It then develops the history of the modelling of the financial market by presenting a literature review of some of the most significant models in this field.

1.2 How the Market Works

A market is simply a place where traders can buy and sell products. Each product has a listed spot price $S(t)$ at time t and this price changes in time in response to the supply and demand for that product as well as external factors like political decisions, weather and other news. There are many markets around the world where different products are available for trade, and some products are listed on more than one market.

A stock market is a market where stocks or shares are traded. A stock or share is a part-ownership in a company. Dividends are often paid to shareholders out of the profits the company makes. The price of the shares reflects the supply and demand for the shares which in turn generally reflects public opinion of the value of the company.

The financial market is more general than the stock market. The financial market is a market for all sorts of financial products, including stocks and bonds, commodities like gold and oil, foreign currencies, and financial derivatives. A derivative is a contract concerned with the trade of an underlying asset. For example, a *European call option* is

a contract giving the holder the right to buy a particular asset at a specific exercise date and price sometime in the future. The price of the option depends on the price of the asset as well as on opinion about how that price will change in the future. The option itself may be traded many times before the exercise date quoted on the contract. There are many types of derivatives traded on the financial market.

The usual way of trading is through a stock exchange using a stockbroker, often through a bank or on the Internet. The stock exchange makes some rules and ensures that traded products are standardised. The stockbroker submits an order to buy or sell to the exchange. The order may be a limit order or a market order. A limit order includes a minimum (when selling) or a maximum (when buying) price which will be accepted by the trader. The trader may have to wait some time before the trade can be exercised according to his/her specifications. A market order contains just the number of shares to be traded and will be filled straight away by available orders of the opposite direction at the best price available.

The exchange keeps a log of all the buy and sell limit orders in a limit order book. The log consists of the number of shares, the price limit and the time the order was placed. For any given product, there will be a gap between the highest price someone is willing to pay (bid) and the lowest price someone is willing to accept (ask) in return for the product. This gap is called the bid-ask spread. The actual price listed for the product by the exchange will be somewhere in between these two values.

The exchange normally has a designated market maker to provide liquidity to traders. Liquidity refers to the ease of turning assets into money. The market maker always has some of the securities on hand for immediate trade. They list both bid and ask prices so that under normal circumstances other traders are always able to trade. If there is a sell order with no matching buy order, the market maker will buy so that the trade is able to go ahead. The market maker receives some trading privileges from the exchange in return for their service.

Traders may be anything from large investment banks, insurance companies and pension funds to small businesses and individuals. The reason most people get involved in trading on the financial market is of course to make money. Prices can change quickly and by large amounts, and traders can make huge profits from this if they buy and sell at the right times. Along with the huge potential for profits comes increased risk. Prices can move in both directions and so traders can also lose a lot of money. Usually traders have a certain amount of risk-aversion: an acceptable limit to the amount of risk they are willing to take on in proportion to the potential profits they can make by getting involved in a certain market. Those who are completely risk-averse can simply put their money in the bank to collect the risk-free rate of return.

Traders may also be motivated to trade in order to reduce their risks. For example, a car manufacturer takes on a certain amount of risk because they are only involved in one industry. If the price of fuel increases or the government increases motor taxes, cars become less attractive and the industry may take a hit. This company may choose to own shares in other types of industry whose profits are broadly anticorrelated to theirs, such as a rail company. Any hits to their industry may also result in profits to the other industry, so the car manufacturer's loss will be offset by the increase in value of their shares in the rail company. Their overall risk is reduced through diversification.

There are thus two main types of trader: those who want to be exposed to risk and the accompanying increased potential profits are called speculators; those who want to reduce risk are called hedgers.

An index is a useful way to see how a particular market is doing. An index is a weighted average of a collection of stock prices. A company's weight in the index is usually determined by its current spot price and the number of its shares that have been traded. Traders can also invest in index funds which track an index's performance. The oldest index in the world is the Dow Jones Industrial Average (DJIA), beginning in 1887. It is made up of 30 US-based companies. Other well-known indices include the NASDAQ-100, an index of the top 101 non-financial companies listed on the American NASDAQ[1] stock exchange, the FTSE 100 maintained by the FTSE Group[2], a subsidiary of the London Stock Exchange, and the S&P500 comprised of 500 companies in the US chosen by Standard & Poor's Financial Services LLC. The daily price of the DJIA index is shown in Figure 1.1 from 1928 to 2012.

1.3 Econophysics

In recent years more and more physicists have become interested in the world of economics and finance. Many are interested in the market as a complex adaptive system with many interacting parts. The financial system also produces huge amounts of data in constant streams and of various frequencies and this provides an interesting subject for research [1–3].

Physicists are generally concerned with modelling the market and the data it produces. We want to know, understand and replicate the sort of data generated by the market. Prediction is obviously the holy grail. Some of the well-known models which have been developed over the last hundred years or so will be described later in this chapter.

[1]NASDAQ stands for National Association of Securities Dealers Automated Quotations, but it is better known by its abbreviation.

[2]FTSE originally stood for Financial Times Stock Exchange. Now it is simply known as the FTSE (pronounced "footsie").

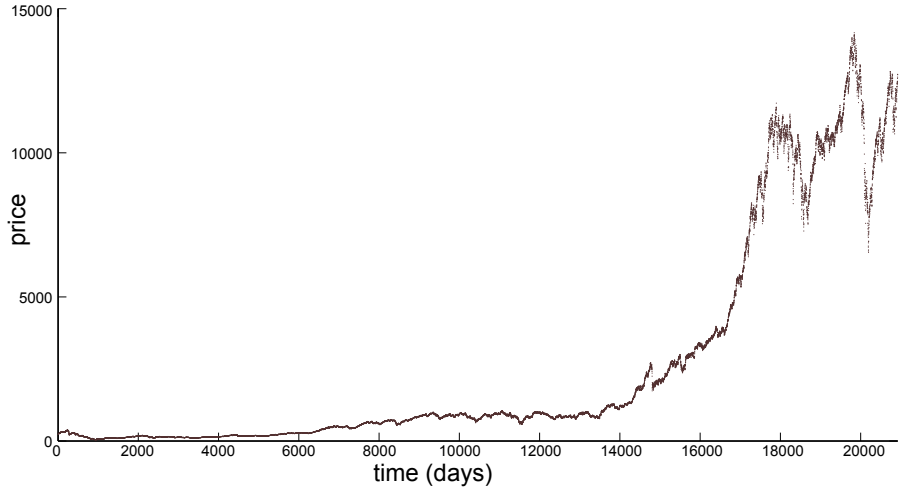

Figure 1.1: Daily prices of the DJIA index from 1928 to 2012.

Some of the methods from statistical mechanics can be applied to financial data. The market can be viewed as a complex system exhibiting critical phenomena and phase transitions. It is a many-body system of interacting parts. The difference between the market and other many-body systems studied by physicists is that in the market, the individual parts are traders who have autonomy and can choose how to behave.

The financial market provides a perfect testing ground for the hypothesis that the laws of statistical physics might apply to human behaviour. Although the participants in a market can make their own decisions, they operate according to a set of rules determined by the exchange where they trade which makes these decisions easier to study. There is also a huge amount of data available for study, which is not the case for other types of human interactions. A whole new interdisciplinary field of study, econophysics, has been born. When studying a fluid flow we are more concerned with the overall system than with the individual position and velocity of each molecule. Similarly econophysics concerns itself chiefly with the aggregate result of many interacting traders or businesses [4].

Econophysics takes the methods from physics and applies them to the economic system. This includes specifically stochastic processes which have been used extensively in the modelling of prices. The ideas from the study of dynamical systems and especially nonlinear dynamics have found a new home in the marketplace [3].

1.4 Technicalities of studying financial data

1.4.1 Units

An important point to agree on before any analysis can be done is the particular variable to be studied. Prices are listed in a variety of currencies, but currencies themselves change in value with respect to each other and so are not a useful unit for reference. Prices can be at many different levels and can move with disparate variances and so they are not suitable for comparison of behaviour. A variable less sensitive to scale and which does well at characterising price movements is needed [3, chapter 5].

For these reasons, it is common in finance to study the log returns Z of the price S:

$$Z(t, \Delta t) = \ln S(t + \Delta t) - \ln S(t)$$

This is a unitless quantity which makes it appropriate for studying data from around the world [5]. The terms "log return" and "return" are often used interchangeably in the finance literature to refer to this quantity.

An obvious choice for a variable to study may be the price increments $\Delta S(t, \Delta t) = S(t + \Delta t) - S(t)$. Since $\Delta S(t, \Delta t)$ is not a unitless quantity, it is not suitable for comparing the movements of shares of companies of different sizes. Another option is the proportional price changes $R(t, \Delta t) = \frac{S(t+\Delta t)-S(t)}{S(t)}$. The principal reason it is useful to study log returns rather than $R(t, \Delta t)$ is that the logarithm is less sensitive to changes in scale. Especially when studying data over a long time period, the growth or decline in the economy over that time has an effect on the size of price changes.

Also, when the time scale Δt is small, the price change $\Delta S(t, \Delta t)$ will also be relatively small and the following holds:

$$\begin{aligned} Z(t, \Delta t) &= \ln S(t + \Delta t) - \ln S(t) \\ &= \ln \frac{S(t + \Delta t)}{S(t)} \\ &= \ln \left(1 + \frac{S(t + \Delta t) - S(t)}{S(t)} \right) \\ &\approx \frac{S(t + \Delta t) - S(t)}{S(t)} \\ &= R(t, \Delta t) \end{aligned}$$

So for small $\Delta S(t, \Delta t)$, the log return $Z(t, \Delta t)$ and the proportional price change $R(t, \Delta t)$ are nearly equivalent.

Figure 1.2 shows all three unit options for daily data of the DJIA index. The data

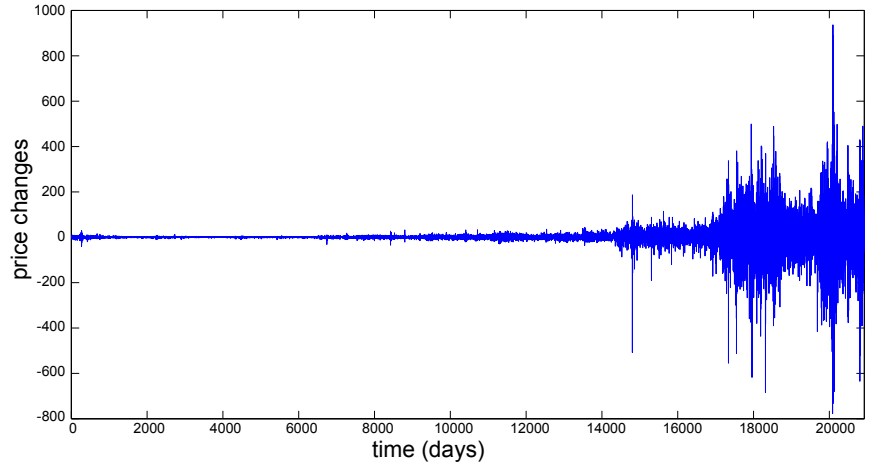

(a) Price increments; $\Delta S(t, \Delta t) = S(t + \Delta t) - S(t)$

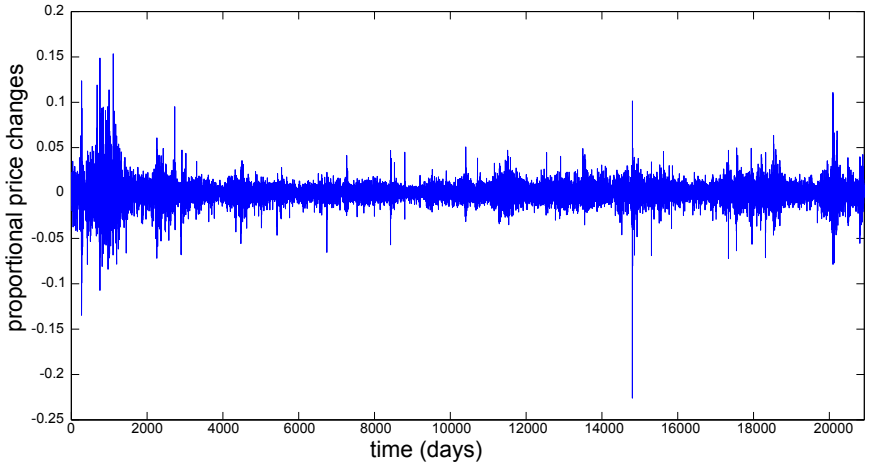

(b) Proportional price changes; $R(t, \Delta t) = \frac{S(t+\Delta t)-S(t)}{S(t)}$

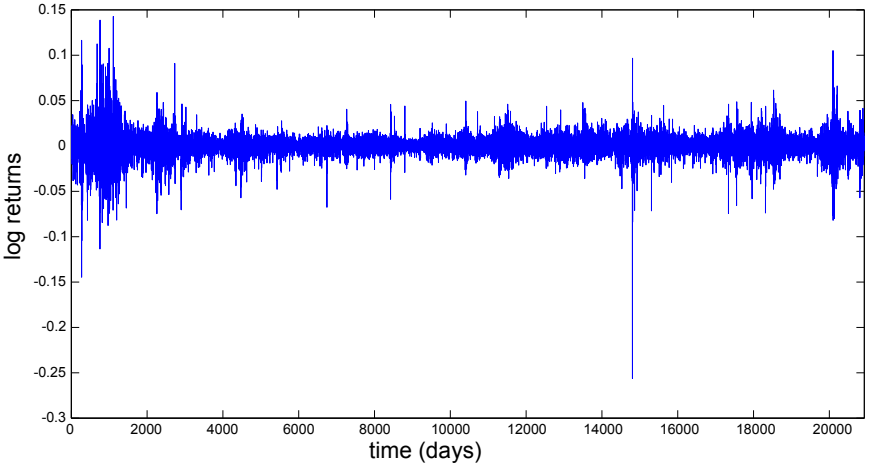

(c) Log returns; $Z(t, \Delta t) = \ln S(t + \Delta t) - \ln S(t)$

Figure 1.2: Price increments $\Delta S(t, \Delta t)$, proportional price changes $R(t, \Delta t)$ and log returns $Z(t, \Delta t)$ of DJIA from 1928 to 2012. $\Delta t = 1$ day.

begins in 1928 and ends in 2012. The economy has grown a lot over those 84 years and the corresponding growth in the average size of price increments makes this clear. The log returns are more consistent over that time and they are useful for this reason.

1.4.2 Scales

The time scales to be used are also an important consideration. Often log returns are calculated using physical time scales, such as the price per minute, day or year. However, there are weekends, holidays and nights when no trades are made. These times can be skipped over and the times when there is active trading can be stitched together as if the non-trading times simply don't exist. This is the common way of measuring time in the financial literature.

Sometimes the overnight or over-weekend log returns are skipped, depending on whether the scale of interest is daily or intra-daily. These changes are often larger than the others because more news has time to arrive over the longer interval between trades. This in turn can result in more drastic changes in the price as traders react to this news when the market opens. However even over the same time scales, volatility is generally found to be higher during trading times than at other times. Reasons may include that news is more likely to arrive during business hours and that informed traders affect prices by the way they trade [6].

Data can also be examined at event or trading time. Event time counts each trade as a time step and so does not correspond to real physical time. There are times when there are many trades per second and others when the trading pace is more sluggish. This sort of data is less freely available than data listed daily or minutely, in physical time. The log returns in physical time are the most commonly studied variable of financial data and this is where the focus will be in my study too.

1.5 It Began with Bachelier

Any discussion of financial modelling begins in 1900 when Louis Bachelier, a student of Henri Poincaré, finished his dissertation entitled "Théorie de la spéculation" [7]. He is now considered the father of modern financial mathematics. In his thesis, Bachelier discussed forward contracts, options and other financial derivatives. His analysis of probability in the context of the stock exchange led him to propose a Gaussian distribution of stock price increments. He developed the mathematical framework for the Wiener process and used this continuous random walk as a model for the evolution of prices. His thesis is the first known work of mathematics applied to finance [8] and is worthy of consideration.

1.5.1 The Wiener Process

In the 19th century, Scottish botanist Robert Brown observed pollen grains and other substances suspended in water under a microscope. He saw how the particles moved continuously in jagged paths [9]. This sort of continuous random walk came to be known as Brownian motion (BM) and is mathematically modelled by a Wiener process.

The standard Wiener process W_t on the interval $[0, T]$ depends continuously on t and has the following properties:

1. $W_0 = 0$
2. W_t has continuous sample paths
3. The sample paths of W_t have independent increments, that is for $0 \leq s < t < u < v \leq T$, $W_t - W_s$ and $W_v - W_u$ are independent.
4. $W_t \sim N(0, t)$ where $N(\mu, \sigma^2)$ is a normal distribution with mean μ and variance σ^2.
5. W_t has statistically stationary increments, that is $W_t - W_s \stackrel{d}{=} W_{t-s} - W_0 = W_{t-s}$ for $0 \leq s < t \leq T$, where $\stackrel{d}{=}$ means equal in distribution.

Some sample paths of a Weiner process are shown in Figure 1.3.

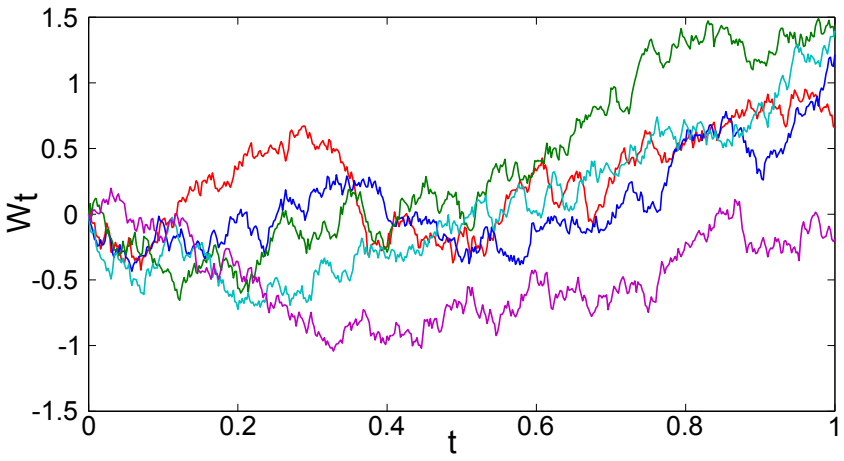

Figure 1.3: Some sample paths of the Wiener process generated in discrete time so that $\Delta W \sim \epsilon\sqrt{\Delta t}$ where $\epsilon \sim N(0, 1)$ and $\Delta t = 1/500$.

1.5.2 Bachelier's model

Let $S(t)$ be the price at time t. In Bachelier's model, the price increments $S(t+\Delta t) - S(t)$ are independent and identically distributed (iid) random variables.

$$S(t + \Delta t) = S(t) + \epsilon$$

where ϵ is taken from some arbitrary stationary distribution with mean μ and finite variance σ^2. Therefore, at time $T = n\Delta t$,

$$\Delta S(t,T) = S(t+T) - S(t) = \sum_{i=1}^{n} \epsilon_i. \tag{1.1}$$

The price increment is the sum of n *iid* random variables. The Central Limit Theorem (CLT) gives us that if $n \gg 1$ ($T \gg \Delta t$), then the distribution of this sum tends to a Gaussian with mean $n\mu$ and variance $n\sigma^2$.

This leads us to Bachelier's result, that price changes over different time intervals such as a week or a month are sums of the changes over shorter time scales and are therefore Gaussian distributed with mean $n\mu$ and standard deviation proportional to the square root of the elapsed time $\sqrt{T}$. This behaviour is essentially a Wiener process with added drift if $\mu \neq 0$.

According to Bachelier's model, the probability distribution of the price S_t at any time t can be found from the initial price S_0, the drift μ, and the standard deviation σ;

$$S_t - S_0 = \mu t + \sigma dW_t. \tag{1.2}$$

On this foundation, Bachelier goes on to discuss financial derivatives in more detail and presents some results on the pricing of options.[3] He found that the value of an option must be proportional to the square root of the elapsed time. This conclusion is one of Bachelier's main results [7].

The main problem with Bachelier's model is that it allows negative prices. Another issue is that, as he admits in his thesis [7], the probability of a particular price change is independent of the current price level. This is to say that this model predicts the increment on a stock currently worth €500 to be the same as the increment on a stock currently worth €5. Intuitively, however, we would expect that the change to a €500 stock would be much greater.

1.6 Geometric Brownian Motion

Geometric Brownian Motion (GBM) was first introduced by the Japanese mathematician Kiyoshi Itō in 1944 [10, chapter 5]. It was 20 years later that Paul A. Samuelson made the application to financial mathematics and price modelling [11].

[3] An option is a contract which gives the holder the right to trade an asset at some point in the future for a given price. The expected value of the future price of the asset is needed in order to calculate a fair price for the option. European call options were described briefly in Section 1.2.

Itō developed a calculus based on stochastic processes. It defines the integration of a function with respect to the differential dW_t of the Wiener process. The result of the stochastic integral is another stochastic process and so it can be defined in a distributional sense. The main advantage of the Itō stochastic integral over the alternative definition of the Stratonovich stochastic integral is that Itō's integral is a martingale. A discrete process X is a martingale if and only if $\mathbb{E}[X_{n+1}|X_0, X_1, \ldots X_n] = X_n$. Given the history of the process, the next expected value is the same as the current value. Knowledge of the historical values is not helpful for predicting future values. The increments of a martingale process are a fair game, expected equal to zero, and so these processes are used extensively in modelling in the areas of gambling and finance.

As mentioned above, Bachelier assumed that the price increment $\Delta S(t, \Delta t) = S(t + \Delta t) - S(t)$ is independent of the price level. It might make more sense if the *relative* price change $S(t + \Delta t)/S(t)$ were independent of the price level. We could conjecture that the random factor $\lambda = S(t + \Delta t)/S(t)$ by which the stock increases or decreases is expected to be the same no matter what the current price level. This leads to a multiplicative (rather than Bachelier's additive) price process:

$$S(t + \Delta t) = \lambda S(t) \tag{1.3}$$

where λ is a random variable drawn from a stationary probability distribution with finite mean and variance. The price at time $T = n\Delta t$ is given by

$$S(t + T) = \lambda_n \ldots \lambda_2 \lambda_1 S(t). \tag{1.4}$$

After taking the natural log of the above equation, we come to

$$\begin{aligned} \ln S(t + T) &= \ln \lambda_n + \ldots \ln \lambda_2 + \ln \lambda_1 + \ln S(t) \\ &= \sum_{i=1}^{n} \ln \lambda_i + \ln S(t) \qquad (1.5) \\ \Rightarrow \ln S(t + T) - \ln S(t) &= \sum_{i=1}^{n} \ln \lambda_i \qquad (1.6) \end{aligned}$$

This difference is the log return $Z(t, T)$. According to this model, it is a sum of *iid* random variables and so will tend to a Gaussian for large T. This multiplicative random walk model thus predicts that $Z(t, T)$ is normally distributed. This model also gives that the log of the price $\ln S(t)$ is normally distributed, from which follows that the stock price itself $S(t)$ has a lognormal distribution.

To find an iterative model for the price, consider the price difference

$$S(t+\Delta t) - S(t) = \lambda S(t) - S(t)$$
$$\Delta S(t, \Delta t) = (\lambda - 1)S(t).$$

Consider an approximation by a constant factor λ. Then let $\lambda - 1 = \mu\Delta t$ for some constant drift rate μ so that the reliance on the time scale Δt is explicit. This leads to

$$\Delta S(t) = \mu S(t)\Delta t.$$

In the limit as $\Delta t \to 0$,

$$dS = \mu S dt$$

or

$$\frac{dS}{S} = \mu dt.$$

There must also be some stochastic element to the price difference so that the variance is nonzero. In keeping with the proposal that the relative price change is independent of the price level, the standard deviation of the price change should be proportional to the price level [12]. This leads to the GBM model

$$dS = \mu S dt + \sigma S dW_t$$

or

$$\frac{dS}{S} = \mu dt + \sigma dW_t \tag{1.7}$$

W_t is the Wiener process described in Section 1.5.1. This is one of the most widely used models of stock prices [12, chapter 12].

The relevant variable is dS/S which indicates that a solution will likely include logarithms. Using the expansion

$$df(x) = \frac{\partial f}{\partial x}dx + \frac{1}{2}\frac{\partial^2 f}{\partial x^2}(dx)^2 + \dots$$

we find

$$d(\log(S_t)) \approx \frac{dS_t}{S_t} - \frac{1}{2}\frac{1}{S_t^2}(dS_t)^2. \tag{1.8}$$

Since we are now dealing with a stochastic process, it will be necessary to employ

some Itō calculus. Itō's calculus gives the following results in the mean square limit:

$$\begin{aligned} dt^2 &\to 0 \\ dtdW_t &\to 0 \\ dW_t^2 &\to dt. \end{aligned}$$

dW_t^2 is not negligible in comparison to dW_t because the expected value of dW_t^2 is dt. This leads us to

$$\begin{aligned} (dS_t)^2 &= \mu^2 S_t^2 dt^2 + 2\mu\sigma S^2 dt dW_t + \sigma^2 S_t^2 dW_t^2 \\ &= \sigma^2 S_t^2 dt \end{aligned}$$

in the mean square limit.

So equation 1.8 becomes

$$d(\log S_t) = \frac{dS_t}{S_t} - \frac{1}{2}\sigma^2 dt.$$

Equation 1.7 gives an expression for dS/S, leading to:

$$\begin{aligned} d(\log S_t) =& \mu dt + \sigma dW_t - \frac{1}{2}\sigma^2 dt \\ =& \left(\mu - \frac{1}{2}\sigma^2\right) dt + \sigma dW_t. \end{aligned}$$

This leads to the following integral equation which can be solved to give a stochastic process for the price.

$$\begin{aligned} \int_0^t d(\log S_s) &= (\mu - 1/2\sigma^2) \int_0^t ds + \sigma \int_0^t dW_s \\ \log S_t - \log S_0 &\stackrel{d}{=} (\mu - 1/2\sigma^2)t + \sigma(W_t - W_0) \\ \ln \frac{S_t}{S_0} &\stackrel{d}{=} (\mu - 1/2\sigma^2)t + \sigma W_t \\ S_t &\stackrel{d}{=} S_0 e^{(\mu - 1/2\sigma^2)t + \sigma W_t} \end{aligned}$$

which is the solution to equation 1.7. The integral of the Wiener process $\int dW_s$ is defined stochastically, not pathwise. In general, S_0 is also a random variable independent of t. I refer interested readers to the many books on stochastic integration; see for example references [10], [13] and [14].

GBM can therefore be seen as the exponential of the Wiener process. This immedi-

ately solves the problem of negative prices encountered with Bachelier's model because the exponential function is nonnegative. GBM also has the property outlined above, that the prices are lognormally distributed. Equivalently, the log returns are normally distributed. To see this, examine the log return of a price process which follows GBM:

$$\begin{aligned}
Z(t,T) =& \ln S(t+T) - \ln S(t) \\
=& \ln e^{(\mu - 1/2\sigma^2)(t+T)+\sigma W_{t+T}} - \ln e^{(\mu-1/2\sigma^2)t+\sigma W_t} \\
=& (\mu - 1/2\sigma^2)(t+T) + \sigma W_{t+T} - ((\mu - 1/2\sigma^2)t + \sigma W_t) \\
=& (\mu - 1/2\sigma^2)T + \sigma(W_{t+T} - W_t) \\
=& (\mu - 1/2\sigma^2)T + \sigma(W_T - W_0) \qquad \text{due to the independent increments of } W_t \\
=& (\mu - 1/2\sigma^2)T + \sigma\epsilon \qquad \text{where } \epsilon \sim N(0,T) \\
& \sim N\left((\mu - 1/2\sigma^2)T, \sigma^2 T\right)
\end{aligned}$$

so the log return $Z(t,T)$ is normally distributed with mean $(\mu - 1/2\sigma^2)T$ and variance $\sigma^2 T$.

1.6.1 Black-Scholes-Merton

The GBM model for stock prices was made particularly famous by the Black-Scholes-Merton equation introduced in 1973 [15] [16, chapter 6]. This famous equation is used for calculating a fair price for options and is derived using Itō's calculus.

The option-pricing formula introduced by Fischer Black and Myron Scholes, and independently by Robert Merton, was developed under the assumption that prices follow a lognormal distribution. The expected price at time t is therefore $\mathbb{E}[S_t] = S_0 e^{\mu t}$. The writer of the option can then calculate the probable price of the stock in the future and so find a fair price for the option.

A European call (put) option gives the owner the right to buy (sell) the underlying stock for the strike price K on the day it matures. The Black-Scholes-Merton formula for calculating their values results in

$$\begin{aligned}
c &= S_0 N(d_1) - K e^{-rT} N(d_2) \\
p &= K e^{-rT} N(-d_2) - S_0 N(-d_1)
\end{aligned}$$

where c is the price of a European call option and p is the price of a European put option.

S_0 is the price at time 0, r is the risk-free rate and T is the time to maturity of the option.

$$d_1 = \frac{\ln(S_0/K) + (r + \sigma^2/2)T}{\sigma\sqrt{T}}$$
$$d_2 = d_1 - \sigma\sqrt{T}$$
$$N(x) = \frac{1}{\sqrt{2\pi}} \int_{-\infty}^{x} e^{-\frac{z^2}{2}} dz$$

σ is the standard deviation of the stock's log returns. $N(x)$ is the cumulative probability distribution function for a standard normal distribution. See references [12] and [10] for details of the derivation.

This important formula had massive impact on the trading world at the time and is still largely employed today with some corrections. It won Myron Scholes and Robert Merton the Nobel prize in Economics in 1997 [17, 18]. Unfortunately Fischer Black died before the prize was awarded.

1.7 Stable Paretian Hypothesis

Others also built on the work of Bachelier. As empirical data began to be accumulated by economists and became available for study, it became evident that the Gaussian distribution does not give an accurate description of stock prices [19]. Benoît Mandelbrot specifically argued that in real data, there are too many log returns which are outliers from a Gaussian prediction and that the actual distribution of returns must therefore have fat tails. He felt that these outliers should not be ignored or studied separately [20]. Also, these outliers cause the second moment of sample data to behave erratically. He found that it did not seem to converge to any limit as the sample size is increased. These reservations about the Gaussian hypothesis were enough to convince Mandelbrot that a "radically new approach" to the issue of log return distributions was warranted [21, 22] [23, chapter 1].

The non-normality of the log returns was a central issue to Mandelbrot's contribution. If the price S_t follows Bachelier's model, then the CLT predicts that price increments will be normally distributed. Mandelbrot proposed that the increments ϵ are *iid*, but that they have infinite variance. This would explain why the CLT does not apply in this case. Mandelbrot proposed the alternative Stable Paretian Hypothesis (SPH).

1.7.1 Stable Paretian Distributions

A stable Paretian distribution[4] is a power-law probability distribution. This type of distribution is desirable in the context of modelling stock prices because it has the features of power-law asymptotic fat tails and a second moment which does not converge to any limiting value. These are exactly the features which Mandelbrot identified in empirical data and wanted to include in his model.

The characteristic function[5] of the stable Paretian distributions is

$$\Psi(t) = \begin{cases} \exp\left[i\delta t - \gamma^\alpha |t|^\alpha \left(1 - i\beta \frac{t}{|t|} \tan\frac{\pi\alpha}{2}\right)\right] & \alpha \neq 1 \\ \exp\left[i\delta t - \gamma|t| \left(1 + i\beta \frac{2}{\pi} \frac{t}{|t|} \ln|t|\right)\right] & \alpha = 1 \end{cases} \tag{1.9}$$

There are four parameters which determine the precise form of the distribution: α, β, γ and δ. There are closed-form expressions for stable Paretian distributions only in a few specific cases of the parameters.[6] The parameters have the following interpretations:

- α is the characteristic exponent, $0 < \alpha \leq 2$. It determines the weight of the tails. The tails are thinner for larger α. When $\alpha = 2$, the Gaussian distribution is recovered.

- β determines the skewness, $-1 \leq \beta \leq 1$. For $\beta = 0$, the distribution is symmetric. When $\beta < 0$, there is more weight in the left tail than the right and vice versa.

- γ is the scale parameter determining the width of the distribution, $\gamma > 0$.

- δ is the location parameter. When $\alpha > 1$, δ is the mean of the distribution. The mean is not defined for $0 < \alpha \leq 1$.

Stable Paretian distributions are stable under addition. This means that if independently distributed stable variables are summed, so long as each has the same values of α and β, the distribution of the sum will also be stable with the same values of α and β. This was also considered a desirable characteristic for modelling stock returns as it means price increments over a time interval will have the same distribution as the price increments during the interval.

[4]Stable Paretian distributions are also called Lévy-stable, and a stochastic process whose movement is generated by such a distribution is often called a Lévy flight. This family of distributions was first described by Paul Lévy in 1925 [21].

[5]The characteristic function of a probability density function is its inverse Fourier transform.

[6]These are the Gaussian distribution ($\alpha = 2$), the Cauchy distribution ($\alpha = 1, \beta = 0$) and the Lévy distribution ($\alpha = 1/2, \beta = 1, \delta = 0, \gamma = 1$) [22].

The Cauchy distribution is stable Paretian with $\alpha = 1, \beta = 0$. Its probability distribution function is [10]

$$f(x; \delta, \gamma) = \frac{\gamma}{\pi} \frac{1}{(x-\delta)^2 + \gamma^2}.$$

Figure 1.4 shows a set of sample data from this distribution. The effect of undefined variance can be seen from the plot of the sample mean as a function of sample size. For data with a defined mean, the sample mean will settle down to the mean of the distribution as the sample size is increased. However for this Cauchy data the sample mean continues to jump erratically even at large sample sizes. This is a symptom of the

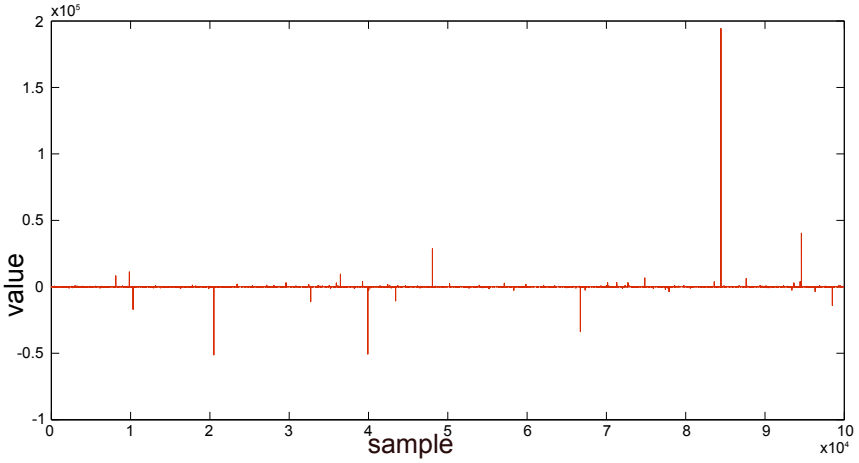

(a)

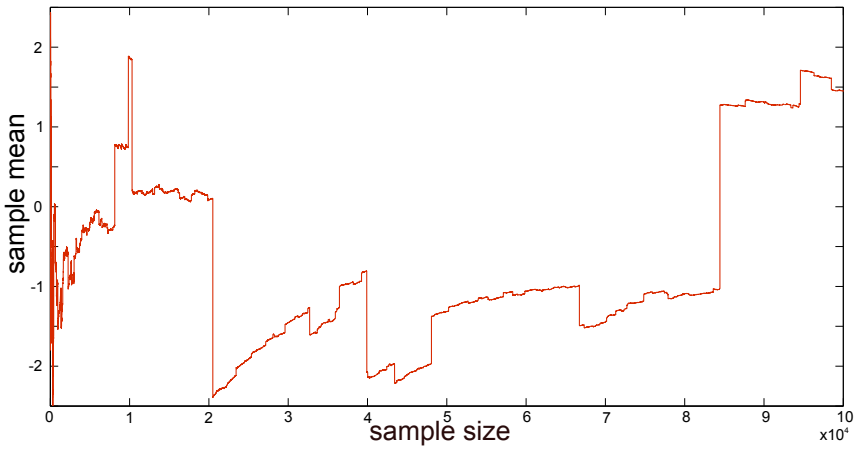

(b)

Figure 1.4: (a) Graph of sample data from a Cauchy distribution with $\gamma = 1, \delta = 0$. (b) Graph of the sample mean of the Cauchy data as the sample size is increased. For large sample size, the mean has still not settled down close to a single value. This is a symptom of the infinite variance of stable Paretian distributions when $\alpha < 2$.

fat tails of the Cauchy distribution.

1.7.2 Mandelbrot's 1963 Model

The SPH model is based on two basic assumptions [22]:

1. The variances of empirically found log return distributions are infinite.
2. The empirical distributions of log returns fit the stable Paretian family of distributions.

Although the CLT does not apply to such data because it has infinite variance, the generalised CLT is relevant. The generalised CLT states that if the sum of a number of *iid* random variables with infinite variance converges to a distribution, that limiting distribution must belong to the family of stable Paretian distributions [22, 24, 25].

Mandelbrot made two essential changes to Bachelier's model [21]. First, he applied Bachelier's process to the log returns Z rather than the price increments ΔS. Secondly he replaced the Gaussian distribution with the stable Paretian family of distributions. This leads to equation 1.1 being replaced by

$$Z(t) = \ln S(t + \Delta t) - \ln S(t) = \sum_{i=1}^{t} \nu_i$$

where random variables ν_i have infinite variance and satisfy the conditions required[7] for their sums to follow a limiting distribution. This is in contrast to the finite variance which was the case for Bachelier's model. The limiting distribution is necessarily stable Paretian with $0 < \alpha < 2$ [22, 21].

The Gaussian distribution belongs to the family of stable Paretian distributions. The difference between Mandelbrot's model and Bachelier's model therefore lies in the value of the parameter α. The Gaussian hypothesis introduced by Bachelier holds that $\alpha = 2$, whereas according to the SPH introduced by Mandelbrot, $\alpha < 2$. Critically, the variance of these distributions is finite only when $\alpha = 2$. When $0 < \alpha < 2$, the tails are fatter or heavier than for a Gaussian and the variance is infinite.

To generate prices with this model from a price $S(t)$ at time t, use $S(t+\Delta t) = e^{\nu} S(t)$ where ν is a random number drawn from a stationary distribution having a power law tail with exponent $\alpha + 1$, $0 < \alpha < 2$, and α is the characteristic exponent of a stable Paretian distribution given in equation 1.9. According to the generalised CLT, this

[7] The conditions have to do with the asymptotic shape of the distributions of the random variables ν_i [10, chapter 4].

process will produce log returns $Z(t)$ whose distribution will tend to a stable distribution with characteristic exponent α.

The fat tails of the Paretian distributions mean that any large price changes in a stable Paretian market are likely to be caused by a small number of large price moves. In a Gaussian market, a large price move is caused instead by many small moves in the same direction. This means the stable Paretian market is more risky than a Gaussian one. This seems to be a better description of the real market as it could explain investors' risk aversion being in excess of that warranted by a Gaussian market [22].

Mandelbrot and Fama both examined empirical data to verify the SPH. Famously, Mandelbrot looked at both daily and monthly log returns of cotton prices [21]. His daily data covered 1900 - 1905 and 1944 - 1958. He had monthly data spanning 1880 - 1940.

The tails of the distribution were assumed power-law in shape with tail exponent α, so

$$\mathbb{P}[Z(t) > u] \sim c(\Delta t)u^{-\alpha}$$
$$\mathbb{P}[Z(t) < -u] \sim c(\Delta t)u^{-\alpha}$$

for some constant $c(\Delta t)$ dependent on the time scale of the log return, Δt.

$\mathbb{P}[Z(t) > u]$ and $\mathbb{P}[Z(t) < -u]$ can be plotted versus u on a doubly logarithmic scale. This gives

$$\log(\mathbb{P}[Z(t) > u]) = -\alpha \log u + \log c(\Delta t)$$
$$\log(\mathbb{P}[Z(t) < -u]) = -\alpha \log u + \log c(\Delta t)$$

so the slope of any linear section on a doubly logarithmic plot gives the exponent α of the tails of the distribution.

Mandelbrot found for the cotton prices that $\alpha \approx 1.7$ for both positive and negative tails for all the data examined. He found discrepancies in the value of the constant $c(\Delta t)$ for different data sets. The various plots appear as horizontal translates of each other. This indicated that the distribution is unchanged up to scale over the different years examined.

This gave credence to the hypothesis of stability since the exponent is unchanged for log returns over different interval lengths ($\Delta t = 1$ day or 1 month) and also at different points in time. The value of α also fitted Mandelbrot's hypothesis that $0 < \alpha < 2$.

Fama analysed daily log returns of all 30 stocks of the DJIA [22, 26]. He found fat tails in every case, further evidence that the Gaussian distribution is not a suitable description

of log returns. He also consistently found $\alpha < 2$ for all 30 stocks. He concluded that the SPH fits the data better than the Gaussian hypothesis [22, 26].

However, there were also some problems with this theory. One of the key assumptions of this hypothesis is that log returns are stably distributed. This leads to the conclusion that returns over longer intervals such as weeks, months or years, have the same distribution as returns per second or per minute. However, it has since been found empirically that low resolution log returns do not have the same distribution as high resolution log returns [27, 28].

Also, the assumption that log returns are independent is wrong. It is now well known that there are slowly decaying autocorrelations in the amplitude of log returns [19]. The feature of volatility clustering[8], a type of nonlinear autocorrelation found in financial log returns, was in fact noted by Mandelbrot at the same time as presenting the SPH [21].

Other findings contradicted the assumption of infinite variance. It was found that although the stable distributions provide a reasonable fit to the centre of empirical distributions, they do not fit the tails well. The tails of empirically found distributions, although fatter than a Gaussian, are significantly thinner than those of the stable Paretian distributions [28].

Also it has been found that the sample mean is not as erratic as predicted by the SPH [28]. As an illustration, a simple analysis has been carried out on minutely data from the Euro Stoxx 50 index. The result in Figure 1.5 shows that as the sample size is increased, the sample mean does begin to settle down to a constant value, in contrast to the behaviour of the Cauchy variable shown in Figure 1.4. This is further evidence against infinite variance.

What about all the empirical evidence supporting the theory? The data sets examined by Mandelbrot were very short compared to the data that later became available to researchers. His longest data set only contained about 3,500 points and so was not large enough to provide good statistics of extreme events contained in the tails. The daily DJIA data examined by Fama were even shorter time series. Most of his data sets ran from the end of 1957 to September 1962, containing only about 1,500 observations per sample [26]. This can be contrasted with data sets examined by researchers today which can contain hundreds of thousands if not millions of values.

Despite these shortfalls, the SPH constituted significant progress in the modelling of stock returns. Rather than based on intuition, it was founded on the observance of the empirical results of trading. Although those observances were later found to be lacking, this is a scientific approach to the problem.

[8]Volatility clustering refers to how periods of high and low volatility tend to cluster together; this phenomenon will be described in detail in Section 2.6.

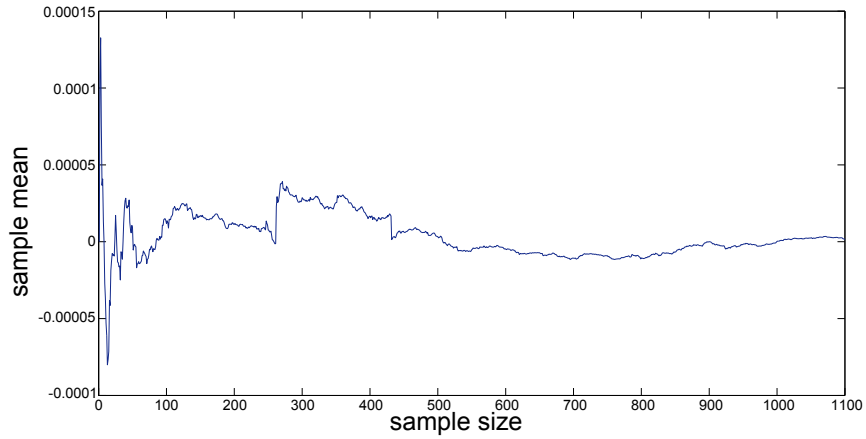

Figure 1.5: The sample mean as a function of increasing sample size for minutely data of the Euro Stoxx 50 index. The data shown is for the first week of May, 2008.

1.8 Mixture of Distributions

Another explanation of the non-Gaussianity of the empirical distribution of log returns was offered by Clark in 1973 and has since been expanded [29–32]. The SPH was based on the assumption that the CLT does not apply to price increments due to infinite variance. Clark proposed that it was another condition of the CLT that was being violated.

According to Clark, the source of the leptokurtic distribution [9] of price increments is the varying rate of the arrival of news. On different days the price moves at different rates due to information being available to traders at different rates. This leads to the Mixture of Distributions Hypothesis (MDH). According to the MDH, the price is a subordinated stochastic process. Rather than a function of time t, the price is a function of a directing process $T(t)$; $S(T(t))$ is subordinate to $S(t)$ [29]. The process $T(t)$ is an indicator of the speed of trading, or event time.

Instead of each day consisting of the same number of incremental price changes, some days have more and others have less, following the process $T(t)$ which is related to the trading volume. The CLT is valid when the number of random variables being summed is constant at least in probability [29]. This is the condition which is violated by the price according to the MDH.

By the MDH, the increments of the directing process $\Delta T(t)$ are lognormally distributed and the increments $\Delta S(t)$ are normal. This combination leads to high kurtosis in the price increments $\Delta S(T(t))$. Empirical test results indicate that the reason for the high kurtosis is that the returns are recorded in physical "clock" time rather than in

[9] A leptokurtic distribution has a thin peak and fat tails. This property of log returns will be discussed in detail in Section 2.3.

event or trading time [29].

1.9 Engle, ARCH, GARCH and more

Although volatility clustering was recognised by Mandelbrot in 1963 [21] and by Fama in his thesis [26], it did not affect their ideas at the time that log returns follow a basic random walk model. This is because the log returns remain uncorrelated even if their amplitudes are not. Engle's autoregressive conditional heteroscedasticity (ARCH) model was the first to incorporate this distinctive feature [33]. These models have become so ubiquitous that the feature of volatility clustering in financial data has come to be known as the "ARCH effect" among economists.

In the GBM model applied to log returns, $Z_t = \mu t + \sigma\epsilon$ where $\epsilon \sim N(0,1)$ is a random number and σ is a constant. Let $\mu = 0$ so that there is no drift. Memory can be introduced to the volatility of the return process by setting

$$\sigma_t^2 = \alpha_0 + \alpha_1 Z_{t-1}^2$$

so that the log return process is now

$$Z_t = \epsilon_t \sqrt{\alpha_0 + \alpha_1 Z_{t-1}^2}$$

where $\epsilon \sim D(0,1)$, D being a distribution that may be normal or leptokurtic.

This is the original ARCH model introduced by Engle in 1982 [33]. One of the main attractions of this type of model is its ability to reproduce the volatility clustering seen in financial data. The data produced has no linear autocorrelation but the moduli and higher order functions of the data are correlated, just like empirical data [34]. The conditional variance varies in time while the unconditional variance remains constant. The conditional variance is also called the scedastic function; hence the name ARCH.

The form of the autoregressive variance can easily be extended to have more memory. An ARCH(q) process has variance of the form

$$\sigma_t^2 = \alpha_0 + \sum_{i=1}^{q} \alpha_i Z_{t-i}^2$$

for some unknown vector of parameters α. The terms in α should satisfy $\alpha_0 > 0, \alpha_i \geq 0, i = 1, \ldots, q-1$ and $\alpha_q > 0$ to ensure that the variance is positive. For large q, volatility clustering is generated by the ARCH process.

The ARCH model is a major departure from the *iid* model of returns. Rather than log

returns being independent, this model gives them an explicit form of condition on their past. Although log returns themselves remain uncorrelated, their higher-order moments are now positively correlated for a lag of q, the order of the ARCH process. It was not the first model to have a non-constant variance, but it was the first model of conditional heteroscedasticity [35].

There have also been many extensions to this model since it was introduced by Engle. For example, the generalised ARCH (GARCH) process as introduced by Bollerslev in 1986 [36] allowed for more flexibility in lag structure and a longer memory.

A GARCH(p,q) process due to Bollerslev [36] has variance of the form

$$\sigma_t^2 = \alpha_0 + \sum_{i=1}^{q} \alpha_i \epsilon_{t-i}^2 + \sum_{i=1}^{p} \beta_i \sigma_{t-i}^2.$$

In this model, dependence on past noise and past variance are separated and can have different lengths and coefficients. When $p = 0$, the ARCH(q) process is recovered.

The GARCH model has in turn been extended in many directions to allow for more flexibility [34]. There now exist a plethora of acronyms ending in ARCH, each signifying a different form of the conditional variance and allowing modellers to include more complexity and specifications in their models; see for example [37, 38].

1.10 Efficient Market Hypothesis

A general theory of how the market works is the Efficient Market Hypothesis (EMH). This concept was independently proposed by both Fama [26] and Samuelson [39] at around the same time. In essence, the EMH states that prices are correct, taking into account all relevant information.

Eugene Fama, in his thesis published as "The Behaviour of Stock Market Prices" in 1965 in The Journal of Business [26], argues for the random walk model of stock prices. He discusses both the independence of successive price increments and also the distribution of these increments. Fama admits that it may not be reasonable to expect the factors which influence stock prices to be independent. For example, traders may imitate the trading pattern of some influential investors and so uncertainty in expectations are not independent. Also, the arrival of new information may not always be independent.

However, the theory asserts that if there are superior traders who know the intrinsic value of the stock, their trading will counteract the herding behaviour of others. Also skilled chart readers will identify bubbles and crashes which are purely speculative and similarly counteract them. The dependence based on the arrival of news is also destroyed by astute traders who correctly anticipate news as well as its effect on the intrinsic value

of the stock.

Fama concludes that "the full effects of new information on intrinsic values will be reflected nearly instantaneously in actual prices" [26], and so the market overall is always correct in its pricing of stocks, even if no individual trader has perfect knowledge. Or "the market uses all relevant information and uses this information correctly to determine" prices [5].

Thus was born the EMH, one of Fama's conclusions from his research: "a situation where successive price changes are independent is *consistent* with the existence of an "efficient" market for securities, that is, a market where, given the available information, actual prices at every point in time represent very good estimates of intrinsic values." [26]

In such an efficient market, any price changes are simply a result of new information becoming available. There are no bubbles because rational fundamental traders will not allow them to develop. Any large price moves must be due to sudden, shocking news reaching the market.

In such a world, it is impossible to make profits in excess of a simple buy-and-hold strategy by examining past prices. Therefore technical analysis for the purpose of finding patterns in historical prices to inform investment strategy should be useless [5].

1.10.1 Is the Market really Efficient?

One of the key elements of economic theory is the EMH first devised by Fama [26] and outlined above. In essence, it states that all important price changes are as a result of new information arriving to the market. Since this information generally appears randomly, price changes must follow a random walk. This means that major price changes, such as the massive drop on "Black Monday", October 19th 1987, should be the result of some major new information. In that day the DJIA lost about 23% of its value, the worst single-day drop in its history. It is clearly visible in Figure 1.6.

Another assumption of mainstream economic theory is that all traders in the market have access to the same information and act on it in the same rational, or at least quasi rational, way. This is the theory of Rational Expectations [40]. According to this theory, if not all traders are rational, at least enough of them are, or on an aggregate level they act in a rational way, so that they can be modelled by some representative rational agents. It is assumed that there is a situation of equilibrium in the market. The arrival of news and the rational behaviour of the traders lead to changes in supply and demand. This in turn affects the price until balance is restored and a new equilibrium position is achieved.

One of the major benefits of mainstream economics is its support of parsimonious models. A clear example of this is the Black-Scholes-Merton model for option pricing, described in Section 1.6.1. This model is based on the random walk, *iid* price increments,

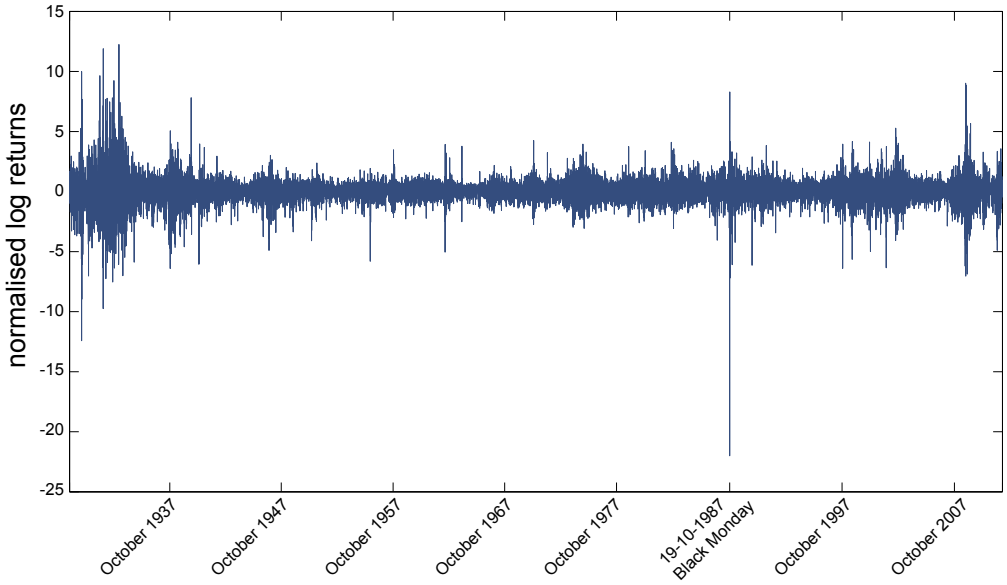

Figure 1.6: Graph of the daily log returns of DJIA from 1928 to 2012 in units of standard deviation, σ. The Black Monday crash was a drop of more than 22σ.

concept. The theory allows analytical treatment of a complex problem. This explains the longevity of the theory despite the errors in it.

The theory of information randomly arriving to the market may seem reasonable. However, the assumption that traders are rational agents with equal access to information is without basis. In reality, there are many different types of traders in the market with varying access to accurate information. Generally, people are not rational. They succumb to emotions such as panic and euphoria. Especially in times of high emotion, traders do not act independently. The market is susceptible to "waves of optimistic and pessimistic sentiment" [41, chapter 12]. The phenomenon of herding behaviour is not admitted by the classical theory.

There is also a certain paradox to the idea of efficient markets. If rational traders make the market efficient, then there is no motive to trade as no excess profit can be made. Therefore rational traders will leave and the market may revert to an inefficient state. This self-contradiction was pointed out by Milton Friedman, American economist and Nobel Memorial Prize winner, as quoted by J. Doyne Farmer [42].[10]

The main problem with this theory is that it has not withstood empirical testing. For example, the cause of the Black Monday crash has not been related to any specific news story [43]. According to the EMH, there should be an obvious major news event behind

[10]It can be argued that there is a certain level of efficiency in the market. Well informed traders identify arbitrage opportunities in the market. Arbitrage refers to cases where the same stock is listed on different stock exchanges at different prices. Traders will quickly buy at the lower price and sell at the higher price. They will make some profit and also their trades will cause prices to readjust so as to remove such arbitrage opportunities from the market. The market can thus be called arbitrage-efficient.

every major price move. The fact that no such news event has been identified casts doubt on the theory. This crash caused economists to rethink the theory of equilibrium [44]. The fat tails of the distribution of log returns had already been noted [21], but this crash drove home the point that the efficiency theory really is not good enough. This has been reinforced by the more recent crash of 2007-2008 [45].

1.11 Agent-Based Modelling - an entirely new approach

The problems identified with the EMH drove financial modelling forward. It was becoming obvious that empirical evidence-based research was necessary, with a move away from tidy analytic models an inevitable result. This is when agent-based modelling came to the fore.

Agent-Based Models (ABMs) are suited to systems made up of many entities interacting with each other and with their environment. ABM does not refer to a specific technique or method. Rather, labelling a model as an ABM describes the perspective from which the model was built. An ABM is built from the perspective of the individual parts rather than the overall process. This is opposite to the aggregate approach of statistical mechanics mentioned in Section 1.3.

ABMs are models in which individual autonomous decision-making components are modelled in order to find the aggregate results of their collective behaviour. The rules governing each agent's behaviour can be defined and then the system is allowed to run. This means that an ABM can be expensive computationally, as each individual's actions need to be defined. This is one reason why ABMs have only become popular in more recent years as computational power has become more available to researchers [46].

This bottom-up method is useful for systems with complex phenomena. The individual actions on a mico level can lead to unexpected behaviour on a macro level. This is called *emergent behaviour* as it is a result of the aggregate actions and could not be anticipated from knowledge of the individuals' rules of behaviour. This refers to situations where the whole is greater than the sum of the parts because the interactions between the parts play an important role in the aggregate result. This is one of the major benefits of ABMs over other models. In this context, major events can occur without an explicit cause-effect relation with a major news item as called for by the EMH.

Because the ABM approach is from the perspective of the individual, it may be possible to find the source of emergent phenomena. Rather than tweaking equations until realistic data is produced, the rules governing agent interactions can be tweaked so

that they behave like real people. Then any counterintuitive aggregate behaviour can possibly be traced back to a particular trait of the agents. This means it can be possible to really understand complex phenomena rather than simply replicate it.

ABMs can also be a natural way to describe a system. When a system is made up of many people, it is more intuitive to talk about the way people act or move than to talk about aggregate statistics like density of people in an area or the proportion of buyers in a market. Agents can be designed to have different reactions to their environment and to each other and they can also learn and adapt, just like real people. These complexities are difficult to describe with differential equations.

The flexibility of ABMs also makes them appealing. Once the model is built, it is easy to adjust the number of agents present, the environment they are in and the rules which govern their behaviour. This makes them ideal for modelling things like disasters to help build good contingency plans.

An example of where ABMs have proven useful is in traffic management [47]. A model can be built of a road network in a major city. Surveys conducted of drivers can inform the input details for the agents, which in this case is vehicles. Details such as where people travel to and how long it takes can be obtained. Agents in the model then are designed to imitate the actions of real drivers. This type of modelling can be especially useful to the city planners. The road network in the model can be adjusted in various ways to find the best way to alleviate congestion. The results of the model help planners make sensible investment in areas that will be of most benefit.

ABMs are an entirely new way of modelling the market. They model real trader behaviour and strategies. They use the stylised facts of financial data as a fitness test. This means that they can offer real insight into how the market works. Agent based modelling will be further explored in Chapter 5 and an entirely new ABM presented in Chapter 6.

1.12 Chapter Summary

This chapter has presented a literature review of the most influential models of the market which have been developed over the last century. Over that time, as more information became available, the understanding of the statistical properties of financial data has increased dramatically. This has been reflected in the development of financial models. From the simple random walk model of Bachelier, we are now in the era of the agent-based model with the emphasis on realistic trading behaviour rather than parsimony. The next chapter will explore the statistical properties of financial data in detail.

1.12.1 Outputs of the work

Below is a list of presentations and publications arising from the work described in this thesis:

- **Poster Presentation** at the Dynamics Days Europe conference, Centre for Biomedical Technology, Madrid, June 3-7 2013.
  Poster title: "Building a triple agent model for financial markets".

- **Conference Presentation** at the Irish Society of New Economists conference, Maynooth University, September 5,6 2013.
  Talk title: "Emergent Properties of a Simple ABM".

- **Publication** in the European Physical Journal B, 87 (6): 129, 2014.
  Paper title: "The origins of multifractality in financial time series and the effect of extreme events"

Chapter 2

Stylised Facts of Financial Data

2.1 Introduction

There are certain universal statistical properties of all financial log return data, whether it comes from the Standard and Poor's index in America or an individual stock listed on the Tokyo exchange. These features also transcend all types of commodities and securities, from pork bellies to foreign exchange prices. These universal qualitative features are called "stylised facts" by economists.

In this chapter I present an analysis of some empirical financial data. The chapter describes many of the stlyised facts which are common to financial time series data from diverse sources. I examine two time series, daily data from the DJIA index and minutely data from the Euro Stoxx 50 index, for these statistical properties. The fact that these two data sets are from different parts of the world and have different frequencies goes to illustrate the universality of the features that will be discussed below.

2.2 Overview of the Data

In this chapter I will examine two sets of empirical log returns for some well-known stylised facts. The first data examined are the daily log returns of the DJIA from 1928 to 2012 which have already been referred to in the previous chapter. It contains 20,922 points. The DJIA is a weighted average of the prices of 30 companies based in the United States. The average is weighted to take into account new shares being issued or dividends being paid by any of the companies so that the index price is consistent. Some of the companies currently included are McDonald's Corporation, The Walt Disney Company and Wal-Mart Stores Inc. The index price and log returns are shown in the top panel of Figure 2.1. The dramatic downturn of late 2007 and 2008 can be clearly seen towards the end of the data and the major Black Monday crash of October 19th 1987 is obvious

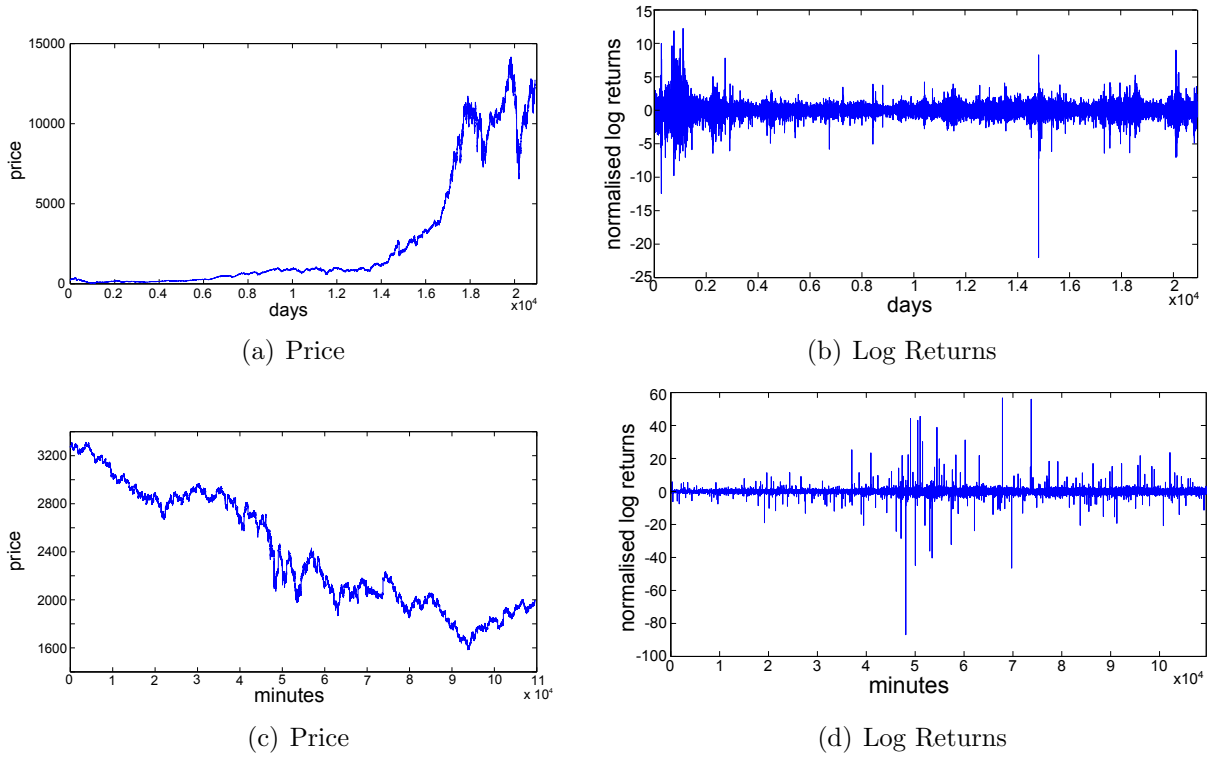

(a) Price

(b) Log Returns

(c) Price

(d) Log Returns

Figure 2.1: Top: Daily price and log return data of the Dow Jones Indstrial Average from 01/10/1928 until 23/01/2012. Bottom: Minutely price and log return data of Euro Stoxx 50 from 02/05/2008 until 27/04/2009.

at around 1.5 x 10^4 days.

Data from the Dow Jones Euro Stoxx 50 is also examined. This is an index of 50 blue chip[1] sector leaders from 12 Eurozone countries which was launched in 1998. The price is recorded each minute and runs for a year, from the start of May 2008 until the end of April 2009. There are 109,545 data points in this time series, shown in the bottom panel of Figure 2.1. The period of high volatility in the middle of the data corresponds to the collapse of Lehman Brothers in September 2008.

The log returns for both DJIA and Euro Stoxx 50 are shown in units of standard deviation to allow for comparison. Summary statistics for both time series are presented in Table 2.1. The properties presented in the table will be discussed in the following sections.

2.3 Leptokurtic Logarithmic Returns

One of the most well-known stylised facts of financial data is that the log returns have fat or heavy tails, as was emphasised by Mandelbrot [19–21]. This refers to the shape of

[1]Blue chip refers to being financially sound and reliable.

data	Δt	N	min	max	$\overline{\mu}$	$\overline{\sigma}$	skewness	kurtosis	H
DJIA	1day	20922	-0.2563	0.1427	$1.89 \cdot 10^{-4}$	0.0117	-0.5931	27.2784	0.5146
Euro Stoxx 50	1min	109545	-0.0935	0.0610	$-4.5257 \cdot 10^{-6}$	0.0011	-2.1397	$1.0335 \cdot 10^{3}$	0.448

Table 2.1: Summary statistics for the log return data examined in this chapter for the stylised facts of financial data. N is the sample size of the data, $\overline{\mu}$ is the sample mean and $\overline{\sigma}$ the sample standard deviation. H is the estimated Hurst exponent of the sample.

the empirical distribution. The tails of the distribution look fat because they contain a lot more extreme events than a Gaussian does.

The shape of the empirical distribution is called *leptokurtic*, from the Greek *lepto* meaning thin or slender, and *kurtos*, meaning bulging or curvature, referring to the thinness of the centre and the fatness of the tails. *Kurtos* is also the origin of the word kurtosis, a measure of the peakedness of a probability distribution. Kurtosis is the fourth central moment:

$$\kappa = \mathbb{E}\left[\frac{(x-\mu)^4}{\sigma^4}\right]$$

where μ is the sample mean and σ the sample standard deviation.

The Gaussian distribution has $\kappa = 3$.[2] The kurtosis of the DJIA and Euro Stoxx 50 data shown in Figure 2.1 are given in Table 2.1. Both have $\kappa \gg 3$ and the kurtosis for the Euro Stoxx 50 log returns is extremely high. Log returns in general have high kurtosis.

In Figure 2.2 the distribution is shown for the DJIA daily log returns as well as minutely log returns for Euro Stoxx 50. Gaussian distributions with the same mean and standard deviation as the empirical distributions are shown as well for reference. Clearly the Gaussian distribution is not a good fit in either case. There are too many log returns close to zero and also too many extreme events compared to a Gaussian random variable. The fat tails are easily seen on a semi-logarithmic scale in Figures 2.2(b) and 2.2(d).

The slow decay of the tails can be quantified by comparison to a power law or Pareto distribution. This can be seen in Figure 2.3. Here the inverse cumulative function $1 - \mathbb{P}[|Z| < X]$ versus X is shown on a doubly logarithmic scale for the DJIA and Euro Stoxx 50 log return time series. The function for the positive and negative tails are also shown separately on this graph. On the doubly logarithmic scale, the power law $y = x^{-\alpha}$ is displayed as a straight line and there is reasonable agreement between this and the tails. For the DJIA data, $\alpha = 4$ and for Euro Stoxx 50, $\alpha = 1.5$. The tail index of financial log return distributions tends to be between 2 and 4, with a lower index indicating fatter tails [48, 49]. This shows that the Euro Stoxx 50 returns have much fatter tails than the

[2]Sometimes kurtosis is defined as $\kappa - 3$ so that a Gaussian distribution has a kurtosis of 0. The correct term for this definition is "excess kurtosis" as it is the kurtosis in excess of that of a Gaussian distribution.

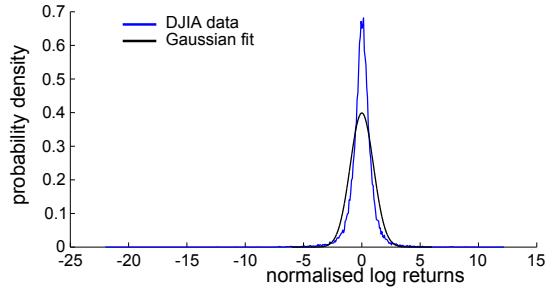

(a) DJIA; $\Delta t = 1$ day

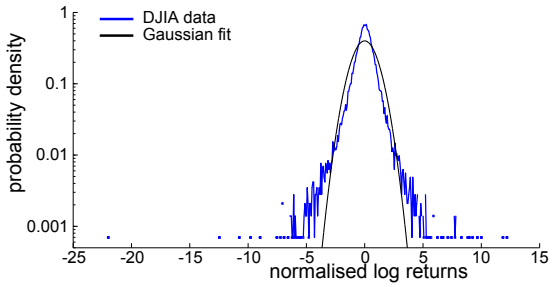

(b) DJIA distribution on semi-logarithmic scale

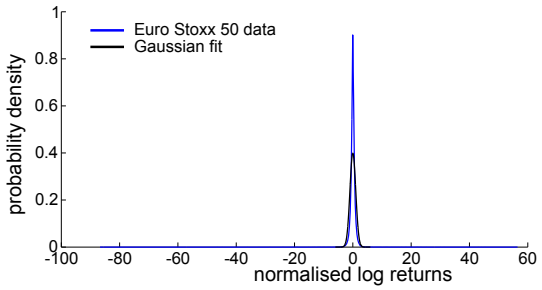

(c) Euro Stoxx 50; $\Delta t = 1$ minute

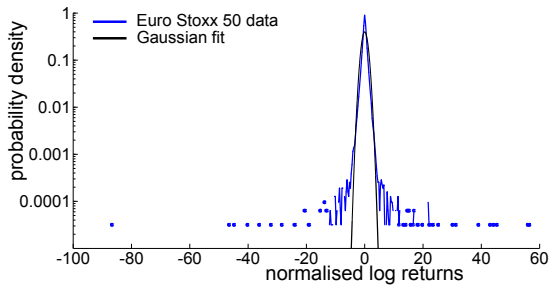

(d) Euro Stoxx 50 distribution on semi-logarithmic scale

Figure 2.2: (a), (b) The distribution of log returns for daily DJIA data, 1928-2012. (c), (d) The distribution of log returns for minutely Euro Stoxx 50 data, May 2008 - April 2009.

DJIA returns. This was also clear from Figure 2.2. The Gaussian is not a good fit to the data for either log return time series and it further illustrates that the tails of the empirical distribution are much fatter than those of a Gaussian.

A leptokurtic distribution is a common characteristic of financial log returns. The particular shape will vary between time, scale and financial product. But this feature of a thin-peaked distribution with fat tails is universal [19, 49].

2.4 Asymmetry of Returns

There are more extreme negative log returns than there are positive. This can be seen when the skewness of the probability distribution is calculated. Skewness is a measure of the asymmetry of the distribution. It is the third central moment:

$$\gamma = \mathbb{E}\left[\frac{(x-\mu)^3}{\sigma^3}\right].$$

The Gaussian distribution is symmetric and so all its odd moments are 0. It is generally a feature of log returns that they have a negative skew [19]. This means that there are more extreme negative log returns than positive. Figure 2.2 shows that this is

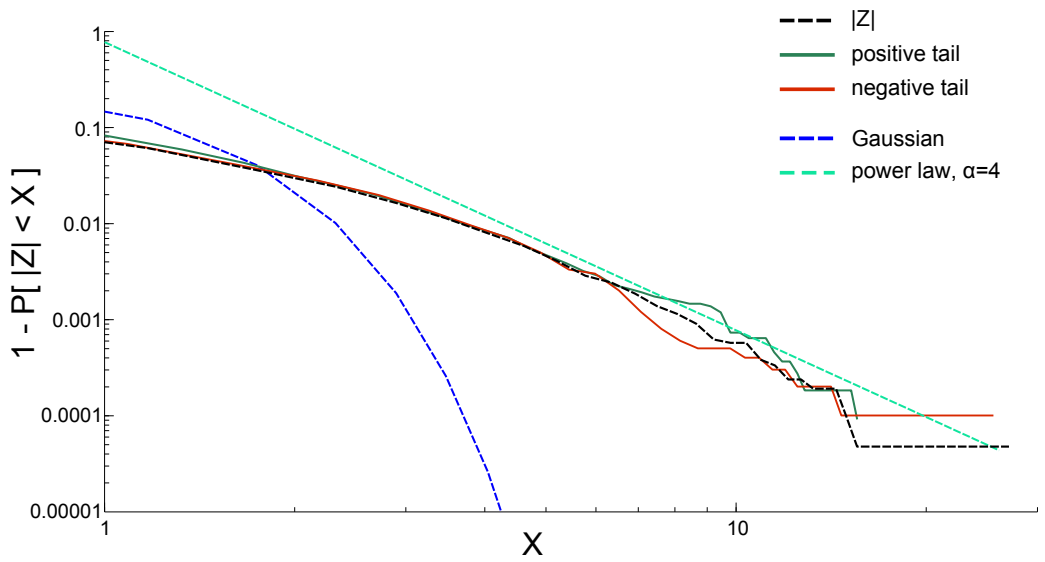

(a) DJIA

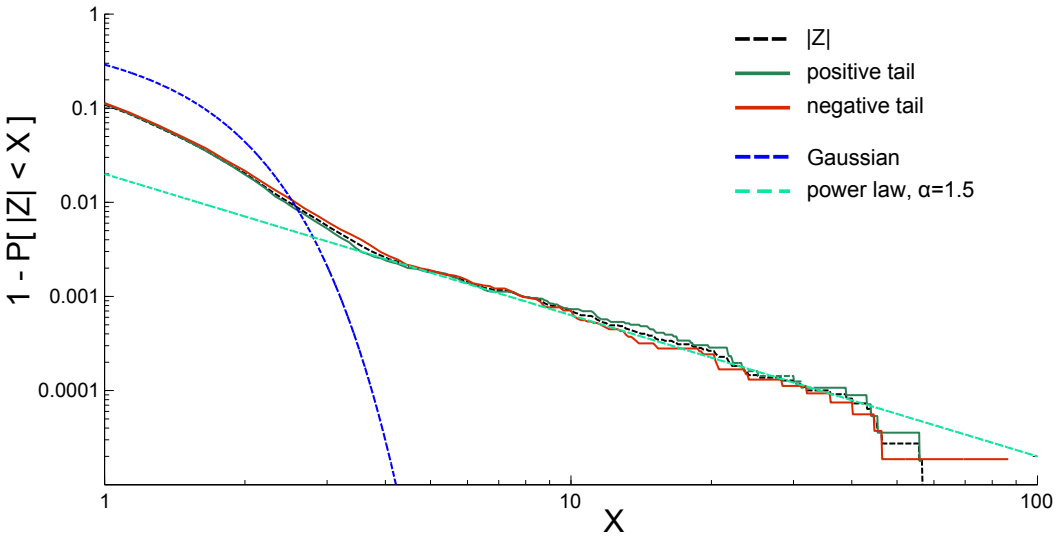

(b) Euro Stoxx 50

Figure 2.3: Graph of $\log(1 - \mathbb{P}[|Z| < X])$ versus $\log(X)$ as well as of the positive and negative tails shown separately for both the DJIA and Euro Stoxx 50 log returns (note the logarithmic scales). A Gaussian is shown for comparison. The pure power law shown for DJIA has exponent 4 and for Euro Stoxx 50 has exponent 1.5.

the case for both the DJIA data and the Euro Stoxx 50 data as in both cases the left tail extends much further than the right one.

The asymmetry can also be seen from Figure 2.3. The negative tail of the DJIA log returns is slowest to decay. This causes the negative skewness. Also, the data for the positive tail finishes before the others because it does not contain events as extreme as those in the negative tail. The negative tail is longer than the positive one for the Euro Stoxx 50 data as well. The skewness for both sets of log returns are given in Table 2.1.

This trait is not one of foreign exchange log returns for currencies with similar monetary policy [5]. Since currencies are traded against each other, if one takes a dive it means that another has jumped in value. This leads to more symmetry in foreign exchange prices than for equities where prices are not so directly anticorrelated.

2.5 Uncorrelated Returns

Price changes are uncorrelated [19] [3, chapter 7]. The direction of the next log return cannot be predicted from the price history. This is evidence for the absence of arbitrage, or the principle of "no free lunch". Arbitrage refers to the opportunity to make riskless profit by trading in the market, as mentioned in Section 1.10.1. If there were correlations in prices this would be possible. However any chance of arbitrage is quickly capitalised on by traders and prices rebalance so that the directions of future moves are unpredictable.

Figure 2.4 shows evidence that log returns are uncorrelated for the data that I have examined. The autocorrelation of the log returns Z falls to within noise level at very short lags. The autocorrelation function (ACF) is calculated by

$$A(X,\tau) = \frac{E[(X_t - \mu)(X_{t+\tau} - \mu)]}{\sigma^2};$$

τ is the time lag.

Empirically, existence of autocorrelation in financial log returns at very short time scales (less than about 20 minutes) has been shown [19, 34]. At these time scales, correlations can be attributed to market microstructure effects. An example of this would be the "bid-ask bounce" which refers to the trade price bouncing from the bid price to the ask price or vice versa. This can lead to some negative autocorrelation at very short time scales [44].

The Dickey-Fuller unit root test [50, 51] is a standard test for correlation in a series. A unit root process x_t is an autoregressive process of the form: $x_{t+1} = x_t + \epsilon_t$, where ϵ_t is a noise term with stationary increments. A unit root process is a martingale and is also a nonstationary process. If the noise terms ϵ_t are also *iid*, then x_t is a random walk.

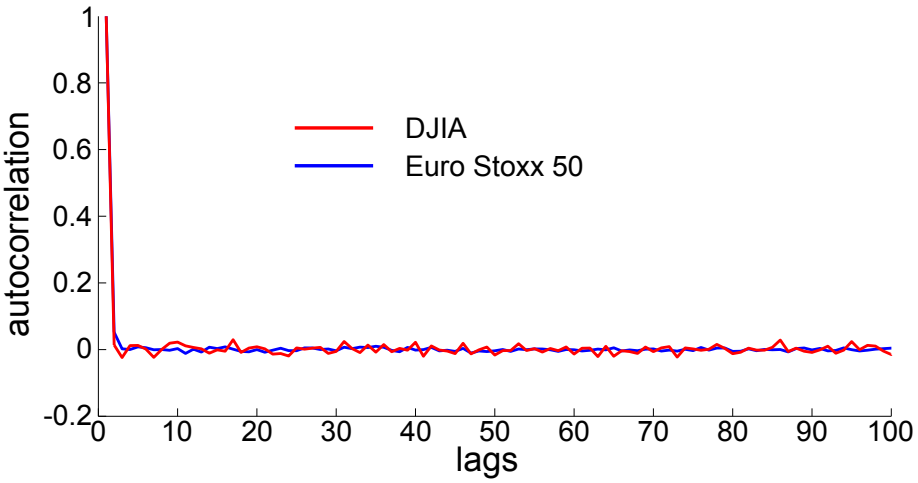

Figure 2.4: Graph of the autocorrelation functions for both the DJIA and Euro Stoxx 50 log returns.

Thus a unit root price process corresponds to a "no arbitrage" condition as it means the price history is not helpful for predicting future prices [5].

In the basic version of the test, the data is fitted to the regression model

$$x_t = \rho x_{t-1} + \epsilon_t$$
$$\Leftrightarrow \Delta x_t = \eta x_{t-1} + \epsilon_t$$

where ϵ_t is a noise term with stationary increments and mean 0, $\eta = \rho - 1$. ρ is the autoregressive parameter and η is the mean-reversion parameter.

The Dickey-Fuller test tests the null hypothesis $H_0 : \rho = 1 \quad (\eta = 0)$ against the alternative $H_1 : \rho < 1 \quad (\eta < 0)$. The augmented Dickey-Fuller (ADF) test tests the same hypotheses for the regression

$$x_{t+1} = \rho x_t + r_1 \Delta x_{t-1} + \cdots + r_n \Delta x_{t-n} + \epsilon_t.$$

This allows for dependence of the process on values further in the past than the Dickey-Fuller test.

I have used MatLab's inbuilt ADF test for both the DJIA and Euro Stoxx 50 price data. The test uses a significance level of 5%. This means that if the probability of obtaining a test statistic at least as extreme as the one observed is less than 5% when H_0 is true, then H_0 is rejected. In the language of statistics, H_0 is rejected if the p-value is less than 0.05. Results of the test are shown in Table 2.2. In both cases the unit root hypothesis is not rejected. This shows that both price series have linearly uncorrelated differences in agreement with expectation.

price data	h	p-value
DJIA	0	0.9611
Euro Stoxx 50	0	0.0541

Table 2.2: Table showing the results of the ADF test. The value of h indicates the result of the test, h $\in \{0, 1\}$. h=0 means that the null hypothesis of a unit root is not rejected. The p-value gives the probability of obtaining a test statistic at least as extreme as the one observed if the null hypothesis is true.

2.6 Volatility Clustering

Volatility is a bit of a slippery word used in the world of economics and finance to describe the spread of log returns. A time of high volatility is one in which there are many log returns of large amplitude in both directions. It is difficult to pin down a strict definition for volatility. Often it is used as a synonym of standard deviation but common measures for it are the absolute values of log returns, squared log returns or an average of either of these over an appropriate time window [1, 52] [3, chapter 7].

From Figures 2.1 (b) and (d), it can be seen that there are periods of time when there are small log returns (volatility is low), and other periods when their magnitudes are large (volatility is high). It is easier to see this by looking at the absolute log returns which are shown in Figure 2.5. The different regimes of high and low volatility are persistent. In 1963 Mandelbrot was the first to identify this feature, noting that "large changes tend to be followed by large changes - of either sign - and small changes tend to be followed by small changes" [21]. This stylised fact has been called *volatility clustering*. The amplitude of the log returns are correlated, even though their signs are not [19, 1, 49] [3, chapter 7].

Volatility clustering can easily be identified by examining the ACF of the absolute values of the log returns. A comparison between the ACFs of log returns Z and their magnitudes $|Z|$ is revealing. Figure 2.6 shows the autocorrelation for both Z and $|Z|$ for DJIA and Euro Stoxx 50. It shows that there is memory in the sizes of log returns although there is no memory in their signs.

There are obvious oscillations in the ACF for the absolute log returns of the Euro Stoxx 50 index shown in Figures 2.6(b) and 2.7(b). The peaks occur at intervals of roughly 480 minutes. There are about 480 minutes in a regular trading day and so these oscillations are a result of intradaily patterns of a high volume of trading close to opening and closing times and the slower pace of trading at lunch time [53, 54]. These patterns do not feature in the daily DJIA data because of its lower resolution.

It is often found empirically that the ACF of absolute log returns has a slow, power-law decay [19, 44]. In Figure 2.7, this is illustrated for DJIA and Euro Stoxx 50. The

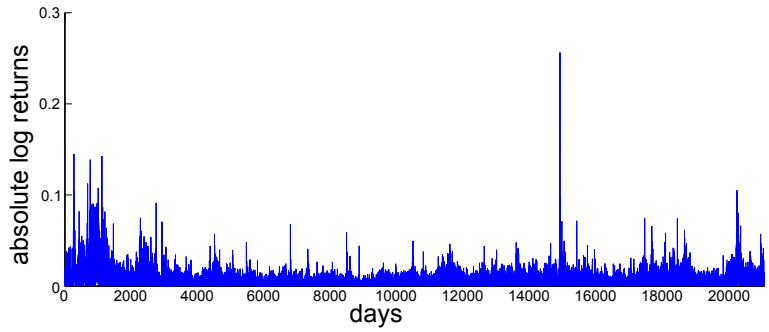

(a) DJIA

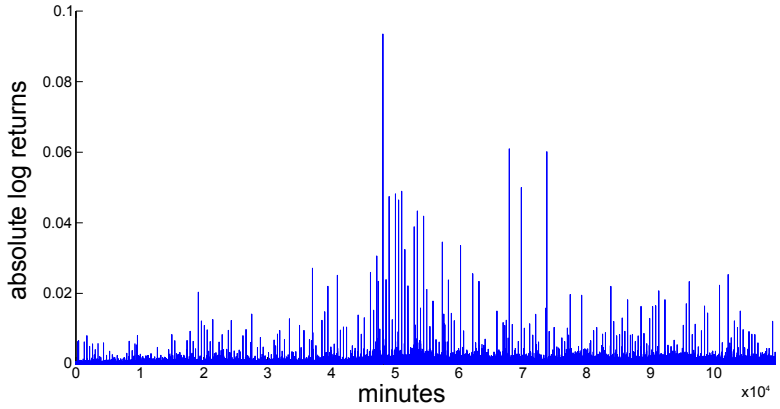

(b) Euro Stoxx 50

Figure 2.5: The absolute log returns of DJIA and Euro Stoxx 50. The nonstationary variance or volatility clustering is clear to see in both cases.

ACF of $|Z|$ versus the lag τ is shown on a doubly logarithmic scale along with a power law with exponent $\beta = -0.2$ in both cases. There is close agreement between the power law and the ACF for $3 \lesssim \tau \lesssim 300$ for DJIA and for $2 \lesssim \tau \lesssim 10000$ for Euro Stoxx 50. The value of the exponent is not universal but generally the power-law decay of the ACF of absolute log returns is a common feature in financial data. The exponent usually falls within the range $-\beta \in [0.2, 0.4]$ [19].

Other measures of volatility that are sometimes used are higher powers of the absolute log returns, that is $|Z|^p$ for some $p > 1$. These also have slowly decaying ACFs compared to that of Z. However, it has been found that the autocorrelation is slowest to decay for $p = 1$ and in fact that the autocorrelation falls almost monotonically as p moves away from 1 in either direction (so long as $p > 0$) [34]. This is illustrated for DJIA daily data in Figure 2.8.

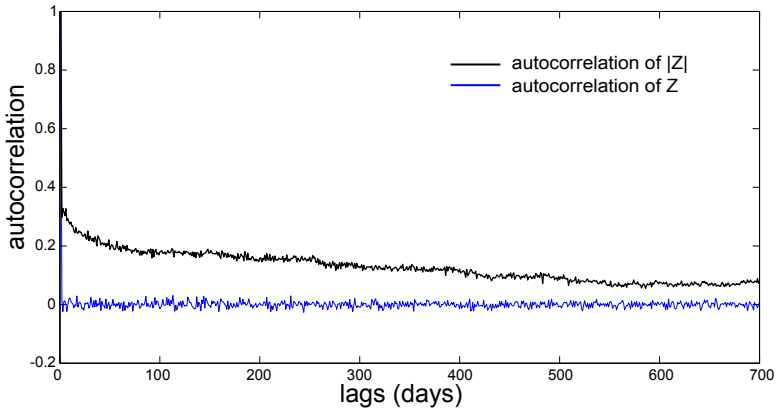

(a) DJIA

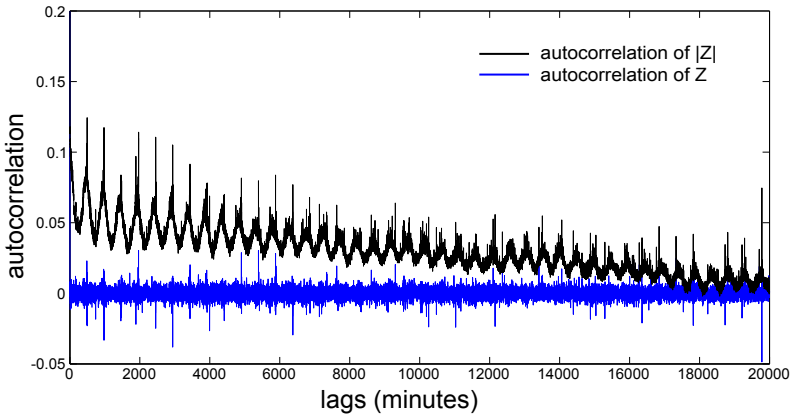

(b) Euro Stoxx 50

Figure 2.6: Graphs of the autocorrelation of log returns, $A(Z, \tau)$, and of the magnitudes of log returns, $A(|Z|, \tau)$, where τ is the lag.

2.7 Aggregational Gaussianity

The log returns described so far are on a daily scale in the case of the DJIA data, or minutely in the case of the Euro Stoxx 50 data. It is possible to have log returns calculated over a huge range of scales, from tick data which is updated at every trade, which can be up to a few times a second, to data updated only annually or even less often.

The distribution of log returns is not invariant under change of scale [19, 53]. The leptokurtosis which has been demonstrated for fine time scales in Section 2.3 diminishes at coarser time scales. This has already been illustrated somewhat by the contrast between the extremely high kurtosis of the minutely Euro Stoxx 50 log returns and the still high but more modest kurtosis of the daily DJIA log returns; see Table 2.1.

The distribution approaches normality at longer time scales [27]. That is, over longer time scales such as annually aggregated data, the distribution of log returns is better

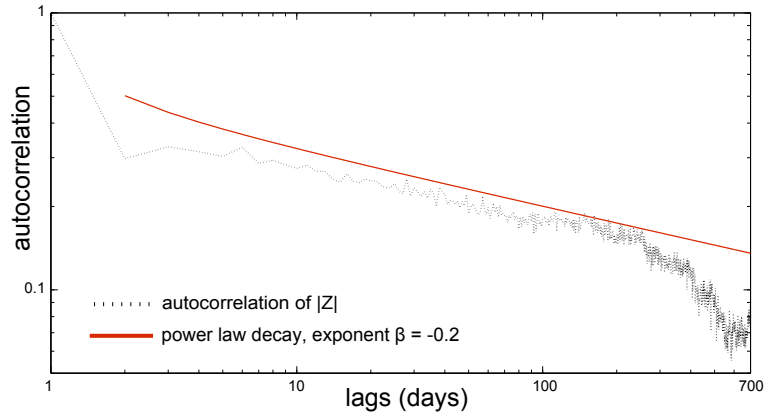

(a) DJIA

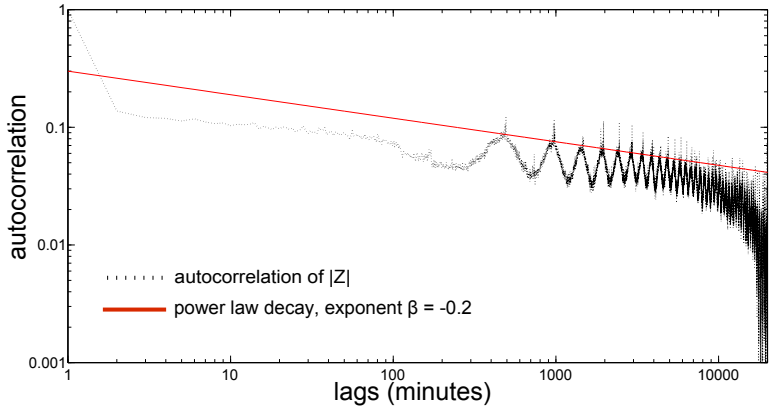

(b) Euro Stoxx 50

Figure 2.7: Graphs of $\log(A(|Z|, \tau))$ versus $\log(\tau)$, where τ is the lag, along with a power-law fit.

described by a Gaussian than it is at shorter time scales. Financial data therefore exhibits aggregational Gaussianity even though it is non-Gaussian at the microscopic level [49, 53].

The Euro Stoxx 50 data that I have been analysing is only a year long and so cannot be tested for this stylised fact. The DJIA data is 84 years long and I construct the probability distribution function for weekly, monthly and annual log returns extracted from the daily data. They are shown in Figure 2.9 on a semi-logarithmic scale along with distribution of the daily log returns and a standard normal curve for comparison. The most extreme events of the daily log returns which were shown in Figure 2.2(a) have been left out of Figure 2.9 for increased clarity.

The distribution of the annual log returns is more closely described by the Gaussian than are the distributions at higher resolution. There are only 84 data points for the annual distribution but it is enough to illustrate the dependence of the shape of the distribution on the time scale of the log returns.

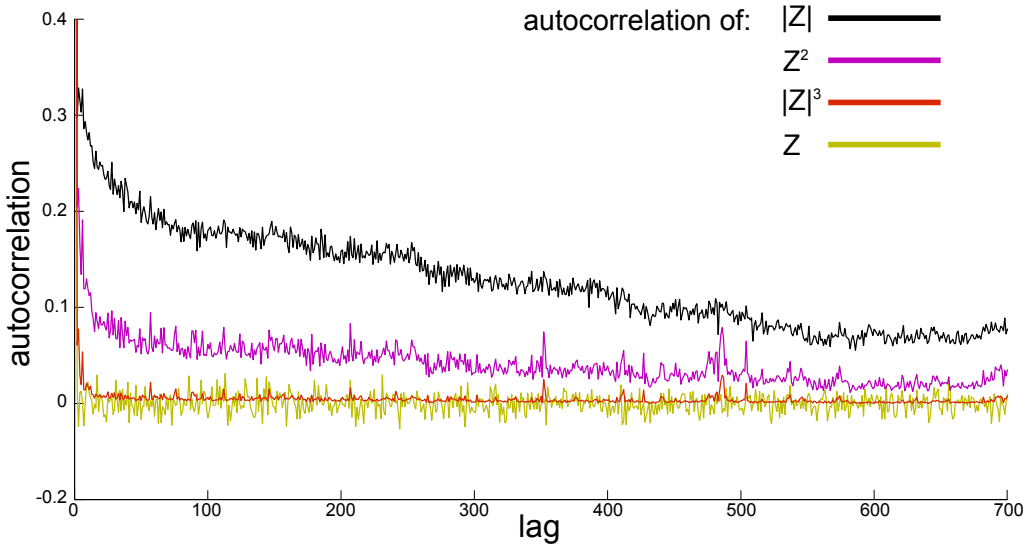

Figure 2.8: The autocorrelation function is most slowly decaying for $|Z|$ compared to other volatility measures.

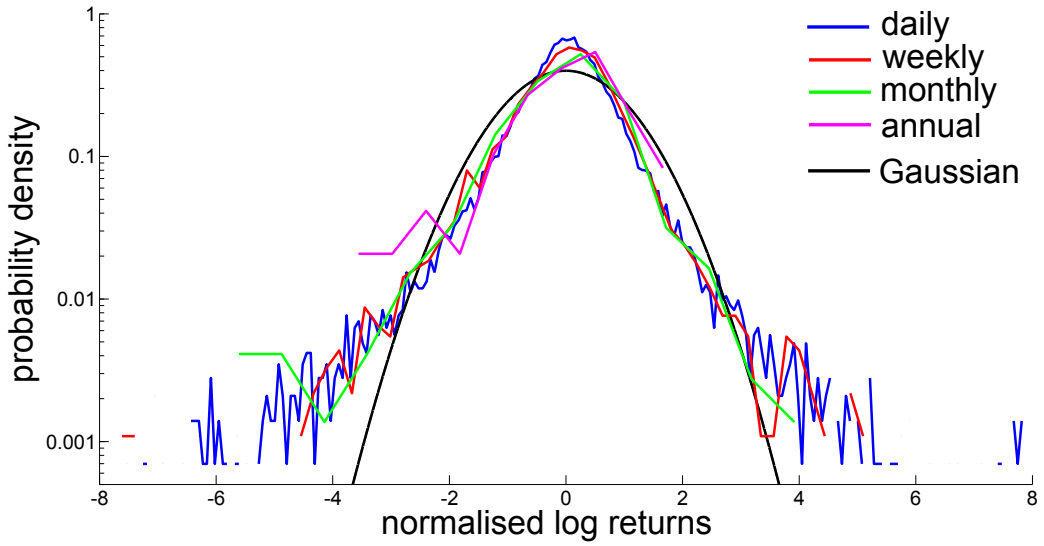

Figure 2.9: Graph of the probability distribution function for daily, weekly, monthly and annual normalised DJIA log returns along with a standard normal distribution for comparison. It is shown on a semi-log scale so the details of the distributions' tails are visible.

2.8 Chapter Summary

This chapter has presented a detailed overview of many of the accepted stylised facts of financial data. Daily data from the DJIA and minutely data from the Euro Sotxx 50 index have been examined and shown to display these features. I have shown that the log returns have fat tails and are uncorrelated. At the same time, the absolute values of the log returns have an ACF which decays slowly, roughly following a power law. The DJIA data has also been shown to exhibit aggregational Gaussianity. The next chapter will introduce another statistical property which is commonly found in financial data: multifractality.

Chapter 3

Introduction to Fractals and Multifractals

3.1 Introduction

Fractal and multifractal structures have been found in many diverse systems. These include heart rate variability, rare-earth elements, the Internet and art [55–68]. Multifractality has been accepted in recent years as another stylised fact of financial log return data [49]. This chapter presents an introduction to fractals and multifractals using some illustrative examples. The partition function and multifractal spectrum are also introduced. These concepts are then applied to financial data. The method of Multifractal Detrended Fluctuation Analysis which allows for multifractal analysis of time series data is described in detail. This chapter also reviews some of the literature covering how multifractals have been used in financial modelling.

3.2 Fractals

The word "fractal" was coined by Benoît B. Mandelbrot, derived from the Latin *fractus* meaning broken or irregular [20, chapter 1]. A fractal is an object which is self-similar and has fine detail, inadequately described by the smooth shapes of classical geometry. Being self-similar, these same fine details can be seen on smaller and smaller scales as you look at higher and higher resolutions of the object. Mandelbrot called it the "science of roughness" [20, chapter 1].

A common example of a natural fractal is a coastline. A coastline is made up of many bays and peninsulas, and each of these in turn have their own smaller bays and peninsulas. Confronted with a map of an unfamiliar coastline, it is difficult to discern

the scale of the map because there is similar detail at all scales.

A coastline is not perfectly self-similar. Rather, it is a statistical fractal. We say this because the scaling is not exact. As you look at the coastline at different resolutions you see similar structure but it will not look exactly the same as the overall coastline. Also, there is a limit to the scaling. As you continue to zoom in on a section of the coastline, eventually you see only rocks and sand and then smaller and smaller particles. At the atomic level for example, the jagged shape of the coastline is no longer discernible. All fractal objects found in nature have these limiting properties.

Purely mathematical fractals can be constructed without these limitations. Studying these helps to clarify the important features of fractal shapes. The von Koch curve is a useful introductory example.

3.2.1 The von Koch curve

Beginning with a straight line of unit length, the von Koch curve can be built iteratively so that its structure is known exactly. The construction is shown in Figure 3.1.

In the first iteration, the middle third of the line is replaced by two line segments each of length 1/3 arranged as the sides of an equilateral triangle over the removed section. In the second iteration, each of these four line segments again have their middle third replaced by a suitably scaled triangular "hat". Now there are 16 line segments each of

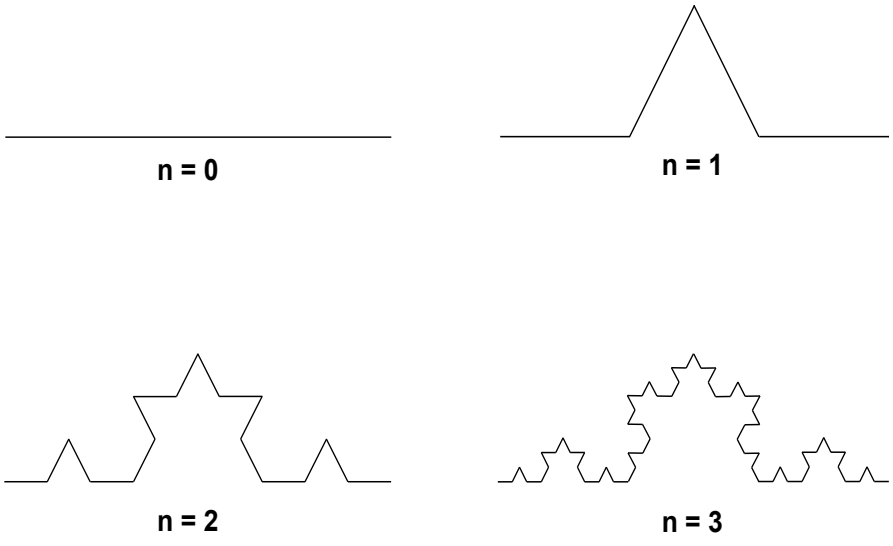

Figure 3.1: The first few iterations of the building of the von Koch curve. The curve at stage $n = 1$ is called the generator because the complete curve can be built recursively from it.

length $1/9$. This process continues so that at iteration n, there are 4^n segments each $(1/3)^n$ long.

The von Koch curve is defined in the limit $n \to \infty$ and so it has infinite length and is nowhere differentiable [69, chapter 1] [70, chapter 2]. The length of the curve, normally a useful descriptor, is not a suitable characterisation of its geometry.

Since the length of the von Koch curve is not well defined, a different description of its character is required. This is the dimension. The regular concept of dimension in Euclidean space can be thought of as a scaling exponent. For example, think of covering a regular two-dimensional square in $\mathbb{R}^2$ of side L with N_s smaller squares of side s. As the size of the covering squares decreases ($s \to 0$), the number N_s of them needed to cover the large square increases according to the scaling law

$$N_s \propto \left(\frac{L}{s}\right)^2$$

The exponent provides the dimension of the square. This method defines the *box-counting dimension* [70, chapter 4] [71, chapter 9] [72, chapter 3]. There are other definitions of dimension but this one is sufficient for the current discussion[1]. In general, the box counting dimension can be found by covering an object of linear extent L with boxes of length s;

$$\begin{aligned} N_s &= \lim_{s\to 0} \left(\frac{L}{s}\right)^D \\ \implies D &= \lim_{s\to 0} \frac{\ln N_s}{\ln {}^{L}/_{s}} \end{aligned} \tag{3.1}$$

The box-counting dimension is the scaling exponent D. The number of boxes needed to cover the object increases as the box size s decreases following a power law with exponent D.

The dimension of the von Koch curve can be found using this method. At the n^{th} stage of the iteration, 4^n line segments of length $(1/3)^n$ are needed in order to cover the curve. So the dimension is

$$D = \lim_{n\to\infty} \frac{\ln 4^n}{\ln \left(\frac{1}{1/3}\right)^n} = \frac{\ln 4}{\ln 3} \approx 1.2619.$$

This dimension is non-integer as is often the case for fractal objects. The dimension

[1]Examples of other dimensions are the Hausdorff dimension, the correlation dimension and the information dimension. The different definitions of dimension coincide for monofractals such as the von Koch curve, but may have different values for multifractals, discussed later [69, chapter 6].

gives an impression of the size of the fractal. The von Koch curve's dimension is between 1 and 2, so it is somehow thicker than a line but not as big as a surface. Also it is a scaling exponent for the fractal, giving some information on the iterative process used to generate it. As the length s of the measuring tool decreases, the measured length of the curve l increases as the measurement can take in more of the fine structure of the curve [73, 74]. The dimension is a measure of the rate of growth of the measured length of the curve l as the inner length scale s decreases:

$$l \sim s^{1-D}$$

This is reminiscent of the coastline paradox recorded by Lewis Fry Richardson [75]. He noted that the length of a coastline or country border would depend on the length of the measuring tool and in particular would get longer and longer without converging to a "true" length as the measuring tool gets shorter.

3.3 Multifractals

A fractal is such due to its shape; it is a purely geometrical property. But there may be more to an object than its shape. An object can be endowed with some distribution so that different parts of the object have different weight or measure. Now it is possible to talk about the *support* which is the shape of the underlying object, and the *measure* which is the weight distributed over the support. The measure is some location dependent integrable property of the object [74].

It is possible for a measure to have very complex structure and it can be described as multifractal if different parts of the measure scale with different scaling exponents. A multifractal cannot be described by one scaling exponent as in the case of (mono)fractals for which the dimension is an adequate description of scaling. Rather, a whole spectrum of scaling exponents is needed to characterise a multifractal.

3.3.1 Binomial measure

The Binomial measure is often cited as an introductory example to multifractals [76, 77, 74]. A simple analysis of the Binomial measure can help introduce the main properties of multifractal measures in general. It can be built in an iterative fashion as was the von Koch curve. The support of the object is a straight line interval $I = [0, 1]$. On top of the line there is a measure μ so that $\mu(I) = 1$, and it is evenly distributed over the whole interval.

At the first iteration $n = 1$, I is divided into two equal intervals. The measure μ is divided into two pieces; $p_0\mu$ is placed on $(0, 1/2)$ and $p_1\mu$ is placed on $(1/2, 1)$, as shown in Figure 3.2. The proportions are chosen so that $p_0 + p_1 = 1$; $p_0, p_1 > 0$ and $p_0 \neq p_1$ so as not to get a trivial result.

At the next iteration $n = 2$, the same process is repeated in both of the subintervals. So p_0p_0 is placed uniformly on $(0, 1/4)$, p_1p_0 is placed on $(1/4, 1/2)$, p_0p_1 on $(1/2, 3/4)$ and p_1p_1 on $(3/4, 1)$. The process continues to be repeated for each new subinterval. The measure is defined for $n \to \infty$ and so it has an extremely jagged shape as shown in the last panel of Figure 3.2.

Let s be the width of an individual box which has uniformly distributed measure. Therefore at the n^{th} iteration, $s = (1/2)^n$. There are different amounts of measure in different boxes. In the leftmost box at iteration n, for example, $\mu = p_0^n$. So for this

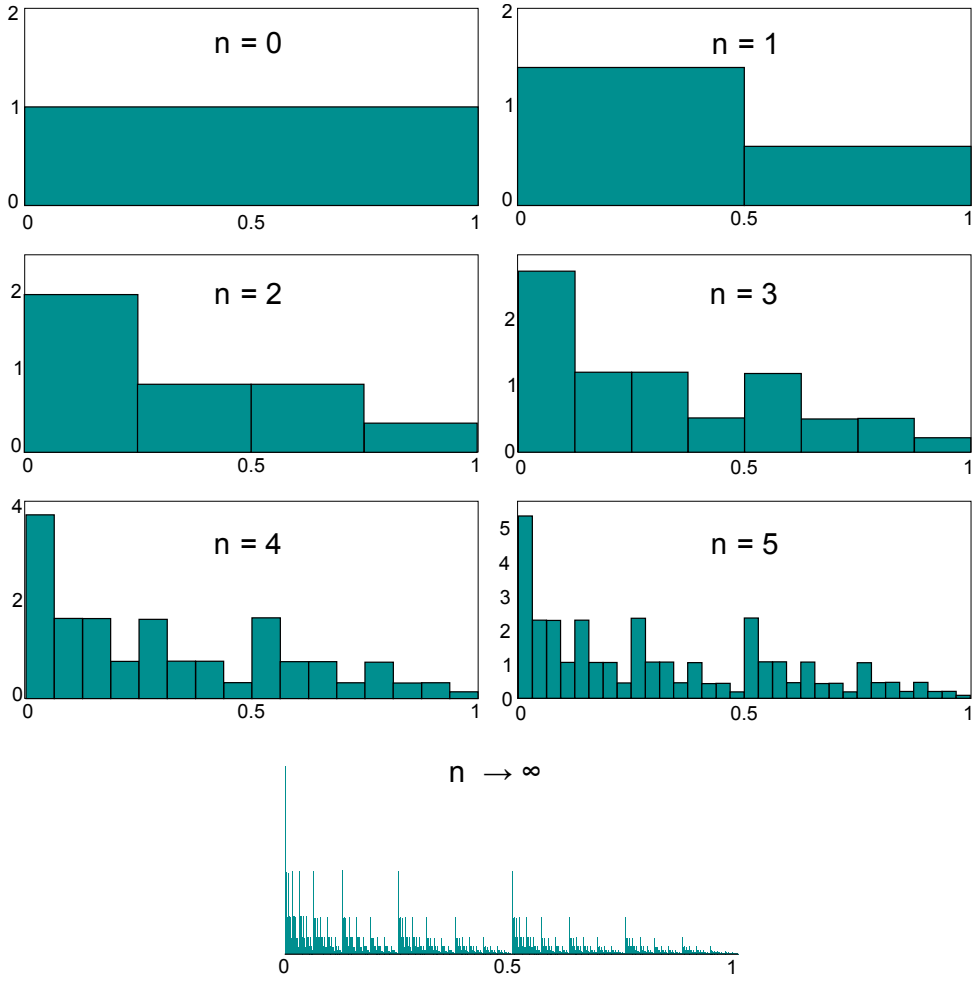

Figure 3.2: The iterative building of the Binomial measure. This construction has $p_0 = 0.7$. The measure μ of any section of the interval is the area under the curve over that section. The Binomial measure is defined in the limit $n \to \infty$

leftmost box, as $n \to \infty$,

$$\begin{aligned} s \sim & \quad \left(\frac{1}{2}\right)^n \\ \mu \sim & \quad p_0^n \\ \implies \ln \mu \sim & \quad \ln s \frac{\ln p_0}{\ln 1/2} \\ \implies \mu \sim & \quad s^\alpha \end{aligned} \tag{3.2}$$

where $\alpha = \dfrac{\ln p_0}{\ln 1/2} = -\log_2 p_0$.

α is called the Hölder exponent and characterises this part of the measure. However, a different Hölder exponent can be found in different areas of the measure. For example, in the rightmost box, $\mu \sim p_1^n, s \sim (1/2)^n$ and so $\alpha = -\log_2 p_1$.

This is why this measure is called a *multi*fractal, because now many scaling exponents are required and not just one. In fact there is a whole spectrum of α values which characterises the measure.

It can be seen from Figure 3.2 that there are different parts of the support which are covered with the same amount of measure. The number of boxes $N(\alpha)$ with measure characterised by an exponent in the range $[\alpha, \alpha + d\alpha]$ increases as $n \to \infty$ or equivalently as $s \to 0$. This number also scales according to the ansatz [78]

$$N(\alpha) \sim s^{-f(\alpha)}, \quad f(\alpha) > 0 \tag{3.3}$$

This relation is similar to equation 3.1, the definition of the box-counting dimension. Appropriately, the subset of segments (which become points as $s \to 0$) in the measure described by Hölder exponent α is said to have dimension $f(\alpha)$ [78]. The multifractal measure is made up of many intricately interwoven fractals, each with their own dimension or scaling exponent α.

Some values of α are more common than others. For example, there will only ever be one box with the maximum amount of measure, p_0^n: the leftmost box. This corresponds to the minimum value of α. Therefore, from equation 3.3,

$$N(\alpha_{\min}) = 1 \Rightarrow f(\alpha_{\min}) = 0.$$

Similarly, for the box containing the least measure on the extreme right, $f(\alpha_{\max}) = 0$. Between these two extremes there are many different Hölder exponents of varying commonality, so that a multifractal spectrum can be obtained. For the Binomial measure,

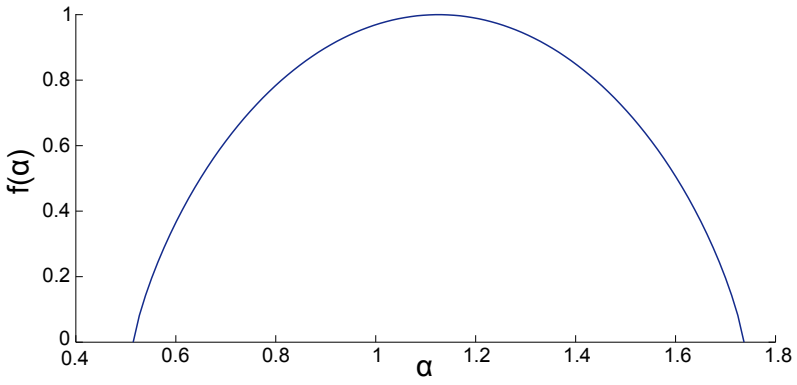

Figure 3.3: The function $f(\alpha)$ versus α for the Binomial measure when $p_0 = 0.7$. $f(\alpha_{max}) = f(\alpha_{min}) = 0$.

the $f(\alpha)$ spectrum can be found analytically[2] to be

$$f(\alpha) = -\left(\frac{\alpha_{max} - \alpha}{\alpha_{max} - \alpha_{min}}\right) \log_2 \left(\frac{\alpha_{max} - \alpha}{\alpha_{max} - \alpha_{min}}\right) - \left(\frac{\alpha - \alpha_{min}}{\alpha_{max} - \alpha_{min}}\right) \log_2 \left(\frac{\alpha - \alpha_{min}}{\alpha_{max} - \alpha_{min}}\right). \tag{3.4}$$

The spectrum is shown in Figure 3.3.

An analytical approach will not work for many multifractals, and numerical techniques must be called upon. A general numerical method for calculating $f(\alpha)$ is via a partition function.

3.3.2 The partition function

Not all multifractal objects are as regular as the Binomial measure. With the Binomial measure it is possible to find how much measure is in each box at any resolution simply by the box's location[2]. However, if such detail is not known, more analysis is required to find the different amounts of measure on the object and how they scale as the box size s is decreased.

The general method for numerically finding the multifractal characterisation of an object X is via a partition function [78, 73][71, chapter 10]. This involves introducing a new parameter q. First cover the object with a grid of boxes with side s. For a given mesh size s, the number of boxes needed to cover the object is N_s. The boxes can be labeled $N_1, N_2, \ldots, N_{N_s}$. Then $\mu(N_i(s))$ is the measure in box N_i of side s, where the measure μ is normalised so that $\mu(X) = 1$.

[2]See Appendix A.

Then the partition function is calculated for a chosen value of q:

$$\chi_q(s) = \sum_{i=1}^{N_s} \mu^q(N_i(s)).$$

This is repeated for different box sizes s until a graph can be plotted of $\log(\chi_q(s))$ versus $\log(s)$. If an appropriate linear region can be found on this doubly logarithmic plot, its slope can be determined and is equal to $\tau(q) = (q-1)D_q$, where D_q is the q^{th} order generalised dimension [79]. D_0 is the dimension of the underlying support.

If the object is a multifractal, repeating for different values of q yields different values of D_q (for a monofractal, $D_q = D_0$ for all q). Eventually a plot of $f(\alpha)$ versus α can be obtained by the Legendre transform borrowed from thermodynamics [71, chapter 10]

$$\alpha(q) = \frac{d\tau(q)}{dq}$$
$$f(\alpha(q)) = \alpha(q)q - \tau(q).$$

The partition function $\chi_q(s)$ will be dominated by different parts of the measure depending on the value of q. For positive q, the boxes with large measure will dominate, whereas for negative q, the boxes with small measure will dominate. Therefore the parameter q allows determination of how different parts of the measure scale within X. If different parts of the measure have different scaling exponents, X is a multifractal.

3.4 Multifractal analysis of time series

Time series data such as the log returns of a stock or index do not lend themselves immediately to multifractal analysis, even via the partition function method. It is necessary to resort to more involved numerical techniques to compute the multifractal scaling spectrum. Critically, for a time series the horizontal and vertical axes do not have equivalent units, and so the concept of the measure being the area under the curve does not follow through from the discussion above. The data cannot be considered as a two-dimensional structure with a possibly multifractal area.

There are a number of methods by which one might examine the fractal properties of time series data. Common ones include the Wavelet Transform Modulus Maxima (WTMM) method [80, 81] and Multifractal Detrended Fluctuation Analysis (MF-DFA) [82, 64]. It has been shown that for data where the true fractal structure is unknown, MF-DFA is the recommended method of these two, showing less bias and being less likely to give a false positive result [83–85]. This is the method which I will use for

my analysis.

The critical thing is to assign a value F to each part of the data by some function[3]. If the assigned value $F = 0$ at only a negligible proportion of points in the time series, the support of the multifractal can be considered as simply a line segment ($D_0 = 1$) as was the case for the Binomial measure [82]. It must then be checked if the assigned value F scales with the segment size s. If there is scaling over a sufficient range of values of s, the multifractal spectrum of $f(\alpha)$ versus α can be produced. The details of this method are given below.

3.4.1 Multifractal Detrended Fluctuation Analysis

MF-DFA is an extension of Detrended Fluctuation Analysis (DFA) [86, 87] which is a method of revealing long-term correlations in data [88]. By DFA and MF-DFA, the value F of a section of the data is the variance of the data from a polynomial fit. It is well suited to time series analysis because it is designed for data of a finite length, without requiring an $N \to \infty$ approximation for validity [82]. Also this method treats the data simply as a one-dimensional line and assigns new values to each segment. This deals with the data having direction-dependent scaling properties and the nonequivalence of the time and value axes [82]. The assigned values are then assessed for scaling and multifractality.

The details of the method are outlined below. The first few steps describe DFA and afterward this is extended to the multifractal case via a version of the partition function described in Section 3.3.2. Begin with a disaggregated time series X such as a set of financial log returns.

1. Transform X into Y by finding the mean-reduced cumulative sums,

$$Y_j = \sum_{i=1}^{j} \left(X_i - \bar{X}\right).$$

   This new data set is aggregated, resembling a random walk rather than a noise series, and has mean 0.

2. Choose a length s. Starting from the beginning, divide Y into non-overlapping segments ν of length s. Since s may not divide evenly into N, make another set of segments starting at the end of the data and coming back so that no data are left out. This results in $2\left[N/s\right] = 2N_s$ boxes covering the entire data set.

[3]I use notation F rather than μ in this context to conform to the literature. Also since the value F assigned by MF-DFA is not strictly a measure, it is appropriate not to use μ here. The fact that F is not a measure will be discussed in Section 3.4.2.

3. Find the least-squares polynomial fit y_ν of chosen order n to the data in each segment $\nu = 1, \ldots, 2N_s$.

4. Find the root-mean-square error or fluctuation between Y and the fit y_ν in each segment ν. This is the value $F(\nu, s)$ of segment ν of size s:

$$F^2(\nu, s) = \frac{1}{s}\sum_{i=1}^{s}\left(Y[(\nu-1)s+i] - y_\nu[i]\right)^2 \quad \text{for} \quad \nu = 1, \ldots, N_s \quad \text{and}$$

$$F^2(\nu, s) = \frac{1}{s}\sum_{i=1}^{s}\left(Y[N-(\nu-N_s)s+i] - y_\nu[i]\right)^2 \quad \text{for} \quad \nu = N_s+1, \ldots, 2N_s.$$

5. Next find the variance of $F(\nu, s)$ over all segments ν of length s,

$$F_2(s) = \left(\frac{1}{2N_s}\sum_{\nu=1}^{2N_s} F^2(\nu, s)\right)^{1/2}$$

.

6. Repeat steps 2 - 5 for different segment lengths s, finding a new value $F_2(s)$ in each case.

7. Plot $\log(F_2(s))$ versus $\log(s)$ and find the least-squares linear fit to the curve. If there is a reasonable linear fit to this data over a sufficient range of s, it indicates that the data is self-affine. The slope of this line, $h(2)$, is an extension of the Hurst exponent which can be applied to non-stationary data; $F_2(s) \propto s^{h(2)}$.

   The steps above describe DFA. This procedure will only find one scaling exponent H for the data set and so cannot differentiate between mono- and multifractals. In a monofractal, there are no periods of extreme high or low volatility, and so the fluctuation F_2 of the data from the polynomial fit y is enough to characterise the scaling. However, for a multifractal, there are periods of extreme high and low volatility and so variance is not enough to describe the scaling. Different order moments should be considered. DFA is expanded to MF-DFA by including the partition function to take this into account:

8. Introduce a parameter q. Adjust the above procedure simply at step 5. Instead of finding just the variance F_2, find the q^{th} order variance F_q for a range of both positive and negative q for each segment size s. This corresponds to the partition

function described in Section 3.3.2.

$$F_q(s) = \left(\frac{1}{2N_s} \sum_{\nu=1}^{2N_s} \left(F^2(\nu, s) \right)^{q/2} \right)^{1/q}$$

For $q = 0$, use the quenched average[4] $F_0(s) = \exp\left(\frac{1}{2N_s} \sum_{\nu=1}^{2N_s} \ln(F(\nu, s)) \right)$. Repeat for different values of s as before.

9. For each value of q, plot $\log(F_q(s))$ versus $\log(s)$. Find the least-squares linear fit to each curve. If an appropriate linear region of sufficient length (more than one order of magnitude of s) is found for each value of q, it can be concluded that there is scaling in the data.

10. If there is scaling in the data, calculate the slopes $h(q)$ of the linear fits. If $h(q)$ varies with q, it indicates that X is multifractal. If X is monofractal, the slopes produced by different values of q will all be the same.

11. In the case of varying $h(q)$, find the multifractal exponent $\tau(q)$,

$$\tau(q) = qh(q) - 1 - qH'$$

where $H' = h(1) - 1$ is the nonconservation parameter[5] and proceed to the $f(\alpha)$ spectrum via the Legendre transforms:

$$\alpha(q) = \frac{d\tau(q)}{dq}$$
$$f(\alpha(q)) = \alpha(q)q - \tau(q).$$

A plot of $f(\alpha)$ versus α is the multifractal spectrum for the time series data X.

3.4.2 Comments on MF-DFA

With this method, the first step is to detrend the data. This removes any drift from the time series and means that MF-DFA is not sensitive to nonstationarities in the data. It is known that there are seasonal effects in financial data on different time scales, such as the "January effect" and the "weekend effect," and a slump in trading around lunchtime is commonly noticeable in intra-daily data [5, 89, 54]. Also there may be trends in the

[4] See Appendix B for details.

[5] This is an adjustment to the original definition of τ given by Kantelhardt et al [82], $\tau(q) = qh(q) - 1$. It accounts for the fact that $F^2(\nu, s)$ is not strictly speaking a measure on the time series Y. This is discussed below in Section 3.4.2.

market over longer time scales due to other influences such as a persistent "bear market" in which prices tend to drop or a "bull market" in which prices rise due to aggregate trader sentiment. On the time scales of years, prices have generally been found to increase at an exponential rate [1].

All such trends will be removed by the detrending in Step 1. This leaves just the fluctuations about the mean which comes from having so many different traders operating in the market, each with their own strategy. In this study, the focus is on these stochastic, little understood movements. The order of detrending n allows discrimination in the type of trends that are removed. The trends themselves could be studied separately.

The parameter q is included as a means of finding the multifractal spectrum. When q is positive, the variance F_q will be dominated by segments with large value. When q is negative, it will be dominated by segments with small value $F(v, s) < 1$. In this way, it picks out areas of the data with extreme high and low standard deviation. This makes it possible to differentiate between the scaling behaviour of high and low value areas of the data. If these scale differently, it means that the time series is a multifractal and a range of scaling exponents α is needed to characterise the scaling.

When $q = 2$, the standard DFA procedure is recovered. If the process is stationary, DFA will lead to the standard Hurst exponent. This is why $h(q)$ can be called a generalisation of the Hurst exponent, as in Step 7 above [82]. If the series is stationary, the detrending will not alter it as there is no trend.

Generally in standard multifractal analysis, the function F of interest is a measure [78, 73]. A measure μ on a set S has, among others, the following properties:

1. $\mu : S \to [0, \infty]$
2. $\mu(A) \geq 0$, for all measurable $A \in S$
3. $\mu(\emptyset) = 0$
4. If $\bigcup_{i=1}^{N} A_i = B$ for disjoint sets A_i, then $\sum_{i=1}^{N} \mu(A_i) = \mu(B)$

Based on these properties, if A and B are measurable subsets of S and $A \subseteq B$, then $\mu(A) \leq \mu(B)$. The function F used in MF-DFA does not have this property [90, 91]. It is possible for the root-mean-square deviation from the fit to decrease as the segment size s increases so that $F_q(\nu_1, s_1) > F_q(\nu_2, s_2)$ although $(\nu_1, s_1) \subset (\nu_2, s_2)$. This accounts for the need for the correction to the definition of $\tau(q)$ noted in Step 11 above. References [90, 91] contain a derivation of the correction.

The value F could be converted from the definition given in Step 4 into a measure by

removing the averaging procedure and instead defining

$$F^2(\nu, s) = \sum_{i=1}^{s} \left(Y[(v-1)s+i] - y_\nu[i]\right)^2 .$$

This value would necessarily increase with s. However the definition of Step 4 above is well established and so I will use it with the correction to $\tau(q)$.

The generalised dimension D_q does not appear in the MF-DFA method. However D_q can be found via MF-DFA. The two definitions of $\tau(q)$,

$\tau(q) = (q-1)D_q$ from the standard partition function method (Section 3.3.2) and
$\tau(q) = qh(q) - 1 - qH'$ from MF-DFA

are equivalent for a stationary series with compact support [82]. This gives

$$\begin{aligned} \tau(q) =& (q-1)D_q = qh(q) - 1 - qH' \\ \implies D_q =& \frac{qh(q) - 1 - qH'}{q-1} \end{aligned}$$

It follows that in the case of the MF-DFA formalism, $D_0 = D_q|_{q=0} = 1$. D_0 is the dimension of the underlying support. This shows that MF-DFA is suitable only for multifractals with support of dimension $D_0 = 1$. Time series data without too many zeroes meets this criterion [82].

3.4.3 Interpretation of the Spectrum

In the case of a perfect mathematical multifractal such as the Binomial measure, the $f(\alpha)$ spectrum is symmetric and reaches zero at both extremes as shown in Figure 3.3. The left side of the spectrum represents areas of high measure and the right represents areas of low measure. The symmetry thus reveals that areas of very high and very low measure are present in the multifractal in similar proportions.

In the context of the partition function χ_q, for negative values of q, χ_q is dominated by areas of small measure which are then shown on the right of the $f(\alpha)$ spectrum; for positive values of q, χ_q is dominated by areas of high measure which are shown on the left of the $f(\alpha)$ spectrum. In the numerical method of MF-DFA, measure becomes the value F, the distance of the data from a polynomial fit, and F_q replaces χ_q.

If a range of scaling exponents are required to describe the scaling of F for a particular time series X, then X is deemed to be multifractal. This does not necessarily mean that a complete spectrum of $f(\alpha)$ with $f(\alpha_{min}) = f(\alpha_{max}) = 0$ will be obtainable. It may

be that scaling is found only for a limited range of q. However, X is multi- rather than monofractal once more than one scaling exponent is required.

3.5 Application to Finance

The application of multifractals to finance was introduced by the founder of the multifractal framework, Benoît B. Mandelbrot [20, chapter 1]. He first introduced the idea of multifractality in 1968 in the context of turbulence, but saw its application to finance because of its heavy tails and long power-law dependence. These two features are also argued to be present in financial data [19]. In fact it was the investigation of financial charts which initiated Mandelbrot's study of "roughness" [20].

The Multifractal Model of Asset Returns (MMAR) was proposed by Mandelbrot et al [76, 92] as an alternative to the ARCH models which were introduced by Engle to produce volatility clustering [33], as described in Section 1.9. The MMAR also generates log returns with volatility clustering. The motivation for the MMAR was to incorporate the heavy tails as well as the long-term dependence of financial log returns.

The MMAR employs a similar concept of trading time being distinct from physical time as used by Clark in the MDH [29], discussed in Section 1.8. It assumes that the price process is multifractal. The model describes the price as

$$S(t) = B_H\left(\Theta(t)\right).$$

B_H is fractional Brownian motion (fBM) with Hurst exponent H. Where BM has Hurst exponent $H = 1/2$, fBM has a Hurst exponent $0 < H < 1$. When $H > 1/2$, B_H is persistent, while B_H is antipersistent when $H < 1/2$. fBM thus has long memory and the process $S(t)$ can reproduce the volatility clustering of financial data.

$\Theta(t)$ is the cumulative distribution function of a multifractal measure. The multifractal element $\Theta(t)$ deforms B_H into a multifractal process and so the resulting price $S(t)$ has multiscaling properties. The main assumption of the MMAR is that the distinct trading time $\Theta(t)$ warps the financial time series into a multifractal structure. It takes the multifractality of the financial time series as a given.

The MMAR also allows for "outliers," large deviations which make up the fat tails of the return distribution and which had often previously been considered anomalies rather than a feature of financial time series. The authors insist that even the most extreme events should be accounted for by an appropriate model [20, 88].

The MMAR has been adapted to form the Poisson Multifractal Model (PMM) [93]. The difference between the PMM and the MMAR is the form of the multifractal mea-

sure. In the PMM, the multifractal measure whose cumulative distribution function gives the trading time $\Theta(t)$ is a Poisson multifractal. The multipliers used to form the multiplicative cascade[6] in a Poisson multifractal change at random rather than predetermined points in time. This means that the resulting process $\Theta(t)$ is "grid-free". Another important property of the PMM is its Markov structure which is a result of the Poisson multifractal [93]. The PMM also shares the desirable traits of the MMAR in that it has a similar autocorrelation structure and produces fat-tailed log returns. The PMM in turn influenced the development of the Markov Switching Multifractal (MSM) [94]. The volatility in the MSM is stochastic, a product of a finite number of Markov components.

Another family of multifractal models is based on the multifractal random walk (MRW) [95, 96]. The MRW features stochastic volatility with a correlation function which decays slowly with logarithmic behaviour. The probability distribution of the increments of the walk has fat tails and also features a transition to a Gaussian distribution for large time scales. The increments themselves are uncorrelated while the volatility has correlations with power-law decay.

The MRW has been extended to account for the negative skew which is found for the distribution of log returns [19, 97]. It is also the basis for the Quasi-Multifractal model [98] and the Self-Excited Multifractal (SEMF) model [99]. The innovation of the SEMF model lies in the fact that values of the process depend on the past and there is no dependence on exogenous shocks to produce the stylised facts. This makes it suitable for modelling stylised facts which are believed to arise endogenously within the system.

It appears to be a well-established fact that financial data in general has multifractal structure [49]. It is therefore important that any model of the financial process take this into account. As has been shown in this section, much progress has been made in incorporating multifractality into financial modelling in recent years.

3.6 Chapter Summary

This chapter presented a general introduction to fractals and multifractals using the examples of the von Koch curve and the Binomial measure. It also included an explanation of the partition function, the general numerical method for extracting the multifractal spectrum for a multifractal measure. This concept was expanded into MF-DFA to allow for the multifractal analysis of time series data. This method of analysis was described in detail. I then reviewed some of the literature which shows how multifractality has been incorporated into some financial models. In the next chapter, a detailed multifractal analysis of empirical financial data from the DJIA and Euro Stoxx 50 will be carried

[6]The multiplicative cascade is a generalization of the Binomial measure described in Section 3.3.1.

out. This will clarify what it means for a time series to have a multifractal structure and motivate the consideration of multifractality in the context of financial modelling.

Chapter 4

Testing Financial Data for Multifractality

4.1 Introduction

Many studies have found multifractal scaling in financial data [100–106]. Multifractal analysis increases our understanding of the financial system and helps to characterise it. An understanding of the multifractal nature of financial data can enable deeper insight into the dynamics of financial products. It provides an additional benchmark by which to measure the fitness of financial models. This in turn can help in the design of well performing portfolios and in risk management [102].

The purpose of this chapter is to examine the DJIA and Euro Stoxx 50 log returns for multifractality. I apply MF-DFA to both empirical financial time series. Where multifractal scaling is found, the spectrum of scaling exponents is calculated via MF-DFA. Further investigations are made to identify the origin of the multifractality in the time series. Multifractality in time series might be predominantly due to the distribution of the data or the temporal correlations [82], and so both of these origins are investigated for the time series analysed in this chapter.

4.2 Parameter Selection

I have applied MF-DFA, described in detail in Section 3.4.1, to the disaggregated time series of the log returns of both DJIA and Euro Stoxx 50. Any non-trading periods such as nighttime and weekends are not included in the data. For the intradaily data, there is no time gap between the closing price on one day and the opening price on the next trading day; these prices are viewed as consecutive. The exclusion of overnight log returns

from the minutely time series made no difference to the results of the analysis and so they have been retained.

The length scales s used have a minimum of 10 and a maximum of $[N/4]$, where N is the length of the time series. This is the rule of thumb suggested by Kantelhardt [82]. At the maximum scale there are therefore 8 boxes since there are $2N_s$ boxes for each s. The increments Δs are uniform on a logarithmic scale. In selecting the detrending order n for the analysis, it is important to consider the possibility of overfitting the data. Since the smallest segment size is 10, $n = 1 - 3$ should be sufficient [64]. I found that $n = 1$ led to scaling results comparable if not better than those achieved by $n = 2, 3$ and so the data is detrended by order $n = 1$ polynomials.

A wide range of 1001 values of the parameter q are chosen, with $q \in [-50, 50]$. This is a very wide range in comparison with other studies [103, 64, 82, 77] where it is standard to use $q \in [-5, 5]$. However, for smaller ranges of q, less of the multifractal spectrum is revealed. I have found that $f(\alpha) \approx 0$ for the examined data as $q \to \pm 50$, and this captures the full spectrum [88]. The fact that the spectrum reaches zero at both ends means that for any resolution at which we choose to examine the data, there is only ever one segment which has the maximum value F_{max} and only one which has the minimum value F_{min} as was the case for the Binomial measure discussed in Section 3.3.1. If $f(\alpha_*) = 0$ for some value $\alpha = \alpha_*$, then $N(\alpha_*) \sim s^0 = 1$. So there is only one segment which has F scaling with this particular value of α.

Multifractality has been reported in cases where there is only the spurious scaling which can arise in non- or monofractal time series [107–109, 85, 110], and so caution is required. It is critically important to check the linearity of the log-log plots as described in Step 9 of the method outlined in Section 3.4.1.

It can be difficult to identify a linear region from the log-log plots alone. Plotting the slope of the line over a moving window should reveal roughly constant slope over the length of the line before linearity is accepted. These plots of the local slope make it clear if there is any curvature in the lines. For perfect mathematical multifractals, these local slopes would be exactly straight. Some oscillation away from a straight line can be expected for statistical multifractals as we are dealing with here. However, if there are any sustained curves revealed by considering the local slopes, any further multifractal analysis must be abandoned. If there is no significant linear region revealed by the local slopes, we cannot conclude that there is multifractal scaling in the data. The local slopes of the log-log plots shown in this chapter are calculated for a moving window of points which allows for some smoothing of the results while still being detailed enough to reveal any nonlinearities.

The analysis was carried out in MatLab. The code provided by Ihlen [64] which was

applied to physiological data proved useful. I made some adjustments and additions to the code so that it exactly carries out the steps outlined in Section 3.4.1.

4.3 Results from MF-DFA

4.3.1 Log-log plots and $f(\alpha)$ spectra

The doubly logarithmic plots of $F_q(s)$ versus s for the DJIA data for different values of q are shown in Figure 4.1(a). The size of the segments s ranges from 10 to 5230. By checking the local slopes of the log-log plots in Figure 4.1(b) it is possible to identify a scaling region over two orders of magnitude from $s = 10$ to $s = 2,000$. Although the slopes are not constant, they oscillate around a constant within this region. This region of scaling was then used to proceed to create the multifractal spectrum shown in Figure 4.2.

The $f(\alpha)$ spectrum constructed for the DJIA data is the classic shape of an inverted parabola as was found for the Binomial measure displayed in Figure 3.3. It has its maximum at $f(\alpha) = 1$. This value gives the dimension of the underlying support of the data which is assumed to be a straight line by MF-DFA. We see that $f(\alpha) \approx 0$ as $q \to \pm 50$. This shows that this range of q is appropriate to use. It also shows that the DJIA log returns have scaling in areas of very high and very low volatility, since the scaling of F_q continues to depend on q even for $|q| \gg 0$.

The results of the scaling check for the Euro Stoxx 50 data are shown in Figure 4.3. In Figure 4.3(a), as s decreases there is a sudden drop in the value of $\log(F_q(s))$ for $q < 0$ at $s \approx 65$. This is not a numerical issue but a genuine feature of the data. Since F is a measure of the distance of the data in any segment from a degree one polynomial fit, low values of $F_q(s)$ indicates that a segment of size s is very well fitted by a straight line.

The abrupt change in $F_q(s)$ can be explained by the presence of a section of 59 consecutive zeroes in the log returns [88]. When the data X is zero, its cumulative sum Y is a constant value. When a segment ν of Y with length s is within an interval of constant value, that segment can be exactly fitted by a horizontal line. This means that $F(\nu, s)$ will be close to zero. The smallest F dominates in F_q when $q < 0$ which explains why the drop in $\log(F_q)$ as s decreases below the length of the interval of zeroes only occurs for $q < 0$. Any scaling there may be in the data does not survive to scales smaller than $s \approx 65$.

It is not clear from Figure 4.3 if there is scaling in the data or not, even for $s > 65$. The multifractality is less certain than for the DJIA case. The linearity is not of the same quality as that observed for the DJIA data shown in Figure 4.1. It could be argued that the local slopes in Figure 4.3(b) are not constant over a sufficient range of s and

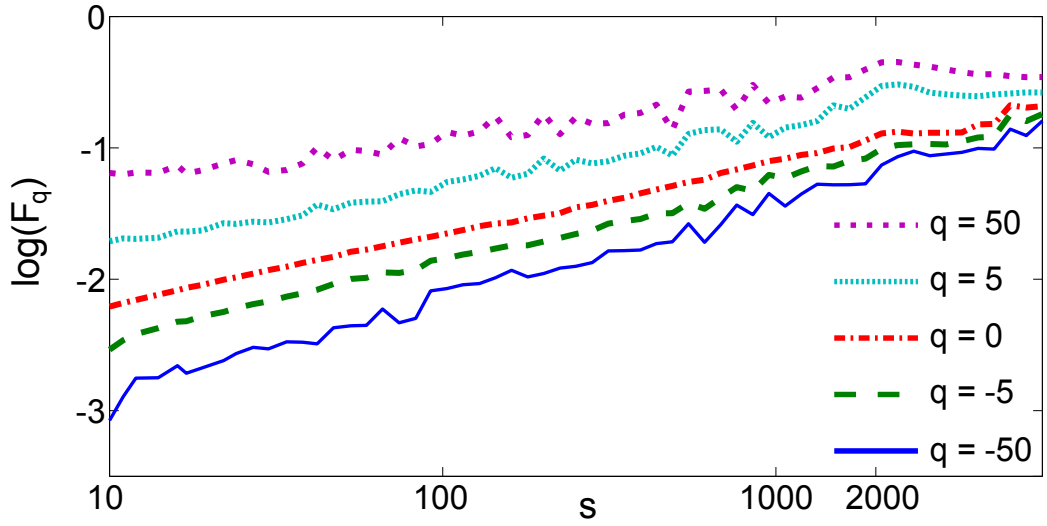

(a) Plots of $\log(F_q)$ versus $\log(s)$.

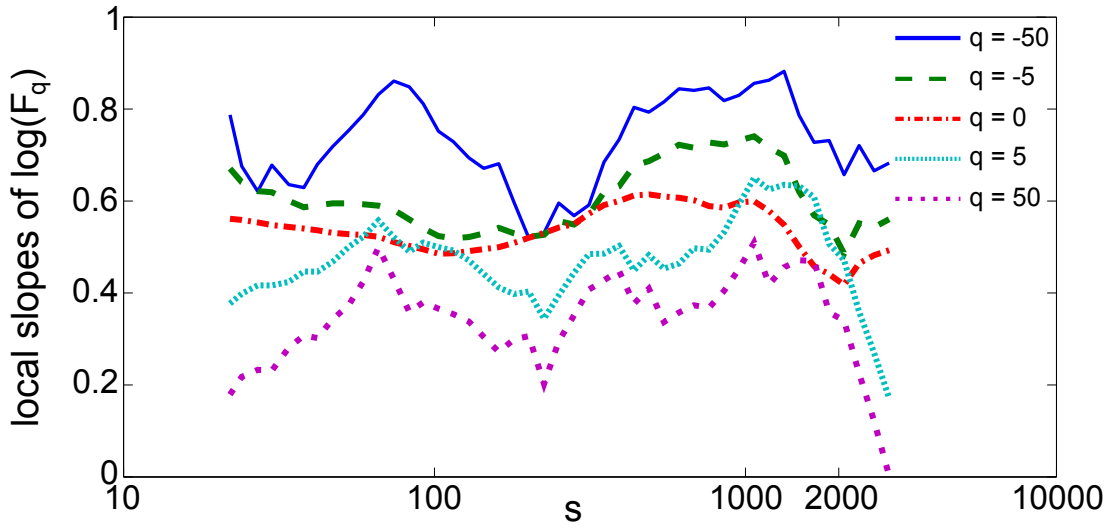

(b) Local slopes of $\log(F_q)$.

Figure 4.1: Graphs of the log-log plots and local slopes of the scaling function $\log(F_q)$ versus $\log(s)$ for the daily DJIA data for selected values of q. The local slopes are calculated over a moving window of 15 points. The slopes remain reasonably constant for $s \in [10, 2000]$.

so indicate a lack of scaling in the Euro Stoxx 50 data. In this case, this data could be presented as a counterexample to the stylised fact of the multifractality of financial log return data [49].

It could also be argued that scaling is present over more than two orders of magnitude; for $65 \lesssim s \leq 10000$ [88]. The multifractal spectrum for the range $65 \lesssim s \leq 10000$ is shown in Figure 4.4. The left side of the spectrum is stretched out and $f(\alpha) < 0$ for $\alpha \lesssim 0.63$.

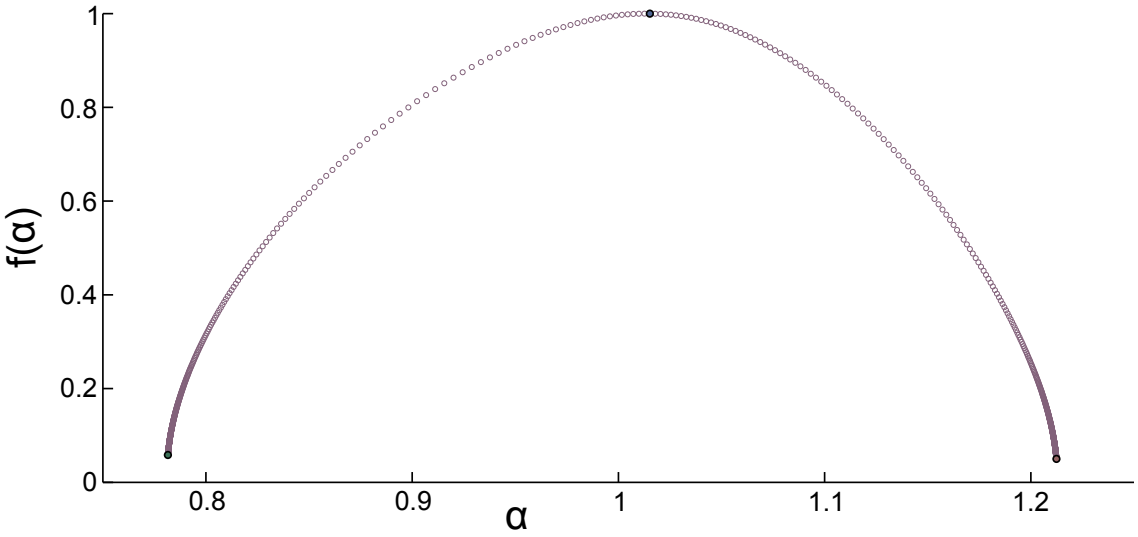

Figure 4.2: The multifractal spectrum for DJIA over the length scales $s \in [10, 2000]$.

The left side represents the areas of high F_q. These are the areas of the data which are badly fitted by a straight line or alternatively where individual points are far from the mean trend.

If the data follows the scaling law of equation 3.3, the number of segments of data $N(\alpha)$ whose value $F(\nu, s)$ has characteristic exponent in the range $[\alpha, \alpha + d\alpha]$ scales as

$$N(\alpha) \sim \left(\frac{s}{N}\right)^{-f(\alpha)}.$$

where N is the length of the time series. In this case, $f(\alpha) < 0$ would mean that $N(\alpha)$ decreases as $s \to 0$. Since this does not make sense, the negative $f(\alpha)$ for $\alpha \lesssim 0.63$ in the case of the Euro Stoxx 50 data shows that the extreme events do not follow this scaling law. The region of the spectrum where $f(\alpha) < 0$ and $\alpha > 0$ is called the latent part [111, 112]. The existence of a latent part is evidence of poor scaling, and possibly even a breakdown in scaling, of the most volatile segments. This will be discussed further in Section 4.3.2.

The fact that Figure 4.3 may indicate a lack of scaling and yet the spectrum in Figure 4.4 can still be produced shows that real caution is required when conducting multifractal analysis. A wide smooth spectrum does not imply that the data actually has multifractal scaling.

The presence of an interval of 59 consecutive zeroes in the Euro Stoxx 50 data constituting an hour of a completely stagnant price seems suspicious. There is also a section of 19 consecutive zeroes, one of 15 as well as some shorter intervals of zeroes throughout the data. To better understand their effect on the scaling, the three longest intervals are

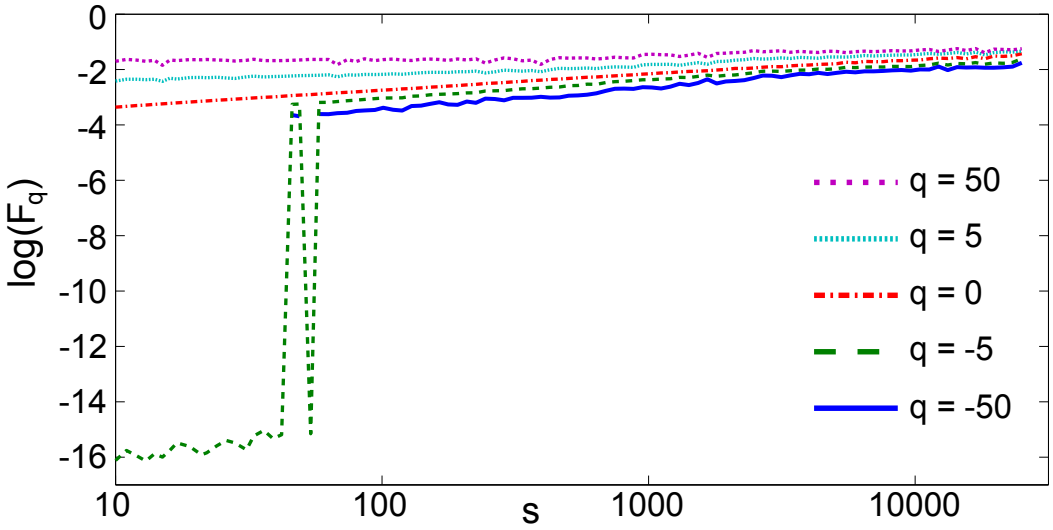

(a) Plots of $\log(F_q)$ versus $\log(s)$.

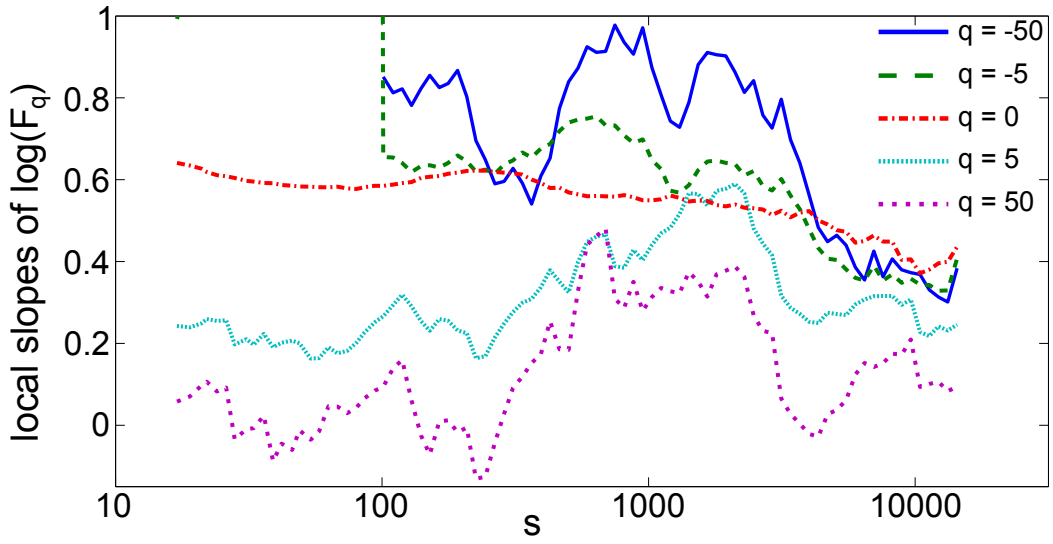

(b) Local slopes of $\log(F_q)$.

Figure 4.3: Graphs of the log-log plots and local slopes of the scaling function $\log(F_q)$ versus $\log(s)$ for the Euro Stoxx 50 minutely log returns for selected values of q. It is obvious that there is no consistent scaling for $s < 65$. The local slopes are calculated over a moving window of 15 points.

removed so that the smallest segment size $s = 10$ is longer than the longest interval of zeroes left in the data. The scaling check is then performed on the modified data and the results displayed in Figure 4.5. In the log-log plots for the modified Euro Stoxx 50 data there is no longer the sharp drop in $F_q(s)$, as can be seen by comparing Figure 4.5(a) and Figure 4.3(a). These results confirm that the sections of zeroes are to blame for the sharp decrease in $F_q(s)$ in Figure 4.3(a). However the local slopes do not appear to

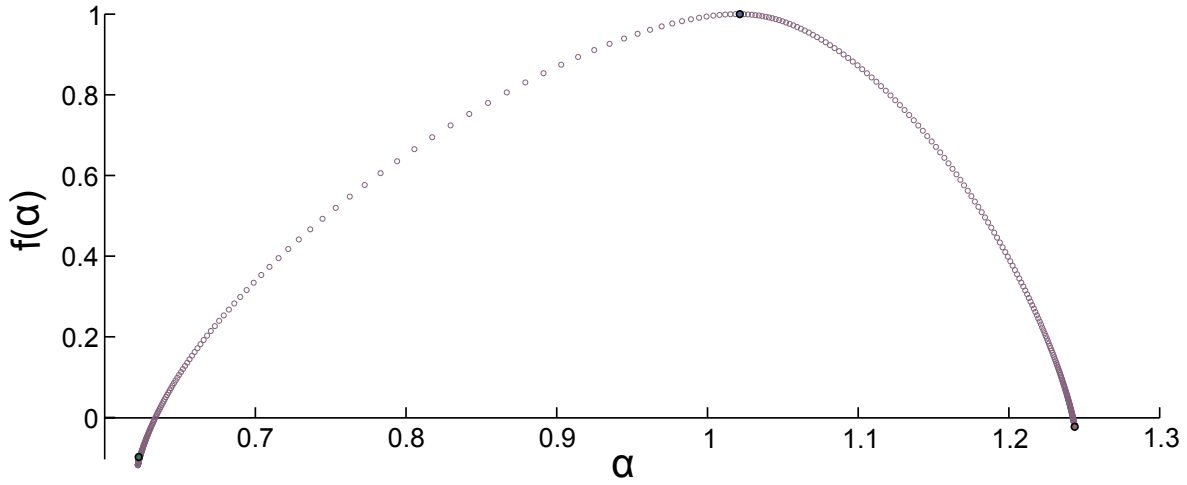

Figure 4.4: The multifractal spectrum for Euro Stoxx 50 over the length scales $s \in [65, 10,000]$.

Data	$f(-50)$	$\alpha(-50)$	$f(0)$	$\alpha(0)$	$f(50)$	$\alpha(50)$	$\Delta\alpha$
DJIA	0.049882	1.2124	1	1.0126	0.058373	0.78155	0.43087
Euro Stoxx 50	−0.023382	1.2437	1	1.0184	−0.0981	0.6226	0.62162
Euro Stoxx 50, zeroes removed	0.0361	1.2606	1	1.0226	−0.00038	0.55587	0.70495

Table 4.1: Summary of the main results of MF-DFA on the daily DJIA and minutely Euro Stoxx 50 log returns for a range of values of $q \in [-50, 50]$. Here $\Delta\alpha = \alpha_{\max} - \alpha_{\min}$.

be oscillating about constants and so I conclude that this modified data does not have scaling.

The spectra in this chapter are shifted to the right in comparison to those in the literature [103, 106, 77]. This can be accounted for by the updated definition of $\tau(q)$ in Step 11 in Section 3.4.1. A summary of the results of MF-DFA for both data sets is contained in Table 4.1.

4.3.2 The source of multifractality

It is generally accepted that there are two possible sources of multifractal scaling in time series data [82]. It could be predominantly due to (1) the data being drawn from a broad probability distribution or (2) long-term correlations of small and large fluctuations. Both of these influences can individually be removed from the data to reveal the impact they have on the multifractality of the time series.

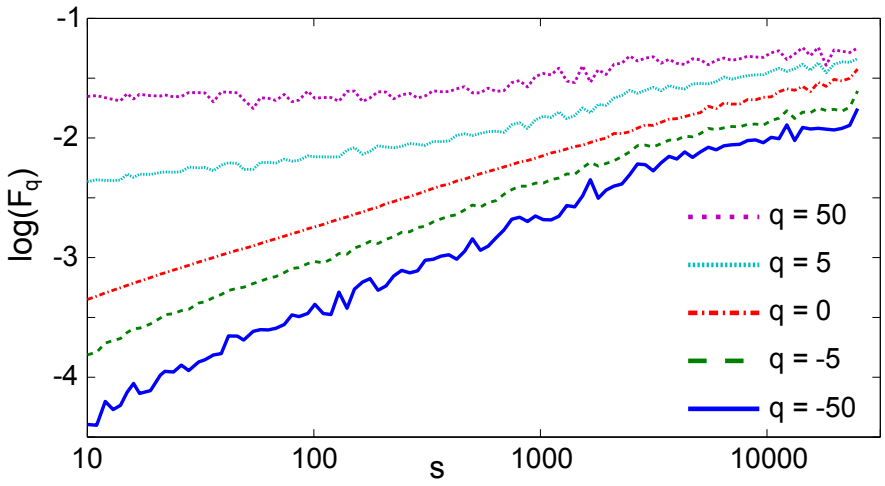

(a) Plots of $\log(F_q)$ versus $\log(s)$.

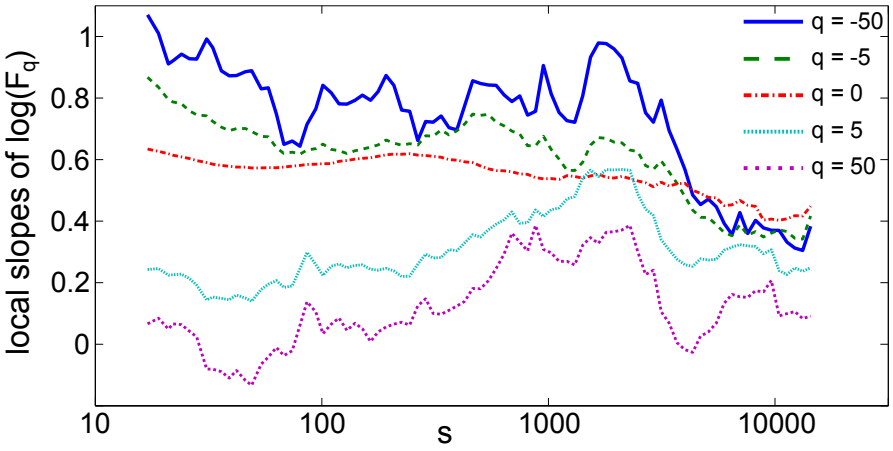

(b) Local slopes of $\log(F_q)$.

Figure 4.5: Graphs of the results of MF-DFA analysis on Euro Stoxx 50 minutely log returns which have had three intervals of zeroes removed. Plots are shown for selected values of q. The local slopes are calculated over a moving window of 15 points.

Source of Scaling - Distribution

The distributions of both the daily DJIA and the minutely Euro Stoxx 50 log returns are extremely leptokurtic. The log returns are very wild at times, as can be seen in Figures 2.1(b) and 2.1(d). The most extreme event for DJIA is Black Monday, 19th October 1987. It constituted a drop of over 22σ for this index. The Euro Stoxx 50 data contains even more extreme events.

Both distributions have been normalised and are shown along with the Standard Normal curve for comparison on a semi-logarithmic scale in Figure 4.6. The Euro Stoxx 50 data is not shown completely; a negative log return of -86σ and some positive log

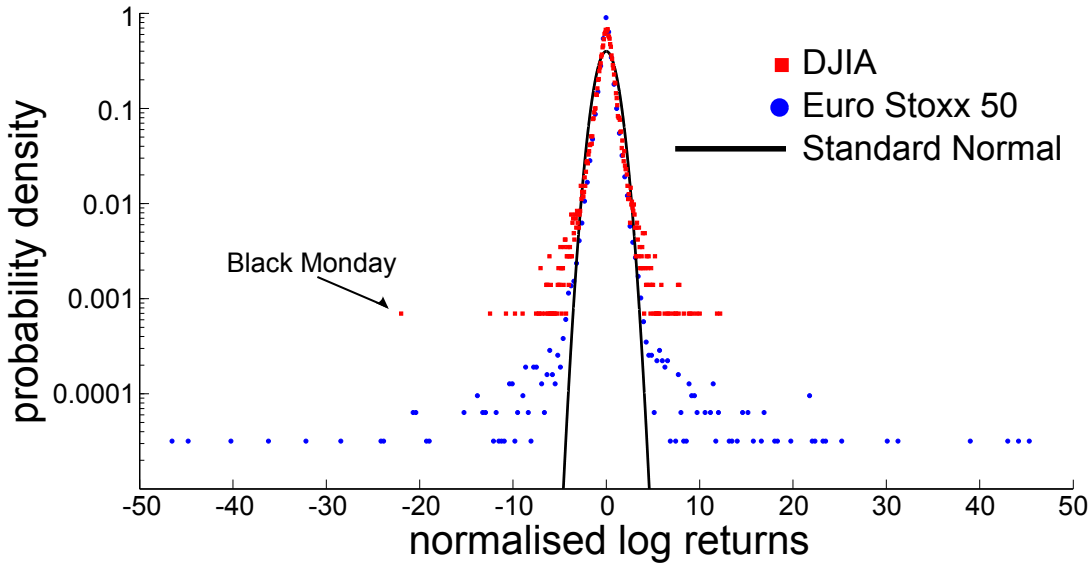

Figure 4.6: Graph of the normalised empirically found distribution of the DJIA (red squares) and Euro Stoxx 50 (blue circles) data along with the Standard Normal curve for comparison. It is shown on a semi-logarithmic scale to make the fat tails clear.

returns of approximately 60σ are excluded to make the graph clearer.

The effect of the distribution on the scaling in the time series can be revealed in a number of ways [103]. One method involves truncating the tails of the distribution. If large positive and negative log returns are reduced, the data will retain its temporal correlations while the fat tails of the distribution will be removed. This truncated data can then be tested for multifractality to reveal what influence the distribution of log returns has on the $f(\alpha)$ spectrum.

Any log returns z in the data which satisfy $|z| > c\sigma$ are replaced by $\text{sgn}(z)c\sigma$ where σ is the standard deviation of the original data and c is the chosen truncation point. Then the usual analysis can be conducted on this new data set to find the scaling properties.

I have done this for both DJIA and Euro Stoxx 50. The truncation point c varies from 1 to 10 for DJIA and 1 to 15 for Euro Stoxx 50. The number of points which have been truncated for each value of c are shown in Table 4.2.

The local slopes of the plots of $\log(F_q)$ versus $\log(s)$ for $q = 25$ are shown in Figure 4.7. Since the truncation reduces the volatility of the data set, the areas of high F are affected. It therefore is reasonable to only examine the graph of $F_q|_{q>0}$ as these are the ones dominated by large F. $F_q|_{q<0}$ are unaltered by the truncation procedure.

The oscillations of the local slopes of F_{25} for the truncated DJIA data shown in Figure 4.7(a) become more severe for more severe truncation. However the scaling is preserved for most values of c. Extreme events are evidently not imperative to the multifractal scaling in this time series.

c:	1	2	3	4	5	6	7	8	9	10	11	12	13	14	15
DJIA	3875	957	362	162	75	45	27	13	10	5	4	3	1	1	1
Euro Stoxx 50	14166	2516	671	299	206	161	128	109	90	79	68	57	53	45	42

Table 4.2: The inverse cumulative frequency table showing the number of log returns whose absolute value in units of standard deviation is larger than the given truncation point c for both the DJIA and Euro Stoxx 50 time series.

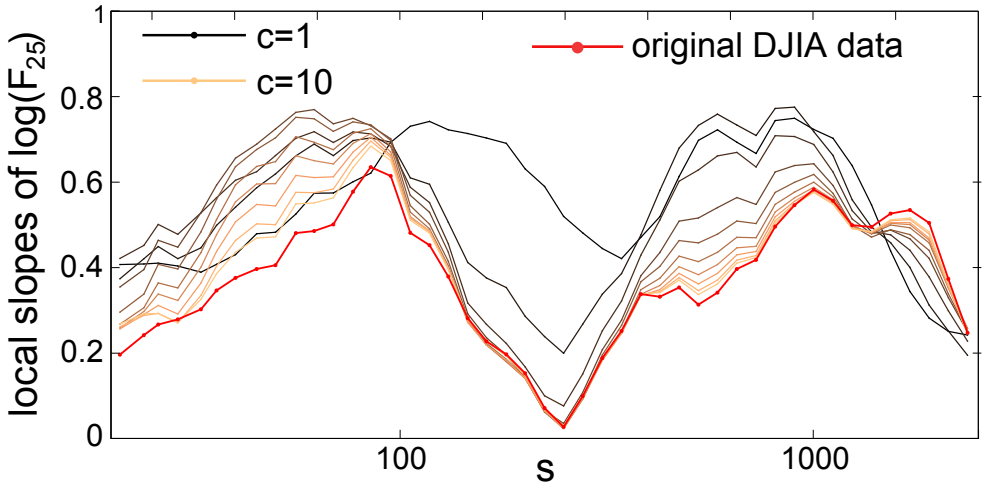

(a) DJIA

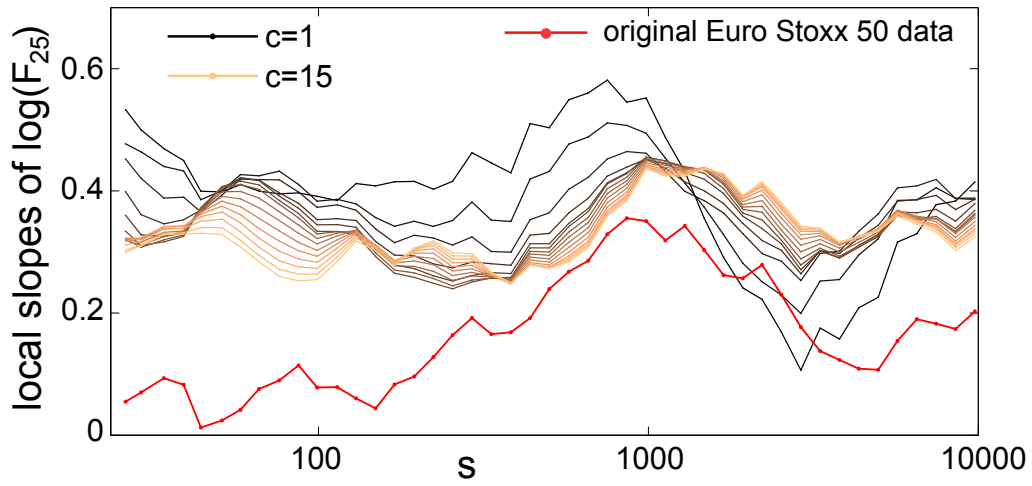

(b) Euro Stoxx 50

Figure 4.7: Graph of the local slopes calculated over 15 points of $\log(F_{25})$ versus $\log(s)$ for DJIA and Euro Stoxx 50 log returns for a range of truncation points $c\sigma$. The colour of the lines becomes lighter as c increases from the minimum value to the maximum value indicated on the graph. The slope for the original data in both cases is the red line.

The local slopes of F_{25} for the truncated Euro Stoxx 50 data in Figure 4.7(b) are closer to constant than that of the original data. The scaling is actually improved by modest truncation. Apart from the most severe cases of $c = 1$ and $c = 2$, the slopes are reasonably constant. The severe leptokurtosis of the Euro Stoxx 50 log returns is shown to be a hindrance to the scaling. This was initially indicated by the stretched left-hand side of its $f(\alpha)$ plot shown in Figure 4.4 in Section 4.3.1. This can be contrasted with the much more symmetric $f(\alpha)$ plot for the Euro Stoxx 50 data truncated at $c = 15$ shown in Figure 4.8.

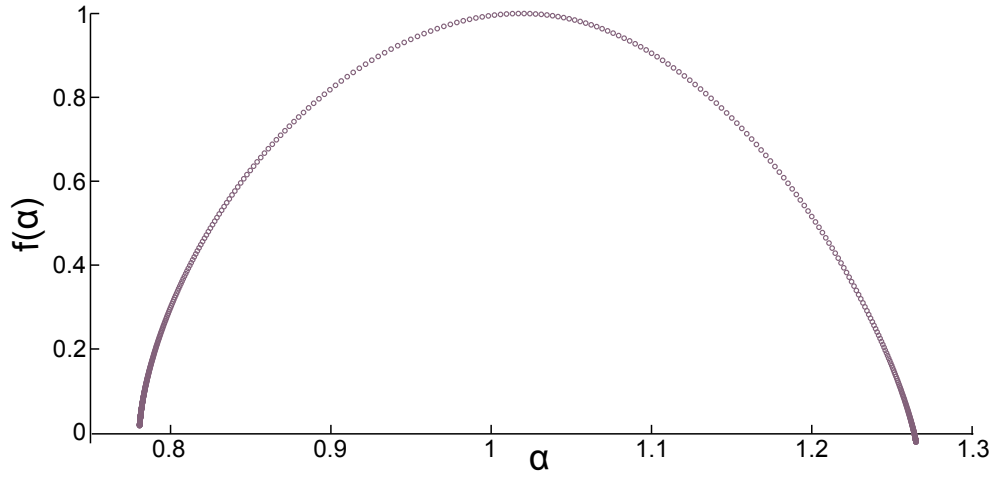

Figure 4.8: Graph of the multifractal spectrum, $f(\alpha)$ versus α, for the Euro Stoxx 50 data after it has been truncated so that any log returns $|z| > 15\sigma$ have been replaced with $z = \text{sgn}(z)15\sigma$. It has been constructed for $s \in [65, 10000]$.

As can be seen from Figure 4.6 and Table 4.2, the vast majority of log returns for both DJIA and Euro Stoxx 50 are close to zero, within a couple of standard deviations of the mean. However the few extreme events do have a significant effect since the shape of the $f(\alpha)$ spectrum for Euro Stoxx 50 changes dramatically with the reduction of only 42 points from the data (less than 0.04% of the points).

The spectrum for the truncated data, shown in Figure 4.8, is narrower than that of the original Euro Stoxx 50 data ($\Delta\alpha = 0.48$ here compared to 0.62 for the original, see Table 4.3). This result is consistent with others which have found that the multifractal spectrum narrows when extreme events are truncated [103, 113]. This is to be expected as the narrower range of α reflects the reduced heterogeneity in the data when extreme events have been tamed. However, where others [103, 109, 113–116] have used the spectrum width $\Delta\alpha$ as a metric of the level of multifractality, I have conducted a more detailed analysis. The plots of $\log(F_q)$, their local slopes, and the resulting $f(\alpha)$ spectrum are all inspected, giving more insight into the effect of the extreme events. The extreme events

Data	$f(-50)$	$\alpha(-50)$	$f(0)$	$\alpha(0)$	$f(50)$	$\alpha(50)$	$\Delta\alpha$
DJIA	0.049882	1.2124	1	1.0126	0.058373	0.78155	0.43087
Euro Stoxx 50	−0.023382	1.2437	1	1.0184	−0.0981	0.6226	0.62162
Euro Stoxx 50, zeroes removed	0.0361	1.2606	1	1.0226	−0.00038	0.55587	0.70495
truncated Euro Stoxx 50, $c = 15$	−0.021838	1.265	1	1.0169	0.017184	0.78068	0.48431

Table 4.3: Summary of the main results of MF-DFA on the daily DJIA and minutely Euro Stoxx 50 log returns for a range of values of $q \in [-50, 50]$. These values are also reported in Table 4.1. The truncated Euro Stoxx 50 data has extreme events replaced with smaller ones. Here $\Delta\alpha = \alpha_{\max} - \alpha_{\min}$.

cause the spectrum to become asymmetric. The left side of the spectrum in Figure 4.4 is stretched due to poor statistics in those extreme areas of the time series. Therefore the spectrum width $\Delta\alpha$ alone is unreliable in this case to base conclusions on about the strength of multifractal scaling [88].

Some studies have found that extreme events cannot simply be thought of as scaled-up versions of smaller events [117–119]. Extreme events appear to be drawn from a different distribution. The results of the analysis of Euro Stoxx 50 lend some support to this idea. While the scaling in the complete data set is uncertain, the scaling improves when large positive and negative returns are reduced. This indicates that they may belong to a separate scaling regime or they may not scale at all. However the number of extreme events is too small to test them separately for scaling.

Source of Scaling - Correlations

Temporal correlations may also be responsible for the multifractal structure [82, 103]. A way to check if correlation in the data is responsible for the scaling is to shuffle the data as suggested by Kantelhardt et al [82]. Shuffling removes time correlations and any scaling that remains must be due to the probability distribution from which the data is drawn. The distribution of values is not affected by reordering the series.

Any individual shuffle may still contain some correlations, so to be sure to completely rid the data of all correlations, both the DJIA and the Euro Stoxx 50 log returns were shuffled 100 times, each random permutation beginning with a new random number generator seed in MatLab. The function F_q was found for each of the shuffled data sets. These were then averaged to find $\overline{F_q(s)} = \frac{1}{100}\sum_{i=1}^{100} F_{q,i}(s)$, where the index i identifies the shuffled data sequence. I then checked the plots of $\log(\overline{F_q(s)})$ versus $\log(s)$ for different values of q for linearity. The results are shown in Figures 4.9 and 4.10. The same analysis was conducted with the quenched average, $\overline{\log(F_q(s))}$, with indistinguishable results [88].

For the averaged shuffled data, the log-log plots are smooth as is to be expected since

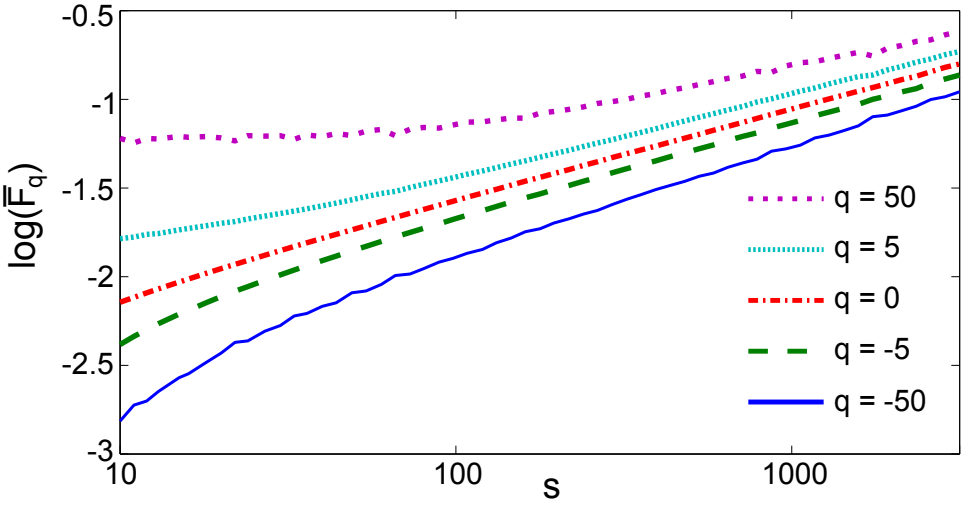

(a) Plots of $\log(\overline{F_q})$ versus $\log(s)$.

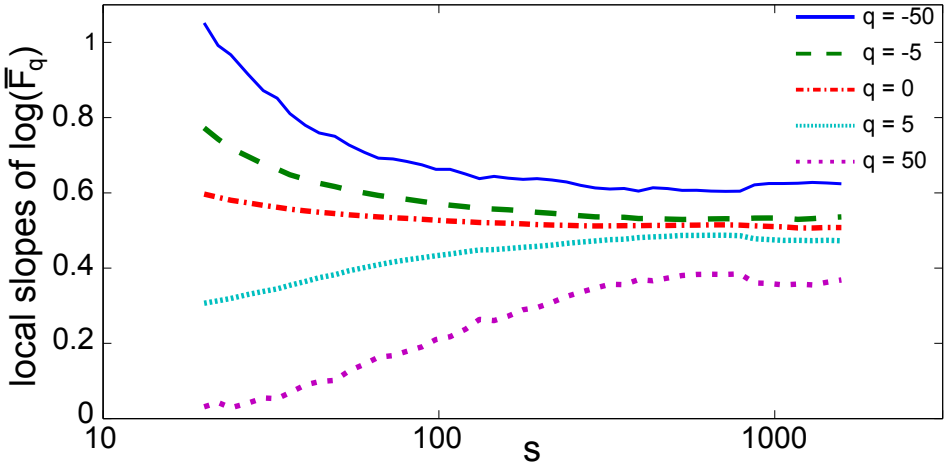

(b) Local slopes of $\log(\overline{F_q})$.

Figure 4.9: Shuffled DJIA data: (a) Graph of the log of the averaged scaling function, $\log(\overline{F_q})$, versus the log of the scale, $\log(s)$, for selected values of q as shown on the graph. (b) Graph of the local slopes of the lines in (a) calculated over 15 points for the same values of q.

it is averaged over so many shuffles. However, there is no evidence of scaling here. The log-log plots in both cases initially may appear linear but a linear region can only be identified with certainty by checking if the local slopes of the log-log plots are constant.

It is clear from Figure 4.9(b) that there is no scaling in the shuffled DJIA data. The slopes consistently decrease with s for $q < 0$ and increase with s for $q > 0$. For $s > 300$ the slopes are fairly constant but this linear region is too small to proceed to the multifractal spectrum. Thus we do not have the rationale to proceed to calculate $h(q)$ and must

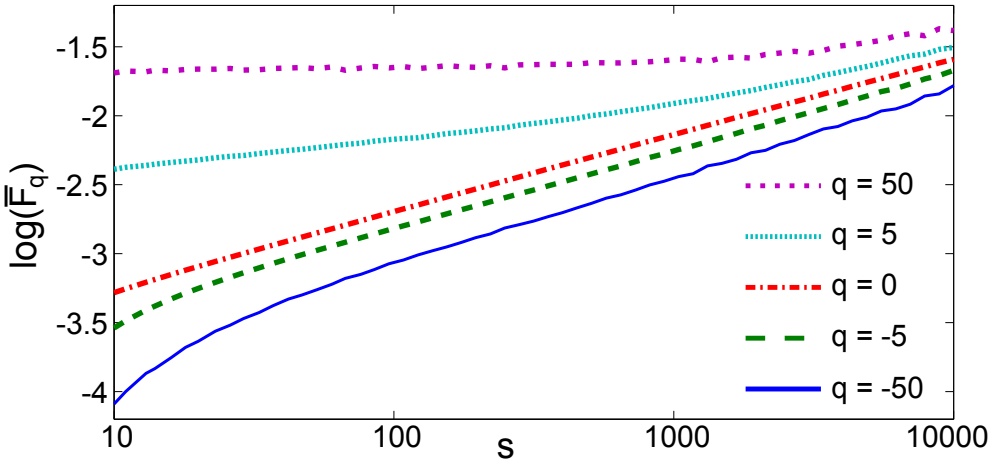

(a) Plots of $\log(\overline{F_q})$ versus $\log(s)$.

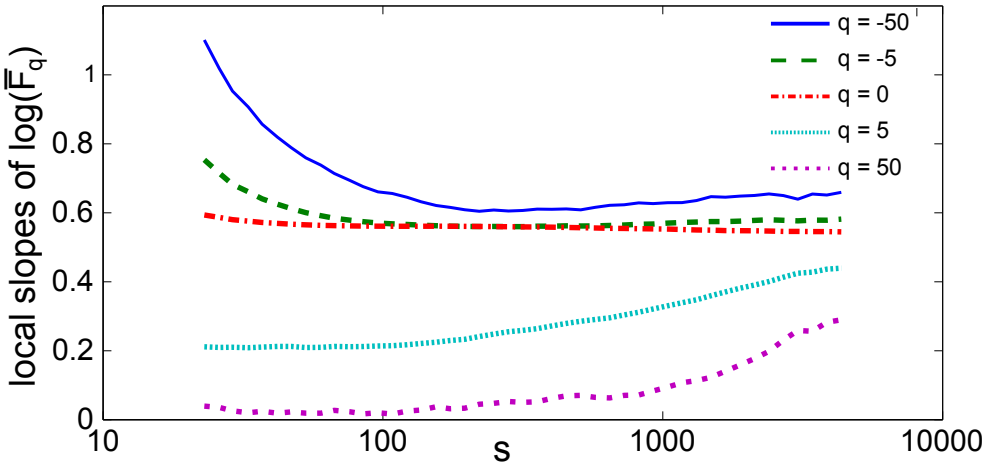

(b) Local slopes of $\log(\overline{F_q})$.

Figure 4.10: Shuffled Euro Stoxx 50 data: (a) Graph of the log of the average scaling function, $\log(\overline{F_q})$, versus the log of the scale, $\log(s)$, for selected values of q as shown on the graph. (b) Graph of the local slopes of the lines in (a) calculated over 15 points for the same values of q.

instead conclude that multifractal scaling is absent in this shuffled data set.

For Euro Stoxx 50, whose scaling results are shown in Figure 4.10, there is arguably a section of linearity from $100 < s < 10000$ for $q \leq 0$, while this scaling is not present for $q > 0$. As is common for financial log returns, there are many values close to zero and few far from zero. In the context of MF-DFA, this translates into many areas of small F and few areas of very high F. When it comes to conducting MF-DFA on the shuffled log returns, it is therefore expected that scaling may be revealed by negative q (small F, right side of the spectrum), while there may not be sufficient extreme log returns to see

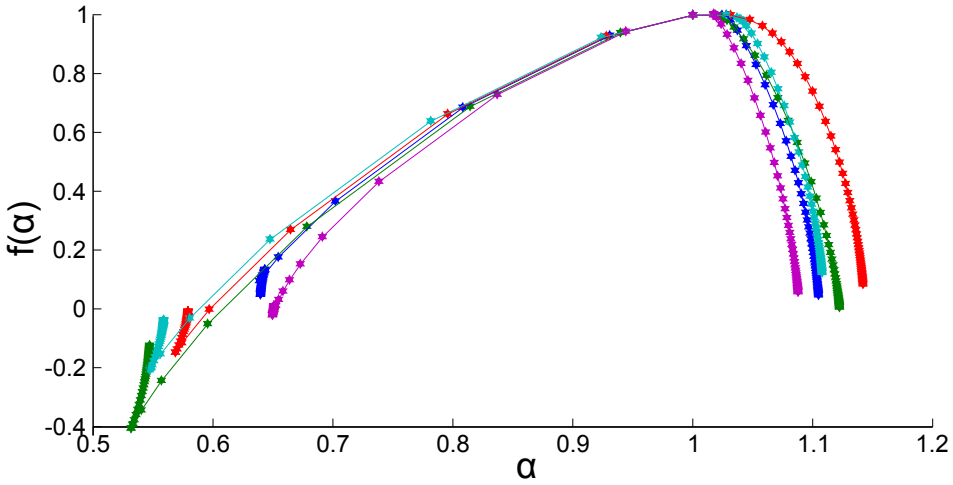

Figure 4.11: Graphs of $f(\alpha)$ versus α for five separate shuffles of the Euro Stoxx 50 log returns.

scaling for positive q (high F, left side of spectrum).

The $f(\alpha)$ spectrum has been constructed for $100 < s < 10000$ for five separate shuffles of the Euro Stoxx 50 log returns which are shown together in Figure 4.11. The right side of the spectrum contains a lot of points and is well defined in each case. However the left side of the spectrum is poorly defined. This is because areas of very high F are rare in the data and so good scaling statistics are not possible. It can therefore be concluded that the shuffled Euro Stoxx 50 log returns have reduced multifractality. In this case the spectrum width $\Delta\alpha$ is clearly useless as a measure of the level of multifractality in the time series.

Other studies [101, 103, 105, 120, 114] have found multifractal scaling in shuffled financial data. However, as no explicit investigation of the logarithmic plots and their local slopes was conducted, the conclusion that multifractal scaling is present is not justified.

The order of detrending may have some influence on the results. It is well known that the linear correlations in financial data are very short-lived whereas there are long-term non-linear correlations [19] so it may be argued that nonlinear detrending should be performed. The detrending carried out in the study presented in this chapter is linear, but I found similar results for higher order detrending, $n = 2, 3$[1]. This shows that the lack of scaling is a real characteristic of the shuffled data and not a symptom of a poor choice of the detrending order.

I also employed different strengths of shuffling. Rather than reordering every point in the data, it is possible to divide the data into intervals of length l [85]. Then keep

[1]See Appendix C for results found using higher order detrending.

each set of l adjoining points together in the same order while shuffling the order of the intervals. This can show how robust the scaling is to the long-term temporal correlations.

I conducted this analysis on the DJIA log returns. Intervals of lengths $l = 10, 50, 100, 500, 1000$, and 5000 were kept intact and the order of the intervals was shuffled randomly 100 times. Then the plots of $\log(\overline{F_q})$ versus $\log(s)$ were found. Figure 4.12 shows the slopes of the log-log plots for $q = 25$. As it is not practical to show the local slopes for the full range of q values, I chose to display results for $q = 25$.

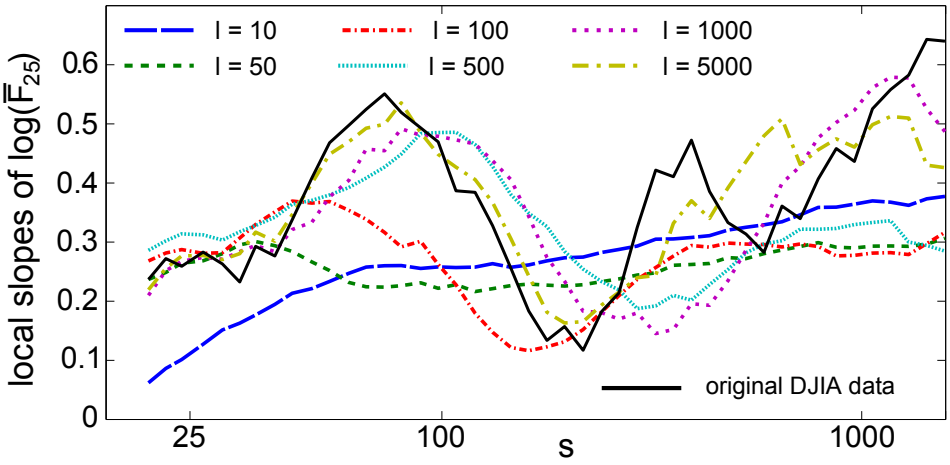

Figure 4.12: For various interval lengths l, the local slopes of $\log(F_q)$ versus $\log(s)$ is shown for $q = 25$ for the DJIA data. The slope for the original data is the black line, being the same as the corresponding line in Figure 4.1(b).

The scaling is worst for the shortest interval length, $l = 10$. The local slope of the scaling function increases steeply with the box size. For $l = 10$, any temporal correlations longer than 10 days have been destroyed by the shuffling. For longer intervals, more memory of the data is preserved and correspondingly the scaling improves.

For the data shuffled with $l = 500$, the scaling is preserved. At this length and for longer intervals, the slopes are oscillating about a constant and don't show sustained curvature in a single direction. This value of l gives an indication of the length of temporal correlations that are significant to the multifractal scaling in the data. It is possible to infer that the data has memory to the order of 100's of days. Although the scaling survives some modest shuffling, more extreme reordering is detrimental to the multifractal structure. The scaling is not robust against a substantial change in the ordering of the log returns.

The results presented in this section provide evidence that long-term correlations, which are removed by the shuffling procedure, are a major source of the multifractality in both the DJIA daily data and the Euro Stoxx 50 minutely data [88].

4.4 Conclusions

I have carried out a systematic study of the multifractal properties of two financial time series: daily DJIA log returns from 1928 to 2012 and minutely Euro Stoxx 50 log returns from 2008 to 2009. Careful attention was paid to finding an appropriate linear region in the logarithmic plots of the scaling function F_q versus the segment size s before concluding that multifractal scaling is present and proceeding to the plot of $f(\alpha)$ versus α. This examination makes this study more comprehensive than many others which have investigated financial data for multifractality. I have found that the metric $\Delta\alpha$ is not sufficent for measuring the level of multifractality in the data. Rather, the log-log plots, local slopes and the multifractal spectrum should all be examined carefully before drawing such conclusions.

The scaling is open to interpretation for the Euro Stoxx 50 time series. The uncertainty illustrates the need for caution and for further analysis techniques to be developed in this area. A set tolerance of linearity of the $\log(F_q)$ versus $\log(s)$ plots is required within which multifractality can be accepted.

In the case of the DJIA daily data, the multifractal spectrum is nearly perfectly symmetric. The one for the minutely Euro Stoxx 50 data, on the other hand, is stretched on the left and $f(\alpha) < 0$ for $\alpha \lesssim 0.63$. The shape of its asymmetric $f(\alpha)$ plot reveals that the extremely volatile areas of the data scale differently from the rest of the data or perhaps do not scale at all. The number of extreme events is too small to test them separately for scaling.

Adjustments were made to the distribution of the log returns to reveal its effect on the scaling. The results indicate that the extreme events do not conform to the scaling law which is followed by the smaller log returns. In the case of Euro Stoxx 50, the scaling is improved when the most extreme events are removed. This is consistent with the asymmetric shape of its multifractal spectrum. It can be concluded that the extreme events are actually inimical to the multifractal scaling found in the Euro Stoxx 50 log returns.

The results of this analysis on these two time series lead me to the conjecture that the resolution of the time series has an impact on the results of MF-DFA. At small resolutions (e.g. minute) where log returns are more highly leptokurtic, the extreme events can distort the scaling, while such distortion is absent at larger resolutions (such as days). The 42 most extreme points reduced in the Euro Stoxx 50 time series by the truncation have a major impact on the scaling results. The data appear to be made up of a multifractal subset and these outliers.

The temporal correlations in both data sets have been shown to be a significant source

of the multifractal scaling. The scaling does not survive at all in the DJIA time series and is much reduced in the Euro Stoxx 50 time series when the data is reordered, which removes correlations.

In general there is no consensus in the published literature as to whether it is the fat tails of the distribution or the temporal correlations which contribute most to the multifractal scaling in financial data. It has been found that the distribution contributes more to the multifractal scaling than do the temporal correlations in some daily data [105, 103]. Others have shown evidence of the opposite [121] or that both sources are significantly present [114]. Work on higher-frequency data [106, 115] has found that the correlations are the most likely cause of multifractality. Mixed results have been found for foreign exchange rates [116, 122, 123]. These varied results imply that the main source of multifractality is dependent on the particulars of each specific data set and that there is no universal law applying to all financial data.

4.5 Future Work - Proposal for tightening multifractality

I have found the task of judging whether or not a time series has a multifractal scaling structure to be a difficult one. Examining the plots of $\log(F_q)$ versus $\log(s)$ is the starting point, and finding the local slopes of those plots and examining those too is very important. However even at that stage it is not necessarily obvious whether the data should be accepted as having scaling or not.

In the case of the DJIA data, the fact that multifractal scaling is present was shown to be reasonably clear. However, as was discussed briefly in Section 4.3.1, the multifractality of the Euro Stoxx 50 minutely data is not certain. It could be argued that the plots shown in Figure 4.3 show that the data does not have multifractal scaling. Deciding whether or not there is multifractality in the data calls for some subjective reasoning. I believe that there should be some more statistical analysis tools to help.

It is necessary to impose an objective measure so that multifractality can be determined without relying solely on visual inspection of the log-log plots and their local slopes. The linearity of the log-log plots really lies at the crux of the issue. If the local slopes of the log-log plots are roughly constant or oscillate around a constant value for a sufficient range of the segment size s, the data can be interpreted as having multifractal scaling. If there is sustained curvature in the local slopes, however, the data should not be classified as multifractal. A basic visual inspection definitely has its merits but I think that some statistical tool would be a helpful addition to this process.

A simple approach would be to find the distance of the local slope $m(s)$ from the mean $\overline{m}$ at each point for increasing s;

$$K = \sum_{s=s_{min}}^{s_{max}} (m(s) - \overline{m}). \tag{4.1}$$

We are happy for the slope to oscillate about its mean, and could accept multifractality for $|K| < K_{max}$ for some tolerance level K_{max}. However, large $|K|$ would indicate that that the slope spends much more time above the mean than below it or vice versa. In that case, we could reject the hypothesis of multifractal scaling being present in the data at our chosen tolerance level.

This analysis could not be at the expense of visual inspection of the plots of the local slopes of $\log(F_q)$ against $\log(s)$. Otherwise, this toleration level method may permit acceptance of data as multifractal when in fact the local slopes consistently either increase or decrease for increasing s rather than oscillate about the mean.

Figure 4.13 illustrates this idea of measuring the linearity of the plots of $\log(F_q)$ vs $\log(s)$ by summing the difference of the slope from its mean at each point. This is a very simple proposition which could be expanded into a useful tool for multifractal analysis.

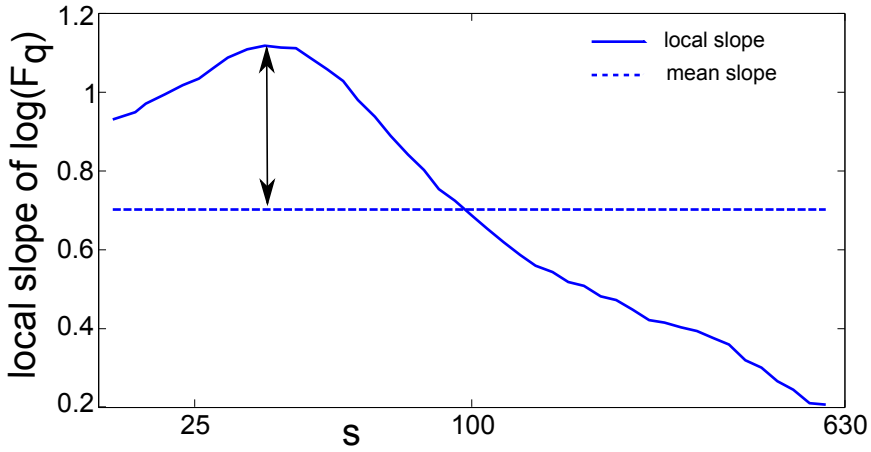

Figure 4.13: Graph of a local slope of $\log(F_q)$ versus $\log(s)$ for one value of q.

4.6 Chapter Summary

This chapter has presented a comprehensive study of the multifractal properties of two financial time series via Multifractal Detrended Fluctuation Analysis. The multifractal spectra for the DJIA and Euro Stoxx 50 data were found. Further investigations identified the temporal correlations as the predominant source of the multifractal scaling in both

cases. The chapter makes a new contribution to the literature in carrying out this analysis and in finding that extreme events in the Euro Stoxx 50 time series are inimical to the scaling. I have also argued that further statistical tools are required in order to carry out multifractal analysis objectively and made a proposal as to how that might be achieved.

Chapter 5

Agent-Based Modelling

5.1 Introduction

I now turn back to the issue of modelling the market. This chapter contains a literature review of some influential ABMs in the area of financial modelling. This will serve as an introduction to this type of modelling for in the next chapter I will develop my own ABM of the financial market.

ABMs are suited for systems made up of many interacting parts or individuals, called agents. Section 1.11 contained a brief introduction to the concept of ABMs. The classification of ABM does not refer to a particular technique. Rather a model is agent-based if it is built from the perspective of the interacting parts instead of from the perspective of the aggregate system [46].

This type of model is especially useful for systems which exhibit emergent behaviour. By their construction, ABMs can be helpful in discovering what type of behaviour leads to the stylised facts common in financial data, which are really emergent phenomena originating from agent interactions and market microstructure. Because they are built from the viewpoint of individual traders, they can show how different types of trading practices affect the log returns. With them it may be possible to peek inside the black box of the market.

As with any type of model, ABMs must be kept simple if they are going to have any explanatory power [124, 125]. As a model gets more complicated, it is difficult to uncover which components of the model are behind the different features of the results [126]. When this happens, the agent-based models are no more helpful in explaining market dynamics than are other more traditional approaches. There have been many attempts to obtain a useful ABM of financial markets which balances realism with tractability [44].

5.2 The Literature

There have been many ABMs built for financial markets in recent years. Each model has a specific purpose and so will include only details relevant to the question it is attempting to answer. There are some useful reports [44, 127, 128] which provide overviews of many models in this field. A selection of the most well-known ABMs are described in this section.

5.2.1 The Game of Life

One of the earliest models in which agents interact with each other and develop over time was John Conway's Game of Life [46, 129]. The game has a basic set-up of a number of counters in an arbitrary pattern on a 2-dimensional grid like a chess board. Each counter has eight neigbouring spaces on the grid, four side-on and four diagonally, which may or may not be occupied by other counters. At each iteration, each counter may survive, die or be born onto an empty cell on the grid according to these rules:

- A counter survives to the next generation if it has two or three neighbours.
- A counter dies and is removed if it has either more than three neighbours (over-population) or else less than two neighbours (isolation).
- A new counter is born on an empty cell which has exactly three neighbours.

The patterns in Conway's Game of Life can evolve in interesting and surprising ways. There are certain patterns which remain unchanged as the game progresses ("still-life" figures) and others which oscillate between some number of patters (Conway called period 2 oscillating figures "blinkers"). There are others which move across the grid. Some release "gliders," patterns which become detached from the central pattern and move away from it [129].

Some patterns can lead to complex phenomena and cascades, emergent behaviour which could not be anticipated from the original pattern of the counters on the grid and the rules of play alone. This game has become very popular and there are many websites dedicated to finding new patterns which lead to interesting behaviour [130–132].

5.2.2 Kim and Markowitz

One of the first modern ABMs applied to financial markets was built by Kim and Markowitz [44, 128]. They built their model in 1989 in an attempt to understand the major crash of Black Monday, October 19th 1987. The model focused on particular trading strategies and the impact they had on the volatility of the market. They had to use

simulation techniques because they were trying to reproduce many features of real-life trading. This problem could not be approached analytically.

Their model contains two different types of agent, rebalancers and portfolio insurers, each with finite wealth. There are two assets available for trade: a risk-free asset with zero interest rate, essentially cash, and a risky one whose price may go up or down. The two types of agent decide how to distribute their wealth between the two assets.

The rebalancers keep the proportion of their wealth in each asset constant. This means that if the risky asset goes up in value, they will sell some to keep the same proportion of their wealth in cash. These agents stabilise the market.

The portfolio insurers instead keep a constant proportion of a section of their wealth in the risky asset. This section of wealth is their total wealth less a floor value, the floor being a lower bound they tolerate for their wealth. This means that they only invest in the risky asset as much as they are willing to lose. If the risky asset goes up in value, their wealth also increases and so they increase their exposure to the risky asset. These agents can destabilise the market.

Kim and Markowitz found that the more portfolio insurers there are in the market, the more instability there is in prices. This lent some credence to the claims that Black Monday was caused by these types of trading strategies [128].

5.2.3 The El Farol Bar problem and Minority Games

William Brian Arthur noted that the classical theory of perfectly rational agents in the market is not realistic [133, 40]. As a situation gets more complicated, people are no longer capable of deducing perfectly logical conclusions. However the problem economists faced was to find something to replace the perfect rationality of the traders in their models. Arthur proposed that the perfectly rational agents with deductive reasoning should be replaced by agents who reason inductively from the information currently available to them [133].

People do not have access to perfect or complete information and neither do they have the capacity for perfect reasoning. However, Arthur argues, we are notoriously good at pattern recognition [133]. We tend to fill in gaps in our understanding with simple models that fit the pattern. We readjust our hypotheses as more information becomes available, perhaps discarding old theories and forming new ones. This is what Arthur has called inductive reasoning.

The El Farol bar problem offers an illustration of inductive reasoning. The problem was devised in response to a bar in Santa Fe, New Mexico, which offers Irish music on Thursday nights [133, 134]. The space is limited in the bar and the evening is only enjoyable if it is not too crowded.

The problem is formulated in this way. Say there are 100 people who might attend the bar. It is only worth going if there are less than 60 people there. Each person forms an independent expectation of the attendance that week. They will go if they expect less than 60 to be there, and they will stay at home if they expect more than 60 to be there. They do not communicate with each other. The only information they have is the previous attendance figures.

The potential attendees reason inductively. They each have an assigned subset of predictors to choose from out of an overall pool of predictors. A predictor of this week's attendance might be for example "The same as last week" or "The average of the last three weeks' attendance." Each agent will use their predictor which has proven to be the most accurate in the past. An agent will go if the predictor says that there will be less than 60 there and stay home otherwise. Then this weeks' attendance figure is released and each predictor's accuracy score is updated [134].

Common beliefs are self-invalidating. If everyone believes that attendance will be low, they will all go to the bar and show that expectation to be wrong. If they all expect attendance to be high, they will all stay at home and so invalidate that expectation. This means that different agents must have access to different subsets of predictors. If they all can use the same predictors, the attendance will simply bounce between zero and 100. This was the insight of Arthur, that different people have access to different information and may process it in different ways. Heterogeneous expectations are necessary for any interesting dynamics to occur.

One result of computer experiments with this model is that the attendance figure converges to 60. The agents' inductive reasoning leads them to this outcome as they learn which of their predictors are most accurate [133].

The Minority Game [135, 136] was an extension to the El Farol Bar problem more suited to economic modelling. Suppose there is a population of N people. At each time step, everybody must choose a side, A or B. Those who turn out to be on the side of the minority win. Of course N should be odd so that there will always be a winning side.

In trading also it is generally those in the minority who win. The minority notice a new trend and buy into it before the majority catch on. The minority profit by leaving the market ahead of the majority by correctly predicting the end of the trend. There are many different strategies in the market; similarly the Minority Game discourages conformity.

The N agents in the Minority Game have predictors which make their decisions, similar to the El Farol Bar problem. The strategies' accuracy scores are updated after each time step. The agents have limited memory; they can only use the last M results to inform their choice. Also the agents have limited information, only learning which side

won at each time and not the actual number of winners in the group.

The results show that the attendance for a given side fluctuates around the 50% mark of the total population. The shorter the memory of the players is, the more fluctuation there is in attendance figures. Large fluctuations are wasteful because when there is a low attendance on the winning side, more could have won without harming the other players. Small fluctuations represent efficient use of resources. Although players have no affiliation to each other and are not considerate of others, the game evolves into a state of sharing so that the most can benefit.

Other variations of the game can be experimented with. Challet [135] describes versions of the model where agents with different memory lengths are present, where agent strategies can adapt in time and where the amount won is dependent on the number of winners. These different versions of the game lead to interesting results. The original game does not deal explicitly with the stylised facts of financial data but there are many extensions to this game which do [136–142].

5.2.4 The Santa Fe Artificial Stock Market

A famous early ABM of which there have been many versions developed is the Santa Fe artificial stock market [44, 127, 143]. This model is focused on how agents learn and adapt. The real difference between this and a standard rational-expectations agent model is that the agents have heterogeneous expectations and have no way of knowing other agents' expectations. This is a feature shared with the agents in the El Farol Bar problem described above.

It is also reminiscent of Keyne's beauty contest [41, chapter 12]. Say you are a judge in a beauty contest. You are asked to pick the contestant that will be most popular among all the other judges, and you win if you do so correctly. Instead of choosing the one you like the best, you have to anticipate the average opinion. If each judge does the same, to win you must devote yourself to"anticipating what average opinion expects the average opinion to be" [41, chapter 12]. Similarly in finance, the trader who correctly anticipates the crowd's action before other members of the crowd wins.

In this environment, it is impossible to form a perfect expectation of future prices and dividends. Each agent in the Santa Fe model has a set of predictors for the market. These predictors are more complex than the ones used by the agents in the El Farol Bar problem or the Minority Game [133, 135]. The predictors are in essence "if-then" statements. Each predictor is a set of market conditions as well as a forecast of the next period's price and dividend. If a predictor's set of market conditions are satisfied, it comes into play. The predictor whose conditions are satisfied and which also has proved the most successful in the past will be used by the agent [143].

Agents in this market learn and adapt in time. Predictors which are rarely used because they are valid for uncommon market conditions or have been shown to be inaccurate are removed from an agent's set of strategies. Those that are used a lot are adapted by mutation (some conditions are changed randomly and others kept the same) and crossover (some conditions are replaced by corresponding conditions in another successful predictor), two methods of genetic evolution.

The real success of this model has been that it can produce many of the stylised facts of real financial data [44, 143]. It can also keep track of the sort of market conditions that are informative to agents. When agents learn slowly, the market evolves toward a rational regime where trading volume is low, there are no bubbles or crashes and technical indicators from the market are useless to the agents. This corresponds to a world where the EMH described in Section 1.10 is true and classical economical theory is valid.

On the other hand, when agents adapt and learn more quickly, technical trading strategies come into use and there are bubbles and crashes, volatility clustering and high trading volume. This matches the real world in which we live where all of these features exist [19].

5.2.5 The Lux and Marchesi model

The ABM by Lux and Marchesi [48, 44] was built with the purpose of explaining stylised facts of financial data, specifically volatility clustering. The model contains two types of trader: chartists and fundamentalists. Among the chartists there are "optimists" who always buy and "pessimists" who always sell. Traders can switch between strategies if the alternate strategy seems more profitable. The probability of switching from chartist to fundamentalist and vice versa depends on how many agents are using the other strategy. This mechanism introduces herding behaviour which means traders are influenced by their neighbours and not just by information about the market. The more agents using a certain strategy, the more likely others are to join them.

Price changes in this model are set by a market maker. The price can either go up or down by a set amount according to certain probabilities. The prices are not insensitive to the level of excess demand however, as a large excess demand will lead to a number of price changes in the same direction until equilibrium is restored.

Volatility clustering is found in the results produced by simulations of this model. These are seen as an "on-off intermittency" in the proportion of chartists present in the market [48]. As long as this fraction is far from the bifurcation point, the log returns fluctuate around zero. However when the fraction of chartists reaches the bifurcation point, the log returns become wild and the system becomes unstable. After some time, the fundamentalists again dominate and the log returns settle to calmer dynamics. This

interaction between fundamentalist and chartist traders and herding behaviour has also been explored by other models [44, 144, 145].

5.2.6 The Minimal Model

Another interesting and more recent ABM is the Minimal Model built by V. Alfi et al [144, 125]. This contains what its authors believe are the four minimal essential ingredients of a useful model of the market:

1. It includes chartist traders who base their trades on technical analysis.

2. It has fundamentalist traders who know the fundamental value of the stock and trade accordingly.

3. It has an allowance of herding behaviour by which agents can switch between strategies if they perceive that the alternate strategy seems to be working better than their own and there are many agents using the alternate strategy.

4. Each agent looks at the price from their own perspective and derives a trade signal (buy, sell or hold) from it.

The authors claim that these four aspects are irreducible and should be included in every ABM [144].

This model is based on the one by Lux and Marchesi [48, 44] described above. In that model there are also fundamentalists who have a stabilising effect on prices and chartists who cause bubbles and crashes. There are also dynamics between the classes of trader as agents can switch between strategies. As in the Lux and Marchesi model, the probability of a trader switching strategy depends both on the perceived profitability of the alternate strategy as well as the number of agents subscribing to that strategy.

The model is built for the purpose of reproducing the stylised facts of uncorrelated, leptokurtically distributed log returns with volatility clustering. These stylised facts are found in the log returns generated by this model [144].

Specifically, the authors see these stylised facts as the result of self-organisation of the market. Through the herding behaviour, traders can switch strategy from fundamentalist to chartist and vice versa and so the market can self-organise. The state of the market is characterised by the proportion of chartists at any time. When the proportion of chartists changes at an appropriate rate, the stylised facts become evident in the results.

In AMBs of the market, stylised facts are usually only present in the results for a limited region of the parameter space [144]. Alfi et al find that the presence of stylised facts is crucially dependent on the overall number of traders in the market. However in the real market place these stylised facts are universal, found in the data produced by the trading of thousands of products in many countries around the world [19]. The real market seems to organise itself into this state. This leads to the natural question of 'Why does the market naturally evolve to a state which produces these stylised facts?'

Alfi et al [144] attempt to answer this question by allowing the agents in the model to opt out of or into trading so that the number of agents actively trading can fluctuate. Agents will trade if their personal trade signal is above a minimum threshold. The number of active agents is found to spontaneously evolve toward the specific number which produces the stylised facts. It looks like self-organised criticality, but a critical state is reached in the thermodynamic limit of large number of particles and large time. Here however, these features are found only when there is a limited number of agents in the market. They can therefore be interpreted as finite size effects and the authors describe the market as being in a state of self-organised intermittency, similar to the on-off intermittency described by Lux and Marchesi [48].

5.3 Models' explanations for the stylised facts

There is no clear consensus in the literature on the reasons for the leptokurtic log returns and volatility clustering which are found in financial data. Many models have focused on reproducing the stylised facts rather than explaining their origin.

The MDH [29] was introduced originally to explain leptokurtic log returns. This was described in Section 1.8. Its focus was on the difference between trading time and clock time, and how this could lead to leptokurtic log returns. The MDH has also been used in the context of explaining volatility as a result of the aggregate impact of heterogeneous information arrival to the market [146].

The ARCH models [33] and the MMAR [76], described in Sections 1.9 and 3.5, can produce volatility clustering and fat tails. However these models do not explain these features in terms of trader activity or market structure [146, 53].

The origins of stylised facts have mainly been dealt with from the ABM perspective [53, 136, 147, 148]. The Santa Fe artificial stock market study concludes that volatility clustering is due to the rate at which agents learn and adapt and use technical trading strategies [143]. A similar ABM by Grannan and Swindle [134] is also built on the foundation of the El Farol Bar problem [133] described in Section 5.2.3. It adds contrarian agents who act against their predictor and also removes traders who perform poorly.

Those authors attribute the volatility clustering to these actions.

The model of Giardina et al [147] attribute the stylised facts to the performance rating of trading strategies (similar to the Santa Fe model), heterogeneous time scales used by traders and the changing activity levels by traders as a response to the price level relative to the fundamental value. This and other models [140–142] have also found that the option to opt out of trading is crucial to the presence of volatility clusters.

An ABM by Cont and Bouchaud [149] in which agents form clusters attributes heavy tails to these clusters which simulate herding behaviour. The model has a random-graph structure and members form independent binary links between each other with a given probability. The communication between agents who then agree on which direction to trade is responsible for log returns with heavy tails and finite variance as found in empirical data.

A proposed reason for the high volatility and fat tails of exchange rate log returns is "overshooting" [5]. This theory is that commodity prices can be slow to change but exchange rates are more flexible. Since these prices move more quickly, the rate can overreact in response to some news and overshoot its new level. This however does not help to explain the fat tails which are also found for equities.

The model by Thurner et al [44, 150] was presented to explain how fat tails and volatility clustering can be caused by leverage and margin calls. Long memory can also be considered a consequence of different traders having access to different information and processing it differently [52]. If news arrives to the market, it is not assimilated into prices immediately as different traders respond at different paces.

In the next chapters I contribute to this body of work as I construct a new ABM and explore the reasons for the stylised facts which are found in the log returns it produces.

5.4 Chapter Summary

This chapter has provided an introduction to the concept of ABMs in finance and a review of the relevant literature in this area. These types of models have become popular as more computing power is now available to researchers. ABMs tackle problems which cannot be approached with analytical methods. The reasons for the stylized facts can potentially be understood as the effects of certain trader behaviour when these types of models are used.

Chapter 6

A new Agent Based Model

6.1 Introduction

This chapter outlines the construction of a new ABM. The motivation for this new model is to add to the understanding of the reasons for some of the stylised facts of financial data. It is built in the same vein as the minimal model by Alfi et al [144]. The goal is to reproduce the key features of financial data with an even simpler model. Although Alfi et al claim that their model is "minimal", new models can continue to add to our understanding of the features of financial data.

Many of the stylised facts of financial data were described in Chapter 2. The ones of principal interest in the context of this chapter are those of leptokurtic log returns and volatility clustering, described in Sections 2.3 and 2.6. I feel that these are the most distinctive features of log returns and they are the ones I am interested in explaining. I hope to achieve further understanding of the origins of these features by means of my ABM presented here. I find that the trading rules of the agents in this model result in some interesting properties of the simulated log returns.

6.2 Building the model

Where some models may investigate the effect of market microstructure on the price or log return process, my ABM is chiefly focused on trader behaviour. It is concerned with the stylised facts of financial data and explaining them from a trader-behaviour perspective. The ABM does not attempt to create a realistic market microstructure and therefore it may miss out on some explanatory factors of the stylised facts. The agents in the model are built in a way that attempts to mimic realistic features in an extremely simplified fashion.

In my model, as in the minimal model by Alfi et al [144] and in the Lux and Marchesi

model [48], there is just one asset available for trade. Each trader may only buy or sell one unit of the asset at a time, and trading takes place at discrete points in time. At each time step, each trader can buy, sell, or stay inactive. The price is calculated from this information and all trades are executed at this price. The agents do not learn or adapt their strategies during the simulation.

The price update mechanism is multiplicative. After agents express their trade decision, the excess demand D_t is calculated. D_t is defined as the number of buyers minus the number of sellers at time t; $D_t = N_{\text{buy},t} - N_{\text{sell},t}$.

Following other models [135, 136, 144, 147], the price S_t at time t is then generated as a function of the excess demand D_t:

$$S_{t+1} = \left(1 + m\frac{D_t}{N}\right) S_t \tag{6.1}$$

where m is a parameter limiting the largest proportional change in the price in one iteration of the model and N is the total number of traders which is fixed for the entire simulation. The factor $\left(1 + m\frac{D_t}{N}\right)$ will cause the same proportional change in the price whether D_t is positive or negative, so that there is symmetry in the price movements.

One of the parameters that the model is most sensitive to is m. It measures the impact of trading on the price. Since D_t/N is the proportion of traders with the majority opinion (either buy or sell, $-1 \leq D_t/N \leq 1$), m controls how much influence this majority has. When $m < 0$, the price moves in the opposite direction to that indicated by the demand of the agents. When $m = 0$, the price is completely static. When $m > 1$, negative prices would be allowed when all traders want to sell ($D_t/N = -1$). These considerations lead me to constrain $0 < m < 1$.

The wealth of each trader is not recorded. It is assumed they all have infinite wealth and so can always afford to buy shares. They are also given enough shares so that they always own some and therefore always have the option to sell. There is no market-maker and so if there are N_{buy} buyers and N_{sell} sellers at some time t and $N_{\text{buy}} > N_{\text{sell}}$, only N_{sell} of the buyers get to carry out their trade and vice versa. Which traders in the majority group get to trade is decided randomly.

In the sections to follow, the traders in the model are described. It begins very simply and gradually more features are added to find what combination of agent behaviour is necessary to produce the stylised facts of financial data that we are interested in. It eventually has three different types of traders operating in the market. These are noise traders who decide randomly whether to buy or sell with probability based on a certain memory of past price changes, technical traders who analyse historical prices to inform their trades, and fundamental traders who know the "fundamental value" of the stock and

trade accordingly. In the completed model, there are N_1 noise traders with a knowledge of just the most recent price change, N_5 with a memory of the last 5 price changes and N_{21} with a memory of the last 21 price changes. There are N_T technical traders and N_F fundamental traders. There are a total of $N = N_1 + N_5 + N_{21} + N_T + N_F$ agents in the model.

Whether it is realistic to classify all traders as belonging to one of some set of predefined types may seem unlikely due to our experience of a very heterogeneous world. However, a recent paper by Tumminello et al. [151] goes some way to justify this classification by the finding that traders do tend to form discrete clusters which perform trades synchronised in both direction and time.

6.2.1 Noise Traders

The model begins with one type of agent. These are myopic noise traders who base their trading decisions only on the current state of the market and so produce a Markov process. They do not take into account any historical prices.

At each iteration of the model each agent must make two decisions. Each agent first decides whether or not to get involved in trading. As described in Section 5.3, allowing agents to be inactive is critical to the presence of the stylised facts. For example, in the model of Alfi et al [144] described in Section 5.2.6, in an attempt to explain the self-organisation of markets into the intermittent state which produces stylised facts, agents only trade if their personal price signal is greater than a minimum threshold.

The opt-out-of-trading feature is included in my model in the following way. If there was a large price move in either direction in the previous trading period, more agents will get involved in trading in this period, according to a function $\Omega_t = \Omega(R_t)$. Ω_t is the proportion of agents that want to trade after observing the latest proportional price change R_t;

$$R_t = \frac{S_t - S_{t-1}}{S_{t-1}} \tag{6.2}$$

The number that trade at time t is therefore $[N_1\Omega(R_t)]$ where N_1 is the total number of traders with single-period memory and $[\cdot]$ denotes the nearest integer function. Ω_t is given by

$$\Omega_t = d + \frac{1-d}{1+e^{-a(|R_t-c|-b)}} = \frac{1+de^{-a(|R_t-c|-b)}}{1+e^{-a(|R_t-c|-b)}}. \tag{6.3}$$

a, b, c and d are constants. Thus in my model it is a collective decision about the proportion of traders who trade rather than a personal decision by each trader based on a personal idiosyncratic signal. Figure 6.1 shows a graph of this function for a few different parameter selections.

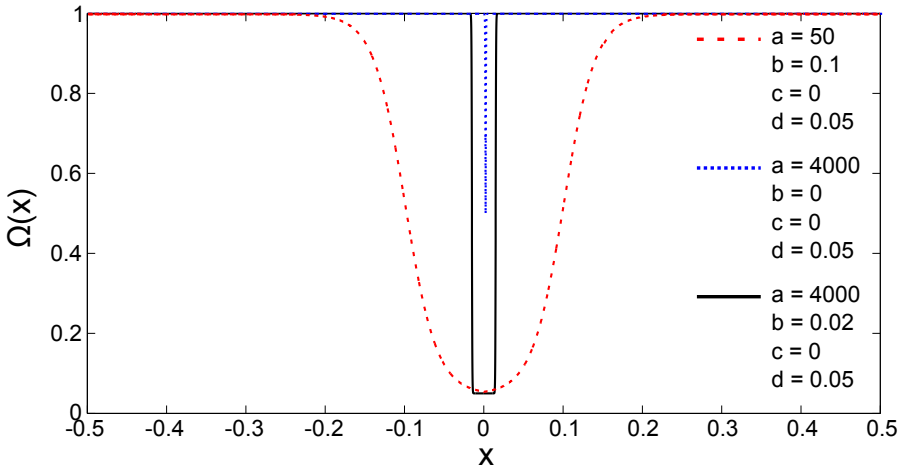

Figure 6.1: Graph of Ω, equation 6.3, the proportion of active traders as a function of the latest proportional price change, shown for various parameter values as indicated on the graph.

The number of agents active in the model is dynamic but is bounded above by the total number of traders N_1 and below by $\left[\frac{1+de^{a(b-c)}}{1+e^{a(b-c)}}N_1\right] \approx [dN_1]$ for the parameter values I will be using. The parameter d, $0 < d < 1$, controls the minimum proportion of agents who are active at any time. Since the number of active traders is rounded to the nearest whole number, it may be 0 if d is small.

The steepness of the function is controlled by a. For higher values of a, Ω_t is more sensitive to the value of R_t. For high a (black line in Figure 6.1), after a large range of the proportional price changes it is either all or a minimum number of the traders who want to trade. For lower a, there is more scope for variations in the number of active traders.

The parameter b controls the width of the interval of values of R_t for which the minimum number of agents trade. For small values of b (dotted blue line in Figure 6.1), there is a very small range of return values for which the minimum number are trading. The width of this range grows with b.

The parameter c gives the location of the minimum of the function. For the simulations it can be set $c > 0$ so that the minimum is located slightly to the right of zero. This means that noise traders are more reactive to small negative price changes than small positive price changes. This seems to be a realistic characteristic but it turns out that the model is not very sensitive to the value of c so long as it is kept within sensible limits.[1]

The minimum number of actively trading noise agents is controlled by d. $d = 1 \implies$

[1] "Sensible limits" means that c should not be so large that the interval of R values for which Ω is a minimum does not contain $R = 0$. If this was the case, many agents would trade when the previous return was 0 but only the minimum would trade after some other nonzero return value.

$\Omega = 1$ for all values of R_t and the number of active noise traders is constant. Since the number of agents trading must be a whole number, the actual number of active traders will be the value $[N_1\Omega]$. This means that if the number of noise traders is small, the minimum number of active traders may be zero at times even though $d > 0$. This has certain consequences which are discussed in more detail in the next chapter.

For the traders now committed to trade, the next decision is whether to buy or sell. Only one share can be traded by each agent at each time step. The decision to buy or sell is made randomly according to a probability distribution based on the previous period's proportional price change. It is a logistic function. Call it P_t. It is the same for each noise trader.

$$P_t = \mathbb{P}[\mathcal{T} = 1|R_t] = \frac{1}{1 + e^{-uR_t}} \tag{6.4}$$

$\mathcal{T}$ is the trading direction, $\mathcal{T} \in \{-1, 1\}$ respectively referring to sell and buy.

$$\mathbb{P}[\mathcal{T} = -1|R_t] = 1 - P_t.$$

For the simulations, this random choice is made by drawing a random number x with uniform distribution, $x \in [0, 1]$, for each trader. This number is then compared with the relevant probability level. If x is less than P_t, the agent will buy. Otherwise he will sell. P_t is shown in Figure 6.2 for various values of the parameter u.

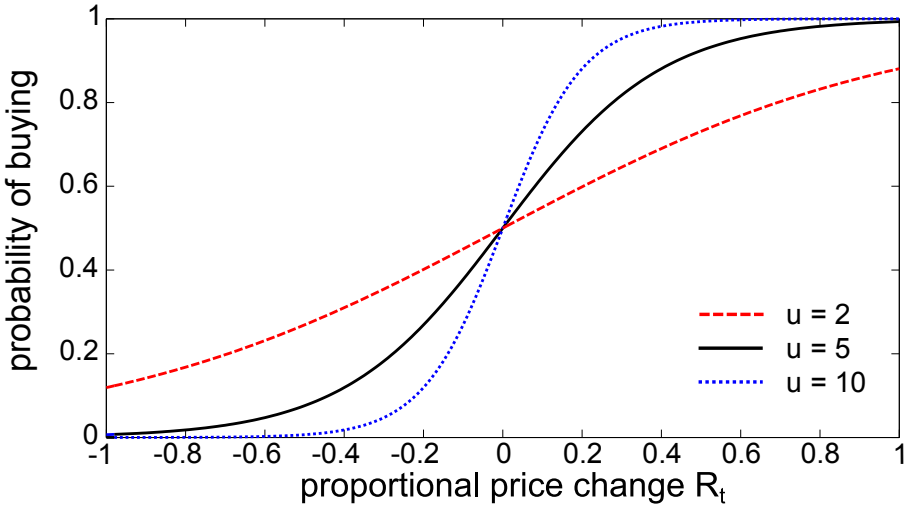

Figure 6.2: Graph of P_t, equation 6.4, the probability of buying.

As can be seen from Figure 6.2, u controls the steepness of the function. It can be interpreted as a "herding strength" parameter. When u is small, P_t is quite flat. This means that the probability of buying will be at its extremes 0 and 1 for only very extreme R_t. This allows for heterogeneity among the noise traders when making their trading choices, so the herding strength is low. When u is large, P_t is steep and so it

reaches its extremes of 0 and 1 for more modest R_t. This means that there is more agreement in the market, or that there is strong herding among the noise traders. This causes high volatility as everyone is trading in the same direction which leads to large jumps in the price.

Having $u < 0$ leads to the counterintuitive situation where noise traders are more likely to buy after observing a negative price move than a positive one. This would amount to having contrarian traders. This could be an interesting option to explore in the future.

If $u = 0$, $P_t = 1/2$ for all values of R_t which makes the noise traders completely ignorant, choosing the direction of their trades by simply tossing a coin. For dynamics which are dependent on the price moves, I set $u > 0$. For small u, the model is more sensitively dependent on the number of each type of trader present. For high u, the price is unstable and leads to an error in MatLab when it reaches very high values. Also when u is large, the generated log returns are strongly correlated. This is because most noise traders in this case agree on which direction to trade, so they will trade in a way which extends the trend and there will be many consecutive log returns of the same sign. This is a state to be avoided as it is not a feature of empirical log returns.

The expected number of agents who want to buy at a time $t+1$, conditional on R_t, is

$$\mathbb{E}_t[N_{\text{buy},t+1}] = N_1 \Omega_t P_t. \tag{6.5}$$

Ω_t is the proportion of active traders at time t, defined in equation 6.3, and $\mathbb{E}_t[\cdot]$ is the expected value evaluated at time t. $\mathbb{E}_t[\cdot]$ is conditioned on the information available at time t, which for these forgetful traders is just R_t. Similarly, the conditional expected number of sellers at time $t+1$ is

$$\mathbb{E}_t[N_{\text{sell},t+1}] = N_1 \Omega_t (1 - P_t). \tag{6.6}$$

The excess demand is $D_t = N_{\text{buy},t} - N_{\text{sell},t}$ and its conditional expected value is

$$\begin{aligned} \mathbb{E}_t[D_{t+1}] &= N_1 \Omega_t \left(P_t - (1 - P_t) \right) \\ &= N_1 \Omega_t \left(\frac{1 - e^{-uR_t}}{1 + e^{-uR_t}} \right) \end{aligned}$$

Now the excess demand D_t gives the next price S_{t+1} by equation 6.1, and so the conditional expected price is:

$$\mathbb{E}_t[S_{t+1}] = \left(1 + m\Omega_t \left(\frac{1 - e^{-uR_t}}{1 + e^{-uR_t}} \right) \right) S_t. \tag{6.7}$$

Now we have an expression for the next expected price completely in terms of the previous two prices. $\mathbb{E}_t[S_{t+1}] = f(S_t, S_{t-1})$ for a function f since $R_t = R_t(S_t, S_{t-1})$. For the sake of brevity, let

$$C_t = \frac{1 - e^{-uR_t}}{1 + e^{-uR_t}}.$$

so that equation 6.7 becomes

$$\mathbb{E}_t[S_{t+1}] = (1 + m\Omega_t C_t)\, S_t. \tag{6.8}$$

Also,

$$\begin{aligned} R_{t+1} &= \frac{S_{t+1} - S_t}{S_t} \\ \implies \mathbb{E}_t[R_{t+1}] &= \frac{(1 + m\Omega_t C_t)S_t - S_t}{S_t} \\ &= m\Omega_t C_t. \end{aligned} \tag{6.9}$$

Note that the above expressions for expected S_{t+1} and R_{t+1} are independent of N_1; in fact the dynamics in the relevant limit of large N are completely described by equation 6.9. These results represent only expected values for the price and proportional price changes. If N_1 is large enough so that the probability $\mathbb{P}[\mathcal{T} = 1]$ could be interpreted as the proportion of traders who choose to buy, then these analytical results would be an accurate description of the simulation results.

Equation 6.8 can be examined to find behaviour for different values of R_t in this large N_1 case. During a bubble period, R_t is large and positive, so $\Omega \approx C \approx 1$. Therefore,

$$S_{t+1} = (1 + m)S_t.$$

The price increases by a factor m, which was defined as the largest possible factor change in the price, as expected.

During a crash period, R_t is large and negative. $\Omega \approx 1$ in this case also, so all agents are getting involved in trading. However, $C_t \approx -1$ for large negative R_t, so

$$S_{t+1} = (1 - m)S_t.$$

and so the price changes by the maximal negative amount allowed as expected.

The dynamics of equation 6.9 can be further simplified by making the approximation

that, for values of R_t close to zero,[2]

$$C_t = \frac{1 - e^{-uR_t}}{1 + e^{-uR_t}} \approx \frac{uR_t}{2 - uR_t} \approx \frac{uR_t}{2}.$$

Then equation 6.9 becomes

$$\mathbb{E}_t[R_{t+1}] = \frac{uR_t}{2} m\Omega_t. \tag{6.10}$$

Fixed points of the dynamics can be found by setting $R_{t+1} = R_t = R_*$. A trivial fixed point is $R_* = 0$. Other fixed points can be found, first assuming $R_* > 0$ (separate values are found for $R_* < 0$ and $R_* > 0$ due to the $|R_t|$ term in Ω, equation 6.3):

$$\begin{aligned}
R_t = R_{t+1} = R_* &= mC_t\Omega_t \\
&\approx \frac{muR_t}{2}\left(d + \frac{1-d}{1 + e^{-a(R_t - b)}}\right) \quad \text{when } R_t \text{ is close to 0} \\
\implies \frac{2}{mu} - d &= \frac{1-d}{1 + e^{-a(R_t - b)}} \\
\implies \frac{(1-d)mu}{2 - dmu} - 1 &= e^{-a(R_t - b)} \\
\implies \ln\left(\frac{mu - 2}{2 - dmu}\right) &= -a(R_t - b) \\
\implies R_* &= -\frac{1}{a}\left(\ln\left(\frac{mu - 2}{2 - dmu}\right)\right) + b
\end{aligned} \tag{6.11}$$

where $c = 0$ in Ω for further simplification[3].

Similarly if $R_* < 0$, it can be found that a fixed point exists at

$$R_* = \frac{1}{a}\left(\ln\left(\frac{mu - 2}{2 - dmu}\right)\right) - b. \tag{6.12}$$

Stability of a fixed point x_* of a function f can be determined mathematically by finding the slope of f around the fixed point. If the slope f' satisfies $|f'(x_*)| < 1$, x_* is a stable fixed point. If $|f'(x_*)| > 1$, the point is unstable. Here we have R_t as a function of $R_{t-1} = R_*$. The derivative is discontinuous due to the presence of the absolute value in Ω_t.

[2] $e^x \approx 1 + x$ if $x \ll 1$.

[3] The parameter c was introduced as it appealed to the intuition that traders are more inclined to react to a negative return than to a positive one of the same size. However, c is small and has no noticeable effect on the results.

It is possible to find the slope using:

$$\frac{d}{dx}|x| = \begin{cases} \operatorname{sgn}(x), & x \neq 0 \\ \text{undefined}, & x = 0 \end{cases}$$

Assuming $R_t \neq 0$ allows the following derivation, still using the $|R_t| \ll 1$ approximation so that $C_t \approx \frac{uR_t}{2}$:

$$\begin{aligned} R_{t+1} &= \frac{muR_t}{2}\left(d + \frac{1-d}{1+e^{-a(R_t-b)}}\right) \\ \frac{dR_{t+1}}{dR_t} &= \frac{mu}{2}\left(d + \frac{1-d}{1+e^{-a(|R_t|-b)}}\right) + \dots \\ &\qquad \dots + \frac{muR_t}{2}\left(-(1-d)\left(1+e^{-a(|R_t|-b)}\right)^{-2}\left(-a\operatorname{sgn}(R_t)e^{-a(|R_t|-b)}\right)\right) \\ &= \frac{mu}{2}\left(\frac{1+e^{-a(|R_t|-b)}\left(1+d(1+e^{-a(|R_t|-b)}) + (1-d)R_t a\operatorname{sgn}(R_t)\right)}{(1+e^{-a(|R_t|-b)})^2}\right) \end{aligned}$$

Inserting the value for the fixed point $R_* > 0$, equation 6.11, after some manipulation leads to

$$\left.\frac{dR_{t+1}}{dR_t}\right|_{R_*} = \frac{(mu-2)^2}{2mu(1-d)^2} + \frac{(mu-2)(2-dmu)}{2mu(1-d)}\left(\frac{(1+d)mu-2}{mu-2} + \ln\left(\frac{mu-2}{2-dmu}\right) + b\right) \tag{6.13}$$

This derivation reveals mu as an important variable. If $mu = 2$ this equation vanishes, meaning that this fixed point R_* is super stable. However, if $mu = 2$, the fixed points R_* of equations 6.11 and 6.12 are located at $\pm\infty$. I later discover that $mu = 2$ gives the most realistic results in the simulated model. The results are reasonably consistent for a range of m and u values, so long as the product mu remains constant.

Adding Memory

Traders who base their decisions on different amounts of historical data are thought to be responsible for some of the stylised facts of empirical data [53]. A first addition to the model is therefore to give some of the traders memory of different lengths. These agents use an average over the last five or 21 steps. Rather than basing their decision on the proportional price change R_t, they use an exponential moving average (EMA)

$$R_{t,n} = w(n)R_t + (1 - w(n))\, R_{t-1,n}. \tag{6.14}$$

The weight $w(n) = \frac{2}{n+1}$ where n is the number of trading periods they remember. These new traders who have some memory are called week and month traders to distinguish them from the original day traders.

$$\text{week traders: } n = 5$$
$$\text{month traders: } n = 21$$

This value $R_{t,n}$ is then used by them in place of R_t in their decisions of whether or not to trade (Ω_t, equation 6.3) and in which direction to trade (P_t, equation 6.4).

I don't expect these noise traders to cause volatility clustering in the log returns resulting from their trades. They are more likely to cause clustering in the direction of trade since a positive price change increases the probability of buying which leads to another positive price change.

So far, the market is populated with unintelligent agents who just trade randomly according to some basic behavioural rules. In the next addition to the model, and following standard practice in many other agent-based models [44, 48, 144], new types of traders are introduced. These are technical traders and fundamental traders. Technical traders or chartists analyse the price history looking for trends while fundamental traders are more concerned with the fundamental profit-generating potential of the company in which they are investing [16, chapter 2].

6.2.2 Technical traders

Technical traders inform their trading choices by indicators from past prices such as moving averages. They use these indicators or signals to attempt to predict future price moves. For example on a price chart, if the moving average of the price crosses over the price it shows that there has been a change in the trend. Technical traders use signals like this as a basis for their trading decisions.

The chartists in the model by Lux and Marchesi [48] are divided into optimists and pessimists. The optimists always buy and the pessimists always sell. They do not analyse historical prices at all. In the Minimal Model by Alfi et al [144], the chartists use a basic moving average of historical prices compared to the current price to identify trends.

The technical traders in my model use a slightly more involved technical analysis of trends in the price in order to make their decisions as this was found to lead to more realistic results. They calculate the Moving Average Convergence Divergence (MACD). Although the aim of this model is to be as simple as possible, the rationale for using this more complicated technique lies in its realism. It also leads to richer dynamics in the results as the traders have a fuller picture of price trends than that afforded by the basic

moving average. Unlike the original noise traders, the technical traders' trading decisions are completely deterministic given the price history.

The MACD technique involves taking two EMAs of the price, A and B, of different lengths l_A and l_B. They then find the difference M_t between these two moving averages. This difference is called the MACD. Then they calculate an EMA of the MACD, s_t, of length l. These steps are described by the following equations:

$$\begin{aligned} A_t =& w(l_A)S_t + (1 - w(l_A))\, A_{t-1} \\ B_t =& w(l_B)S_t + (1 - w(l_B))\, B_{t-1} \\ M_t =& A_t - B_t \\ s_t =& w(l)M_t + (1 - w(l))\, s_{t-1} \end{aligned} \tag{6.15}$$

The weight w depends on the length; $w(x) = \frac{2}{x+1}$. A comparison between the MACD M_t and its EMA s_t indicates trends in the price. If $M_t > s_t$, the price is on an upward trend. If $M_t < s_t$, the price is on a downward trend. If there is a positive trend the technical traders will buy. If there is a negative trend they will sell. These traders amplify any trends they detect.

More explicitly,

$$\begin{aligned} A_t - B_t - s_t > 0 \quad &\rightarrow \quad \text{buy} \\ A_t - B_t - s_t < 0 \quad &\rightarrow \quad \text{sell} \\ A_t - B_t - s_t = 0 \quad &\rightarrow \quad \text{hold} \end{aligned}$$

The technical traders' decision is completely determined by the price history.

This leads to the excess demand by the technical traders:

$$\begin{aligned} D_t =& N_{\text{buy}} - N_{\text{sell}} \\ =& N_T \text{sgn}(A_t - B_t + s_t) \end{aligned}$$

where N_T is the total number of technical traders and $\text{sgn}(x)$ is the sign function given by

$$\text{sgn}(x) := \begin{cases} 1, & x > 0 \\ 0, & x = 0 \\ -1, & x < 0. \end{cases}$$

Therefore, when there are only technical traders operating in the model, the price is

updated according to:

$$\begin{aligned} S_{t+1} &= \left(1 + m\frac{D_t}{N}\right) S_t \\ &= \left(1 + m \cdot \text{sgn}(A_t - B_t + s_t)\right) S_t \end{aligned}$$

There is a problem with having technical traders in the model. The amplification of trends leads the price to either grow to infinity or drop to zero very quickly. All traders also have unlimited buying power and so extremely large prices are a common occurrence. The price can also drop to extremely small values. Because the price update mechanism in this model is multiplicative, there can be no recovery from a zero price. The issue of choosing between a linear and multiplicative price update mechanism is discussed by Alfi et al [125] in the context of their ABM, and it is generally accepted that a multiplicative price is more realistic despite these issues.

Another type of trader is necessary to keep the market reasonably stable. Fundamental traders will fill this role.

6.2.3 Fundamental traders

In order to have fundamental traders in the model, there must first of all be a defined "fundamental value" for the traded asset. In a real trading environment, the fundamental value of a stock can be estimated as the current value of expected future dividend payments. This sort of calculation clearly cannot be performed within this model. Other models which have fundamental traders often set the fundamental value to some constant level for the duration of the simulation [48, 144]. Allowing the fundamental value to vary or giving fundamental traders heterogeneous beliefs may allow for more interesting dynamics [125, 137].

In my model, I let all the fundamental traders agree with each other on what the fundamental value is at any moment. There are two options for the fundamental value, f. It may be fixed to a constant level or it may be set to follow a random walk which is the discrete Euler approximation to GBM:

$$f_t = f_{t-1}\left(1 + \mu_f \Delta t + \sigma_f \epsilon_t\right) \tag{6.16}$$

This is a basic approximation which ignores Itō's calculus. μ_f and σ_f are the mean and variance, and ϵ_t is a random number taken from a standard normal distribution. These are the iterates of a Wiener process. I also set the time steps to $\Delta t = 1$.

The fundamental traders know the fundamental value of the asset. At time t, they compare the price S_t to f_t and decide if the asset represents good value. They will buy

if the price is below the fundamental value and sell if it is above. Their trading strategy pulls the price back towards the fundamental value. They have the opposite effect on prices to the technical traders, and so help to stabilise the market. Like the technical traders, their decisions are deterministic once f_t is known and S_t is revealed. All of the fundamental traders trade in the same direction.

These traders act in response to the relationship between the fundamental value f_t and the price S_t at time t.

$$\begin{aligned} f_t > S_t \quad &\rightarrow \quad \text{buy} \\ f_t < S_t \quad &\rightarrow \quad \text{sell} \\ f_t = S_t \quad &\rightarrow \quad \text{hold} \end{aligned}$$

The demand of the fundamental traders at time t is therefore given by

$$D_t = N_F \text{sgn}(f_t - S_t)$$

where N_F is the total number of fundamental traders in the model.

If these are the only traders in the market, then the new price is

$$\begin{aligned} S_{t+1} &= \left(1 + m\frac{D_t}{N_F}\right) S_t \\ &= \left(1 + m \cdot \text{sgn}(f_t - S_t)\right) S_t \end{aligned}$$

6.2.4 The Complete Model

We now have enough information to put together a system of equations for the model when there are some of each type of agent trading. This will include N_1 noise traders (each with just one-period memory for simplicity), N_T technical traders and N_F fundamental traders. The total number of traders is N, $N = N_1 + N_T + N_F$. The model can be written

as an iterative map with the following coupled equations:

$$
\begin{aligned}
S_{t+1} &= \left(1 + m\frac{D_t}{N}\right) S_t \\
&\text{Noise Traders} \begin{cases} R_{t+1} = \dfrac{S_{t+1} - S_t}{S_t} \\ \Omega_{t+1} = \dfrac{1 + de^{-a(|R_t - c| - b)}}{1 + e^{-a(|R_t - c| - b)}} \\ P_t = \dfrac{1}{1 + e^{-uR_t}} \\ \mathbb{E}[D_{N,t+1}] = N_1 \Omega_{t+1}(2P_t - 1) \end{cases} \\
&\text{Technical Traders} \begin{cases} A_{t+1} = \frac{2}{l_A+1} S_t + \left(1 - \frac{2}{l_A+1}\right) A_t \\ B_{t+1} = \frac{2}{l_B+1} S_t + \left(1 - \frac{2}{l_B+1}\right) B_t \\ s_{t+1} = \frac{2}{l+1}(A_{t+1} - B_{t+1}) + \left(1 - \frac{1}{l+1}\right) s_t \\ D_{T,t+1} = N_T \text{sgn}(A_{t+1} - B_{t+1} + s_{t+1}) \end{cases} \\
&\text{Fundamental Traders} \begin{cases} f_{t+1} = f_t(1 + \mu_f + \sigma_f \epsilon_t) \\ D_{F,t+1} = N_F \text{sgn}(f_t - S_t) \end{cases} \\
\mathbb{E}[D_{t+1}] =& \mathbb{E}[D_{N,t+1}] + D_{T,t+1} + D_{F,t+1}
\end{aligned} \tag{6.17}
$$

This system of equations does not contain any mention of shares or of the personal wealth of the agents. All traders always have the option to both buy and sell, or can be considered infinite in both shareholdings and wealth. Also, in this description of the model, the noise traders all have only a one-period memory (they are all day traders). The equation R_t can be adjusted to $R_{t,n}$ by equation 6.14 to allow for noise traders with longer memory. This map is probabilistic due to the uncertainties coming from the noise traders' probability of buying, P_t, and from the random factor ϵ in the fundamental value f_t.

6.3 Chapter Summary

In this chapter, my new ABM has been developed. The motivation behind this new ABM was to find a very simple model which can reproduce some of the stylised facts of empirical financial time series. This will aid the understanding of the origin of the

stylised facts in empirical data. My ABM is very basic and focuses on trader behaviour rather than market microstructure. So far I have outlined the working elements of the ABM. In the next chapter, the log returns generated by the ABM will be tested for the stylised facts which were found present in the empirical DJIA and Euro Stoxx 50 data which were studied in Chapter 2. I find that the ABM does indeed produce some of the most defining features of financial log return data.

Chapter 7

Results from the Agent Based Model

7.1 Introduction

This chapter contains a discussion of the results obtained from simulating the ABM introduced in the previous chapter. I will first discuss the specifications of the ABM, reviewing the chosen parameter values. The chapter then describes the features of the time series produced by the ABM. Some emergent properties are identified and discussed. The features of leptokurtosis and volatility clustering are especially highlighted and studied in detail. Three ingredients are found to be essential for the production of these stylised facts: the memory of noise traders who make biased random trade decisions, the inclusion of technical traders that trade in line with trends in the price, and the inclusion of fundamental traders who know the "fundamental value" of the stock and trade accordingly. When these three basic types of traders are included, log returns are produced with a leptokurtic distribution and volatility clustering as well as some other statistical features of empirical data.

7.2 Computing Details

The analysis outlined in this chapter involved a lot of computation. I coded my ABM in MatLab. The computer I used for all simulations has the following specification:

- Dell Precision M4600
- Intel(R) Core (TM) i7-2720QM CPU
- 8 GB RAM
- 64-bit operating system

The computation was carried out in MatLab, version R2013a 8.1.0.604 64-bit.

7.3 Model Specifications

The model contains quite a few parameters whose values need to be specified before simulations can begin. The parameter values for each of the defining functions of the ABM are given in Table 7.1. The parameters that the ABM is the most sensitive to are the numbers of the different types of traders who are present in the ABM. Results are presented below for different set-ups of the ABM for which all parameter values are kept constant except for the number of different types of traders. The numbers of each type of trader for the different set-ups are given in Table 7.2.

The parameter m is contained in the price function:

$$S_{t+1} = \left(1 + m\frac{D_t}{N}\right) S_t$$

When m is small, there is little price movement. If fundamental traders are present, the price fluctuates around the fundamental value f. The number of noise traders who get involved in trading is small because the small price movements discourage them from trading through the function Ω. For large m, the price fluctuates wildly and induces an error in MatLab as it approaches numbers too large for the computer. In the mid-range, some more interesting dynamics can occur.

Another influential parameter is u, appearing in the probability of buying, P_t,

$$P_t = \mathbb{P}[\mathcal{T} = 1|R_t] = \frac{1}{1 + e^{-uR_t}}.$$

As was noted in Section 6.2.1, the product mu is more relevant to the dynamics than either m or u alone. I have found that $mu = 2$ leads to the best results.

For a fixed value of m and a varying u, the volatility of the generated log returns increases with u. For higher u, more of the noise traders agree on which direction to trade given the previous price move and so create a large excess demand leading to a large log return.

S	P	Ω				MACD			f	
m	u	a	b	c	d	l_A	l_B	l	μ_f	σ_f
0.4	5	4000	0.02	0.002	0.05	12	26	9	$3 \cdot 10^{-4}$	0.025

Table 7.1: The parameters used for the ABM

model set-up	N_1	N_5	N_{21}	N_T	N_F
Trader Set A	4	4	8	2	2
Trader Set B	0	0	16	2	2
Trader Set C	100	0	0	0	0
Trader Set D	100	100	100	60	60

Table 7.2: The number of the different types of traders in the ABM for the results presented below. N_1, N_5 and N_{21} are noise traders with memories of 1, 5, and 21 times steps respectively.

The proportion of noise traders active at any time is given by Ω,

$$\Omega_t = d + \frac{1-d}{1+e^{-a(|R_t-c|-b)}}.$$

With the parameters used in the simulation given in Table 7.1, Ω is as shown in Figure 7.1 and looks like a step function;

$$\Omega_{\text{step}} = \begin{cases} 1, & |R_t - c| > b \\ d, & |R_t - c| \leq b. \end{cases}$$

There is a sharp transition between proportional price changes after which the minimum number of agents trade and those after which all agents trade.

When the total number of noise traders in the ABM is very small, there is not much scope for different numbers of agents to be active in trading, and so the step function

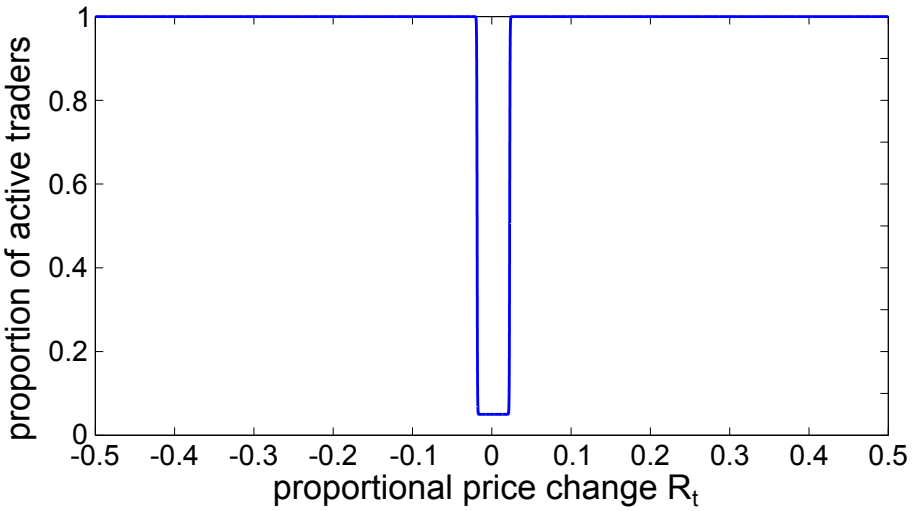

Figure 7.1: Graph of Ω, equation 6.3; $a = 4000, b = 0.02, c = 0.002, d = 0.05$. This is the version of Ω used in simulations of the ABM.

might be sufficient in that case. The form of Ω is important when there are more noise traders in the market, and so the full version of Ω is used in the simulations rather than this basic step function approximation.

The week and month traders use an exponentially weighted moving average of the previous five and 21 trading time periods respectively to inform their trades. A plain unweighted moving average could also be used. The type of moving average employed by the week and month traders has no noticeable effect on the results.

The technical traders employ MACD analysis as described by equations 6.15 given in the previous chapter. They use the lengths l_A, l_B and l given in Table 7.1. These are the standard lengths for this analysis technique.

The fundamental traders know the fundamental value f of the stock. For most of the results presented here this has been set to follow the discrete Euler approximation to GBM and so it takes the form

$$f_{t+1} = f_t(1 + \mu_f + \sigma_f \epsilon_t).$$

The noise terms have a standard normal distribution; $\epsilon_t \sim N(0, 1)$. The drift μ_f and standard deviation σ_f of the fundamental value are given in Table 7.1. These are values used in another model [152] and they have been found to be appropriate here.

A summary of some of the statistical results described below is shown in Table 7.3. Table 7.4 reports the same statistics for computer-generated BM and GBM as well as empirical data from Allied Irish Banks (AIB), DJIA and Exxon Mobil Corporation (XOM) for comparison. The AIB and DJIA data are daily log returns while the XOM log returns are retrieved from the Trades and Quotes (TAQ) database. TAQ is updated with every trade and is extremely high-frequency, often with many prices quoted per second.

	Trader Set A	Trader Set B	Trader Set C	Trader Set D
μ	$1.94 \cdot 10^{-4} \pm 1.97 \cdot 10^{-4}$	$-9.88 \cdot 10^{-6} \pm 2.286 \cdot 10^{-4}$	-0.0074 ± 0.0052	$1.78 \cdot 10^{-5} \pm 2.36 \cdot 10^{-4}$
σ	0.0469 ± 0.0167	0.082 ± 0.0026	0.0833 ± 0.0031	0.0782 ± 0.0013
γ	-1.47 ± 0.897	-0.5385 ± 0.0663	-0.4566 ± 0.0862	-0.4187 ± 0.0277
κ	31.44 ± 35.28	4.6948 ± 0.2507	4.5168 ± 0.2821	4.43 ± 0.120
$H(Z)$	0.365 ± 0.097	0.476 ± 0.0398	0.7544 ± 0.0227	0.3195 ± 0.0279
$H(\lvert Z \rvert)$	0.917 ± 0.023	0.7244 ± 0.0233	0.7312 ± 0.0305	0.5871 ± 0.0292

Table 7.3: Descriptive statistics of the log returns produced by the ABM. The values are reported as $\overline{\mu} \pm \overline{\sigma}$, where $\overline{\mu}$ is the sample mean and $\overline{\sigma}$ is the sample standard deviation. The reported statistics are the mean value μ, the standard deviation σ, the skewness γ, the kurtosis κ, and the Hurst exponent H of both the log returns and their magnitudes. Trader Sets are given in Table 7.2. The results obtained are from 20 runs of the ABM, each of length T=10,000.

	BM	GBM	AIB	DJIA	XOM
μ	$4.421 \cdot 10^{-6} \pm 1.95 \cdot 10^{-4}$	$-2.987 \cdot 10^{-4} \pm 2.36 \cdot 10^{-4}$	$-5.14 \cdot 10^{-4}$	$1.90 \cdot 10^{-4}$	$-1.317 \cdot 10^{-8}$
σ	$0.025 \pm 1.7 \cdot 10^{-4}$	$0.025 \pm 1.87 \cdot 10^{-4}$	0.0368	0.0117	$5.295 \cdot 10^{-5}$
γ	-0.002 ± 0.021	-0.076 ± 0.25	-3.8101	-0.5931	5.7149
κ	2.99 ± 0.038	3.021 ± 0.063	119.7169	27.2784	$1.6892 \cdot 10^{4}$
$H(Z)$	0.482 ± 0.028	0.49 ± 0.038	0.6142	0.5146	0.4517
$H(\|Z\|)$	0.494 ± 0.032	0.485 ± 0.038	0.8890	0.8679	0.8950

Table 7.4: Descriptive statistics of computer-generated and empirical data for comparison with the data generated by the ABM shown in Table 7.3. The statistics for BM and GBM are obtained from 20 samples each of length T=10,000, mean zero and standard deviation 0.025 and are reported as $\overline{\mu} \pm \overline{\sigma}$, where $\overline{\mu}$ is the sample mean and $\overline{\sigma}$ is the sample standard deviation. The statistics have been calculated for the differences of the BM data (due to the presence of negative values) and for the log returns of the GBM and empirical data. The AIB data is daily, 1990-2011. The DJIA data is daily, 1928-2012. The XOM data is TAQ and is for May 2010. The reported statistics are the mean value μ, the standard deviation σ, the skewness γ, the kurtosis κ, and the Hurst exponent H of both the log returns and their magnitudes.

Although the price in the ABM is updated with every trading period, there are different numbers of trades in each period depending on how many active traders there are. This means that the time series produced by the ABM should be comparable to empirical records in physical time (such as AIB and DJIA) rather than trade time (such as XOM).

7.4 Price

Most of the price series produced by the ABM look unrealistic. Examples of generated price time series for different trader sets are depicted in Figure 7.2. I have not found a set of parameter values which produce a realistic price. This is likely due to the unlimited wealth of the traders which is clearly an unrealistic characteristic of the ABM.

The price is bounded below by 0 but is not bounded above. Since the price is multiplicative, when it is on a downward trend it takes smaller negative steps as it gets smaller. When it is on an upward trend, it takes bigger and bigger positive steps until the randomness of the noise traders brings the trend to an end. Setting a limit on wealth would restrict these spikes and may lead to a more realistic price. However, since the ABM is concerned with the features of the log returns rather than the price, this is not a problem.

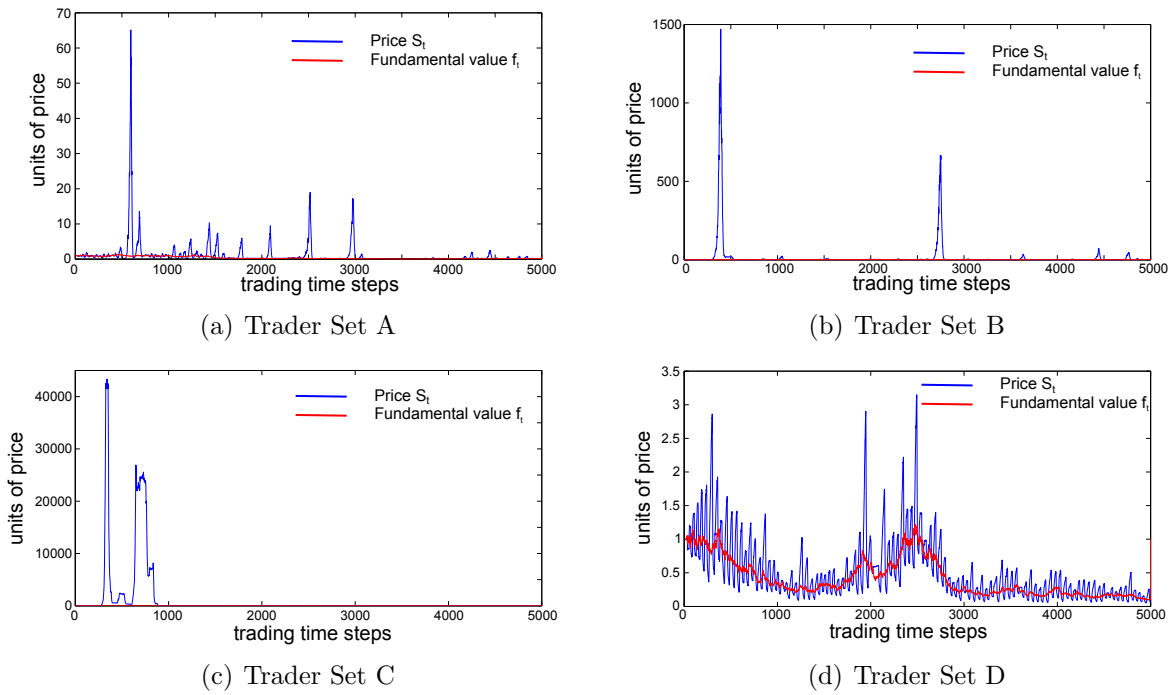

(a) Trader Set A

(b) Trader Set B

(c) Trader Set C

(d) Trader Set D

Figure 7.2: Examples of the price S and fundamental value f generated by the ABM when different numbers of traders are present.

7.5 The Distribution of log returns

Examples of log return time series generated by my model are shown in Figure 7.3. They have been normalised so they have zero mean and unit standard deviation. Figure 7.4 shows the corresponding normalised distributions along with the standard normal for comparison.

The log returns Z produced by the ABM in many different scenarios have been found to be leptokurtically distributed. The model was run many times with different combinations of noise traders without technical or fundamental traders. Different numbers and memory lengths were tested. In each case, the log returns produced had a leptokurtic shape and the Shapiro-Francia test[1] rejected normality at a significance level of 0.1%.

The log returns produced by the ABM when it also includes technical and fundamental traders are also leptokurtic. The distribution of log returns produced in every case is taller and thinner than a Gaussian distribution.

Kurtosis is a measure of how peaked the distribution is. It was defined in Section 2.3 as

$$\kappa = \mathbb{E}\left[\frac{(x-\mu)^4}{\sigma^4}\right]. \tag{7.1}$$

[1]This test is suitable for leptokurtic log returns. It sorts the data into ascending order and finds the correlation between this ordered data and the expected order statistics for data from a normal distribution [153].

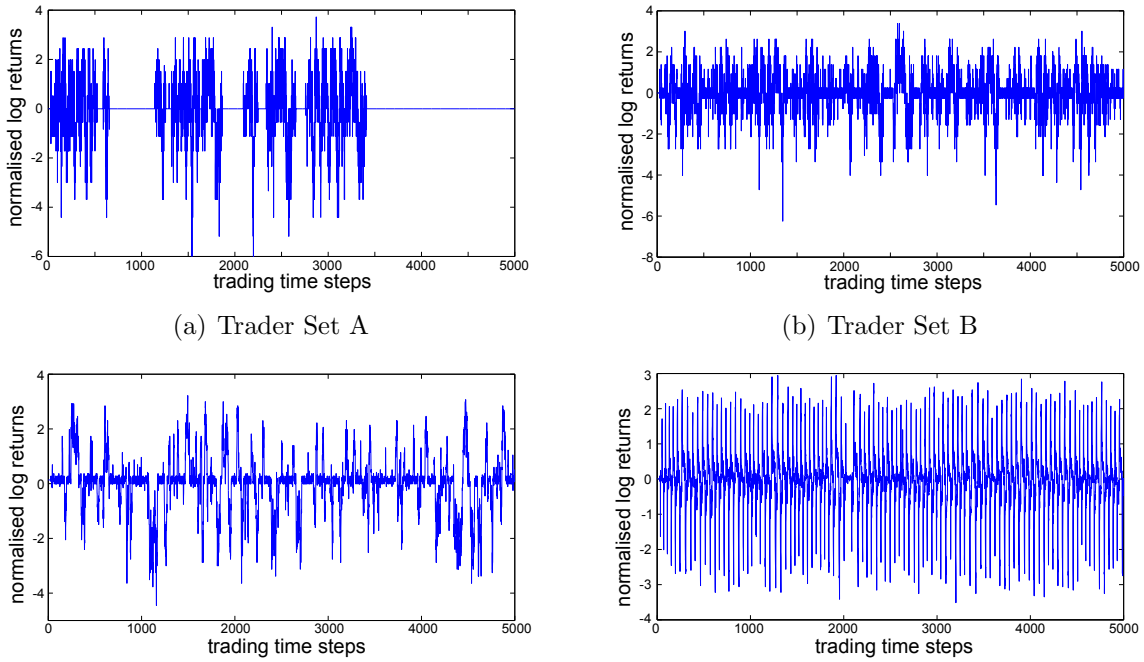

(a) Trader Set A

(b) Trader Set B

(c) Trader Set C

(d) Trader Set D

Figure 7.3: Examples of the log returns produced by the ABM when different numbers of traders are present. They are normalised so are in units of standard deviation.

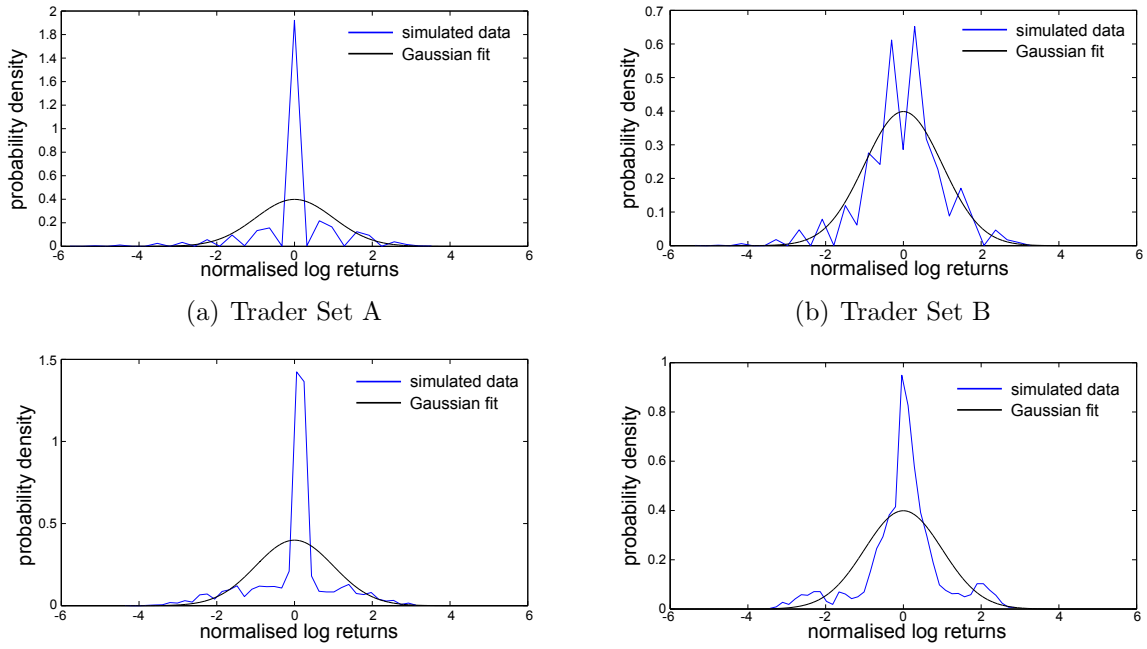

(a) Trader Set A

(b) Trader Set B

(c) Trader Set C

(d) Trader Set D

Figure 7.4: Examples of the distribution of the normalised log returns produced by the ABM when different numbers of traders are present. Each also shows a Gaussian fit for comparison.

For a Gaussian distribution, $\kappa = 3$. The kurtosis of the log returns generated by the ABM are shown in Table 7.3. The kurtosis for all trader combinations is higher than for a Gaussian, but most significantly for Trader Set A. This is due to the many zero log returns produced by this set up of the ABM. These will be discussed below.

The essential feature of the ABM which produces this stylised fact is the function Ω, defined in equation 6.3, and restated again here:

$$\Omega(R_t) = d + \frac{1-d}{1+e^{-a(|R_t-c|-b)}}.$$

This function adjusts the number of active noise traders according to the previous price change. The value of d is critical. If $d = 1$, $\Omega = 1$ and the number of noise traders active in the ABM is constant. Keeping the number of active noise traders at a constant level results in log returns which have a Gaussian distribution. This is the case even when technical and fundamental traders, who are not influenced by Ω, are also present in the ABM. However when the number of active noise traders varies according to Ω with $d < 1$, the log returns have a leptokurtic distribution.

The function Ω mimics realistic trading patterns. In real trading if there is a large price move, perhaps as a result of some news arriving to the market, traders who are normally not very active may be motivated to review their portfolio and make some trades. This leads to more log returns close to zero when these more casual investors are not trading and extreme log returns when everybody wants to trade because they have seen a large price move.

This finding is consistent with other studies which have related the leptokutric distribution of log returns to the varying rate of trading [29, 154–158]. High volatility is related to periods of high trading volume. Since within the ABM each trader can only trade one share at a time, the number of active traders $[\Omega N_N] + N_T + N_F$ is a proxy for volume. The relationship between volume and volatility is discussed in detail in Section 7.8.

Although the ABM produces log returns with a thin-peaked distribution, it does not have the fat tails of empirical data. There are no particularly extreme events. In the examples shown in Figure 7.4, there is no log return further than 6σ from the mean for any of the four time series, each 5000 iterations long. This is less than what is found for empirical data; see for example Table 4.2 which reports on the frequency of different sized log returns in the DJIA and Euro Stoxx 50 data.

Figure 7.5 shows an example of the inverse cumulative distribution for the absolute log returns produced by the ABM. The ones shown are for Trader Set B. Similar results were found for other trader sets. Empirically, as discussed in Section 2.3, log returns are found to have an inverse cumulative distribution whose tail decay can be approximated

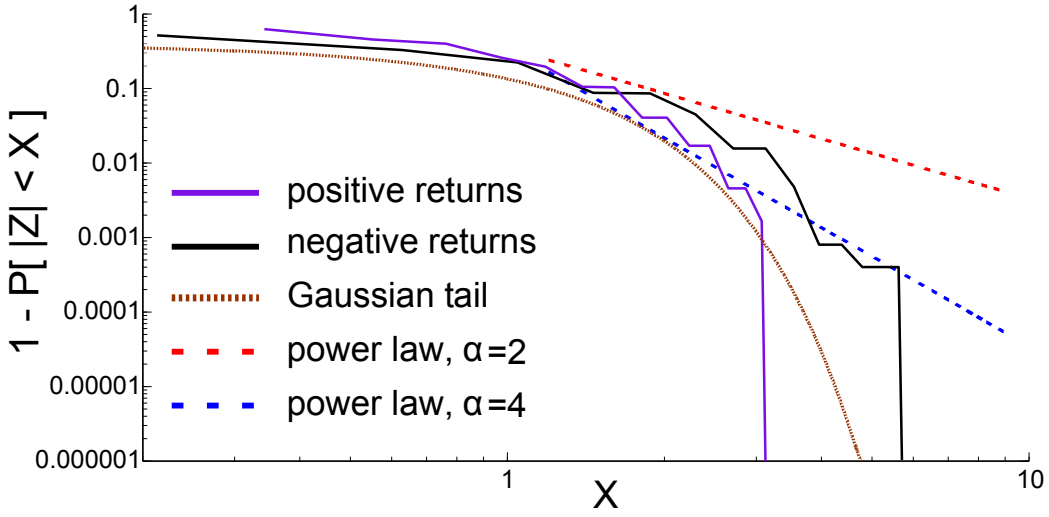

Figure 7.5: Example of the inverse cumulative distribution of the absolute normalised log returns produced by Trader Set B. There is also shown a Gaussian decay and power law lines for comparison.

by a power law with exponent α, $2 < \alpha < 4$ [48]. Power laws with these exponents are shown on the graph along with a Gaussian for comparison. The graph shows that the log returns produced by the ABM do roughly follow a power-law decay for a time but have an abrupt truncation with no extreme events. This can be compared with Figure 2.3 which shows the tail decay for the DJIA and Euro Stoxx 50 data.

The maximum and minimum values of the log returns are limited by the parameter m. However in the simulations, the extreme values set by m are very rarely reached so this limit does not have an undue influence on the truncation of the tails. There is likely not enough heterogeneity amongst the traders in the ABM to allow for extreme events. There are also no information shocks arriving to the market. These are possible areas for extension of the ABM.

The bimodal shape of the distribution for Trader Set B, Figure 7.4(b), is unusual. There are less zero log returns than there are log returns just larger than and smaller than zero. The minimum number of noise traders is responsible for this phenomenon. The minimum number of active noise traders with memory j is very close to $[dN_j]$. For Trader Set B,

$$[dN_j] = [dN_{21}] = [0.05 \cdot 16] = [0.8] = 1.$$

Thus when the minimum number is trading, there is an odd number of traders (5 in this case; one noise trader and two each of the technical and fundamental traders). This means that there will always be a nonzero excess demand and a nonzero log return as a consequence.

This is in contrast to Trader Set A where the minimum number of active noise traders is zero which leads to a zero log return when the technical and fundamental traders are trading in opposite directions and so cancel out each other's demand. This also explains the extended periods of zero log returns seen in Figure 7.3(a) for Trader Set A. When there are no noise traders active, there are just the fundamental and technical traders trading. They usually trade in opposite directions. There are equal numbers of technical and fundamental traders and so the excess demand $D = 0$ which in turn means that the price doesn't change and there is a zero log return.

If the fundamental value follows the approximate GBM process, it continues to fluctuate which will change the trading decision of fundamental traders when it crosses over the price. When this happens, it causes a price change which in turn motivates some more of the noise traders to begin trading again. This is what causes the period of zero log returns caused by Trader Set A to come to an end. If instead the fundamental value is maintained at a constant value, the period of zero log returns will continue to the end of the simulation.

7.6 Uncorrelated log returns

As has been shown before in Section 2.5, empirical financial log returns are not linearly correlated [19, 144] [3, chapter 7]. The price is like a random walk in that the direction of the next price move is not predictable given the price history. The simulation results can be tested for this property.

Figure 7.6 shows that the autocorrelation of the log returns drops close to zero very quickly. The ACF of the log returns for Trader Set A fluctuates away from zero more than for Trader Set B. The prolonged periods of zero log returns which are discussed above in Section 7.5 can be blamed for this fluctuation.

The absolute values of log returns produced by Trader Sets A and B have a much more slowly decaying ACF. This will be discussed in Section 7.7. The log returns themselves will be examined in more detail here.

The ADF test was described in Section 2.5. It tests the hypothesis that a data set is a unit root process. I use it here on the generated price data. Table 7.5 reports on the rejection rate of the unit root null hypothesis H_0 for some time series produced by model simulations with different numbers of traders. For each case the ABM was run twice for a length of 20,000 iterations and the price data divided into sections of length 500 which were all tested separately resulting in 80 tests for each model set-up reported.

The percentage of rejections of H_0 is small for Trader Sets A and B. Trader Sets C and D have bigger rejection rates. The rejection rate is especially high for Trader Set

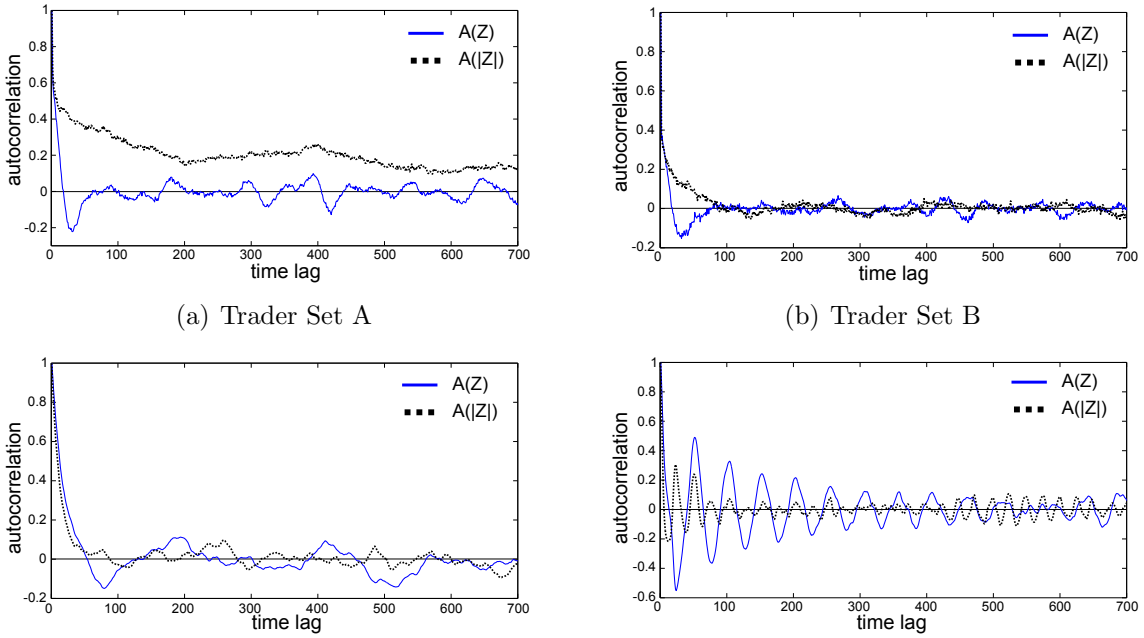

(a) Trader Set A

(b) Trader Set B

(c) Trader Set C

(d) Trader Set D

Figure 7.6: Examples of the ACF of the log returns and their absolute values produced with different numbers of traders in the ABM.

model set-up	S_t	$\ln(S_t)$	Z_t
Trader Set A	3.75%	10%	76%
Trader Set B	3.75%	1.25%	100%
Trader Set C	23.75%	27.5%	100%
Trader Set D	6.25%	2.5%	100%
100 Month Traders only	2.5%	1.25%	100%
20 Technical and 20 Fundamental only	2.5%	6.25	100%

Table 7.5: Out of 80 tests done on price time series of length T=500, this table reports the percentage of the time series produced by different set-ups of the ABM which were rejected as having a unit root by the ADF test. All other parameters for these simulations are as given in Table 7.1.

C. The price generated by Trader Set C is thus shown to be trend-reverting rather than an unpredictable random walk. Trader Set A and Trader Set B have the unit root in the price process which confirms that the log returns are uncorrelated, as are empirical data [48, 19, 126].

The log returns Z_t are expected to be stationary and this is also proved to be true for the results of the ABM by the ADF test. The only log return time series which is not completely rejected as having a unit root is that produced by Trader Set A. This is due to the fact that these log returns have some prolonged periods of $Z_t = 0$. A constant

time series trivially has a unit root since $x_{t+1} = x_t$ means $\rho = 1$ in the regression series described in Section 2.5.

Despite the hopeful results reported for Trader Sets A and B, the unit root hypothesis is rejected a lot more often for longer price series. The ADF test rejects the unit root null hypothesis for longer price data at very small p-values. This means that there is mean-reversion in the simulated data, unlike empirical data. On visual inspection of Figure 7.2 the mean-reversion in the price is obvious. There are sudden huge spikes before the price drops back down. When the price is divided into smaller sections, these spikes do not affect the results so much because there are less of them per tested section.

7.7 Volatility Clustering

With only the original noisy day traders in the ABM, there is no volatility clustering in the simulated log returns. An example is shown in Figure 7.3(c) and the corresponding autocorrelation in Figure 7.6(c). When week and month noisy traders are added, the ACF of the log returns decays more slowly. There is similar decay in the ACF of both the log returns and their magnitudes due to the increased memory of the agents.

Giving some noise traders an even longer memory of 126 time steps (six months' worth of trading days) does not result in volatility clustering either. The memory of the noise traders causes the produced log returns to be correlated. Since log returns in empirical data are uncorrelated [19, 126, 147] as described above, the noise traders alone are found not to produce realistic time series. Many combinations of different numbers and types of noise traders were experimented with. In each case, the log returns produced had some leptokurtosis but no evidence of volatility clusters.

Volatility clustering occurs in the log returns only when technical and fundamental traders are added to the market. Clusters can be identified by eye in Figures 7.3(a) and (b). The volatility clusters produced by the ABM with Trader Set A shown in Figure 7.3(a) are very severe compared with the volatility clusters for empirical data, having prolonged periods of zero log returns. The reason for this was explained above in Section 7.5.

More realistic results are obtained if all of the original noise traders have a month's memory and there are also some technical and fundamental traders operating in the market. This is the case with Trader Set B. Examples of the ACF are shown in Figure 7.6. The magnitudes of log returns generated by Trader Sets A and B are long-term correlated. A slow decay in the ACF of absolute values of log returns is a signature of the volatility clustering that can be seen in Figure 7.3(a) and (b).

The ACF of empirical absolute log returns decays roughly as a power law [44, 147].

Figure 7.7 shows the decay of the autocorrelation for data generated by Trader Sets A and B along with pure power laws for two different set ups of the ABM on doubly logarithmic scales. In both cases, a power law provides a reasonable fit, comparable if not better than the fit to empirical data. Figure 7.7 can be compared with Figure 2.7 which shows the decay for the DJIA and Euro Stoxx 50 log returns. Also see for example Figure 6 in ref. [44].

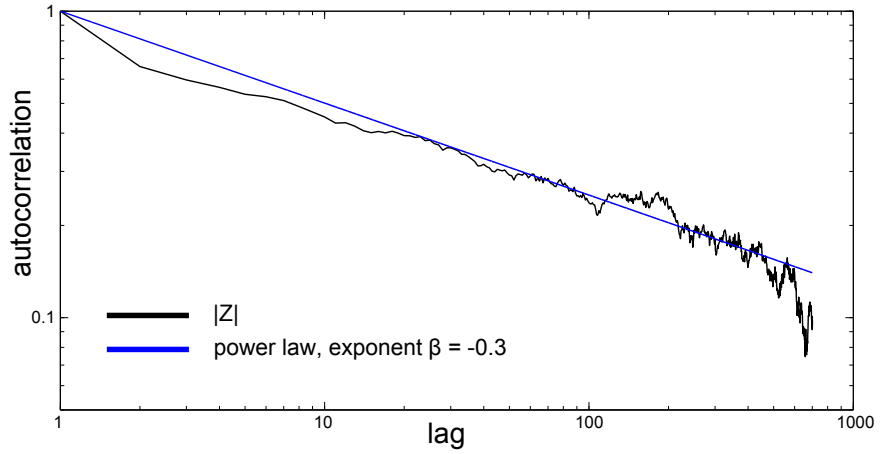

(a) Trader Set A

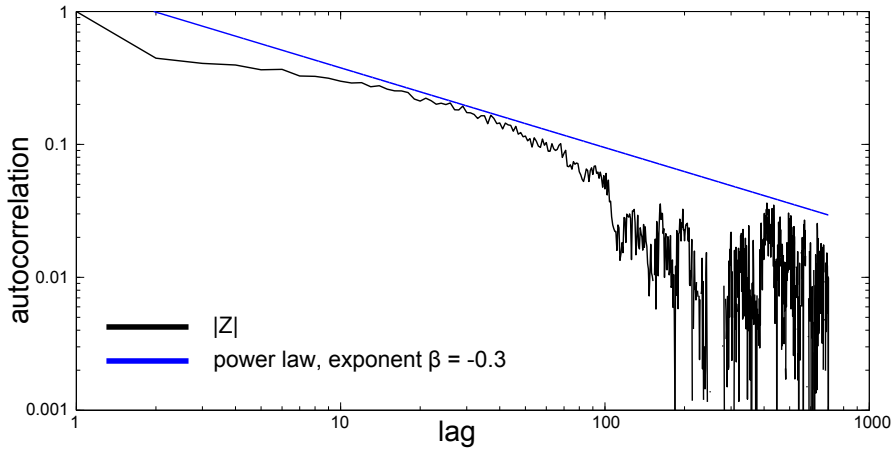

(b) Trader Set B

Figure 7.7: Graphs of the autocorrelation of the absolute log returns generated by the ABM on doubly logarithmic scales. Both are shown with a pure power law for comparison. The power law provides a good fit in both cases.

The technical traders bring memory to the system. However, once there are technical traders, the fundamental traders are an essential addition to keep the ABM stable, so these two factors are impossible to separate. It is reasonable that fundamental traders are necessary to bring an end to the trends instigated by technical traders in a world

where they never believe that a bubble will burst.

The fundamental value crossing over the price triggers the bursts of high volatility. At these moments, the technical and fundamental traders agree with each other and trade in the same direction. There are plenty of noise traders also in the ABM and more of them will get involved in trading after seeing a large price move. This gives the volatility burst some longevity even after the fundamental value has crossed back over the price so that the fundamental and technical traders begin trading in opposite directions again.

If the noise traders are removed from the ABM, the volatility clustering disappears. The interaction between technical and fundamental traders is not enough on its own to create this phenomenon. In the minimal model by Alfi et al [144], volatility clusters are produced by just technical and fundamental traders. In that model agents can switch between trading strategies but that is not possible in my model. The presence of noise traders in my model has a similar effect on the results as the strategy-switching in theirs.

The volatility clustering also disappears for the limit of a large number of agents, and so can be viewed as finite-size effects as in the ABM by Alfi et al [144].

The method of analysis employed by the technical traders also has an impact on the results. If they use a simple moving average of the historical price to compare to the current price as done in the Minimal Model by Alfi et al [144], the volatility clusters do not appear. This confirms that the technical trading strategies are also an essential factor for the creation of volatility clusters in this model.

7.8 The volume-volatility relationship

As mentioned in Section 7.5 in the context of fat tails, it is empirically found that trading volume and volatility are positively correlated [155–158, 147]. The long memory in the volatility of the ABM suggests there may be a similar memory in the volume. In the context of the ABM, the number of active traders at each time t, $N_{active,t} = [\Omega_t N_N] + N_T + N_F$ can be considered a proxy for volume. I have found that the variable $[\Omega_t N_N]$ also has a slowly decaying ACF. An example of the sample ACF is shown in Figure 7.8(a). This graph shows the sample autocorrelation for the total number of active traders N_{active}. Ω_t is the only variable, all other values are fixed for the duration of the simulation.

The long memory in Ω is expected since for day traders it is a function of the absolute value of the proportional price change $|R_t| = \left|\frac{S_t - S_{t-1}}{S_{t-1}}\right|$ which is closely related to the log return Z_t. Ω has even more memory than $|Z_t|$ because for week and month traders it is a function not only of $|R_t|$ but of $R_{t,n}$, a moving average of past values of R_t.

Another possible proxy for the volume is the minimum of the number of buyers and sellers at each iteration of the ABM. G_t=min$(N_{Buy,t}, N_{Sell,t})$ is the number of traders who

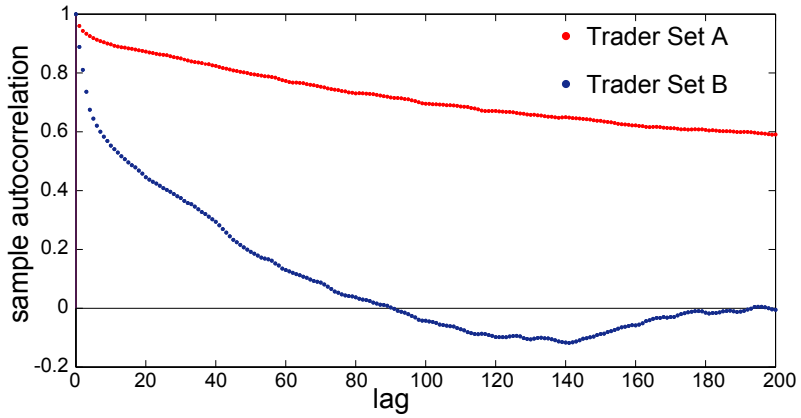

(a) $N_{active,t} = [\Omega_t N_N] + N_T + N_F$

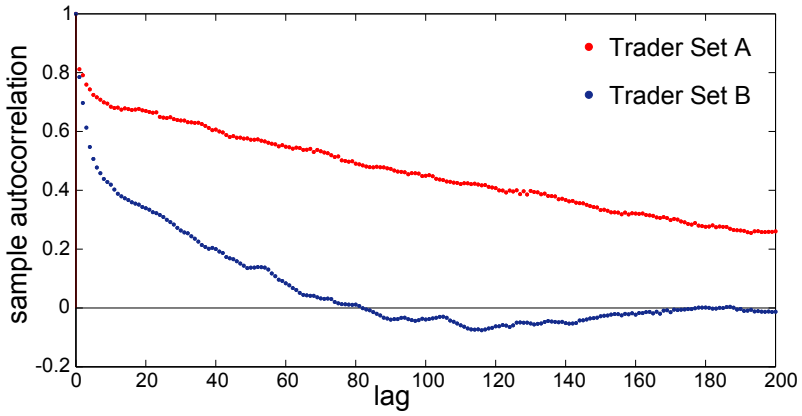

(b) G_t=min$(N_{Buy,t}, N_{Sell,t})$

Figure 7.8: Examples of the graph of the ACF of two proxies for volume for Trader Sets A and B.

actually buy and sell and so this is the number of shares which changes hands during one time step. It also has a long memory as is shown in Figure 7.8(b). Since the price is a function of the excess demand D and not of G, it is expected that the volatility will be less closely related to G than it is to N_{active}. Only Trader Sets A and B are considered here because they produce long correlations in $|Z|$.

Table 7.6 shows the correlation coefficient ρ between the number of active traders N_{active} and the absolute log returns and between the number of trades G and the absolute log returns. $\rho(|Z|, N_{active})$ is quite high for Trader Set A but smaller for Trader Set B. This can be understood by the absence of day traders from Trader Set B. The month traders in Trader Set B are influenced by a moving average of the previous 21 values of R_t which is less directly related to Z_t than R_t itself which is the only input value for Trader Set A. The table also shows that $\rho(|Z|, G)$ is lower than $\rho(|Z|, N_{active})$.

Correlation coefficient values are also shown for Trader Sets C and D but since these

correlation ρ	Trader Set A	Trader Set B	Trader Set C	Trader Set D
$\rho(\|Z\|, N_{active})$	0.7759 ± 0.04	0.4338 ± 0.0166	0.719 ± 0.0154	0.3924 ± 0.0101
$\rho(\|Z\|, G)$	0.6459 ± 0.0529	0.3270 ± 0.0196	0.5277 ± 0.0199	-0.1402 ± 0.0306

Table 7.6: The correlation between N_{active} and $|Z|$ and between G and $|Z|$ for 20 runs of the ABM each with T=10,000. The values are reported as $\overline{\mu} \pm \overline{\sigma}$, where $\overline{\mu}$ is the sample mean and $\overline{\sigma}$ is the sample standard deviation.

sets don't produce other stylised facts, they are not examined in detail.

Figure 7.9 shows both N_{active} and G each plotted against the normalised log returns for examples of simulations with Trader Sets A and B. Table 7.6 shows that the volatility is more closely correlated with N_{active} than with G, but Figure 7.9 gives some insight into the nature of the relationships. These figures show that the relationship is not a simple linear one.

When $|Z| < 2\sigma$, N_{active} appears to take on any permitted value without bias. The same is true of G when $|Z| < 5\sigma$. For larger $|Z|$, N_{active} is on average larger whereas G is on average smaller. The statistics are very small for large $|Z|$ and so it is not possible to infer any conclusions from this result. However similar figures to these resulted from many different simulations and so the results appear to be robust.

These relationships between $|Z|, N_{active}$ and G can be understood as follows. If there is a large $|Z_t|$, $N_{active,t}$ is expected to be large as it depends on $|R_t| \approx |Z_t|$. However, in this case the number of traders with the majority opinion is quite large which necessarily means that $G = \min(N_{Buy}, N_{Sell})$ is small, and so $|Z|$ and G appear to be weakly inversely correlated for large $|Z|$.

This simple analysis confirms N_{active} as a reasonable proxy for trade volume in this model. Its positive correlation with volatility agrees with empirical results for real financial data.

7.9 Hurst Exponent

The Hurst exponent H is a useful measure of the persistence of a time series. $0 < H < 1/2$ indicates that the time series is anti-persistent, so positive values will likely be followed by negative values and vice versa. A Hurst exponent of $1/2 < H < 1$ indicates persistent behaviour, or positive correlation in the time series. If $H = 1/2$, there is no correlation in the data [159].

The average Hurst exponents of the time series produced by the ABM in different set-ups are shown in Table 7.3. For data generated by Trader Sets A and B, the absolute

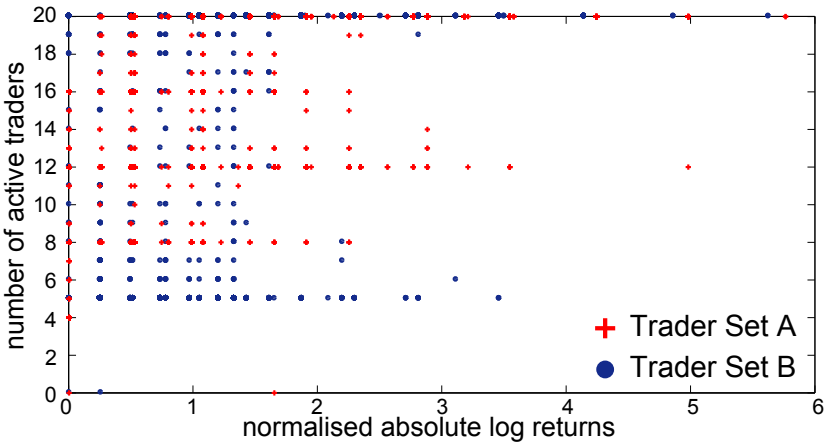

(a) N_{active} vs $|Z|$; $N_{active} = [\Omega_t N_N] + N_T + N_F$

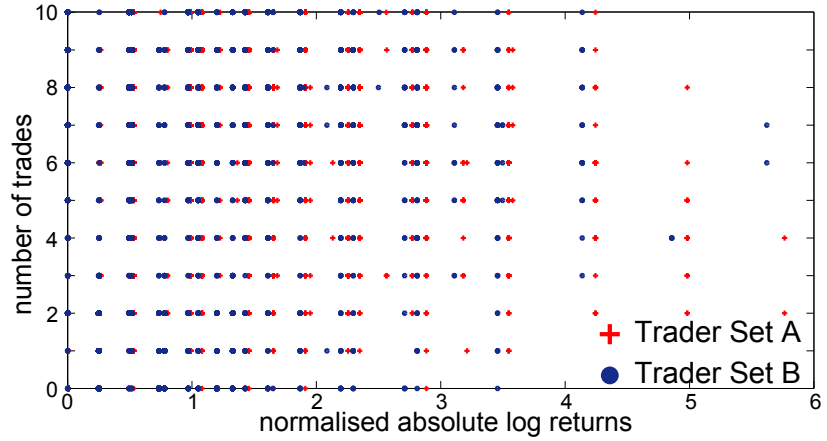

(b) G vs $|Z|$; G=min(N_{Buy}, N_{Sell})

Figure 7.9: Graphs of the number of active traders N_{active} and the number of trades G against the normalised absolute log returns for Trader Sets A and B for a sample data set generated by the ABM.

value of the log returns $|Z|$ have $H > 1/2$ and the log returns Z have $H \approx 1/2$. This is a further indication of volatility clustering as it shows that there is persistence in the magnitudes of log returns whereas the log returns themselves are uncorrelated. It is also consistent with results found for empirical data [160].

7.10 Asymmetry of log returns

Skewness is a measure of the asymmetry of a probability distribution. It is the third central moment of the data, as was defined in Section 2.4:

$$\gamma = \mathbb{E}\left[\frac{(x-\mu)^3}{\sigma^3}\right]. \tag{7.2}$$

The skewness of the log returns produced by the ABM is shown in Table 7.3. The log returns are negatively skewed in all set-ups of the ABM which have been tested and so cannot be ascribed to a particular trading strategy. This is also the case when the parameter c controlling the asymmetry in Ω is set to $c = 0$ and even when $c < 0$ which biases noise traders to be more reactive to positive price moves. For most time series produced by the ABM it is found that the skewness of the price increments ΔS is also negative.

The underlying reason for this negative skew in both the log returns and the price increments remains unclear. It is present for a number of configurations of the initial conditions of the price and fundamental value. Initial conditions have been blamed for skewness in the results of another model [137].

7.11 Aggregational Gaussianity

Another recognised feature of financial data is that as the time lag is increased, the distribution of the log returns begins to more closely resemble a Gaussian [19, 53, 27]. Specifically at long time scales such as annual log returns, the empirical distribution is reasonably fitted by a Gaussian.

Let

$$Z_{t,\Delta} = \log(S_{t+\Delta}) - \log(S_t).$$

So far, the log returns of successive prices ($\Delta = 1$) generated by the ABM have been examined. In order to look for a scale-dependent distribution, log returns at different time scales Δ must be found. If Δ is allowed to increase, the shape of the distribution does indeed change, as is shown in Figure 7.10.

The leptokurtic distribution begins to break down for large Δ. At $\Delta = 10,000$, there is a reasonable fit to a Gaussian distribution within 3σ of the mean, but beyond this the tails are much too fat to be explained by a Gaussian. However, at $\Delta = 100,000$, all values of $Z_{t,\Delta}$ fall roughly on the Gaussian distribution. The results are shown on a semi-log scale to allow for greater visibility of the tails.

The reason for the aggregational Gaussianity lies with the fundamental value f. f

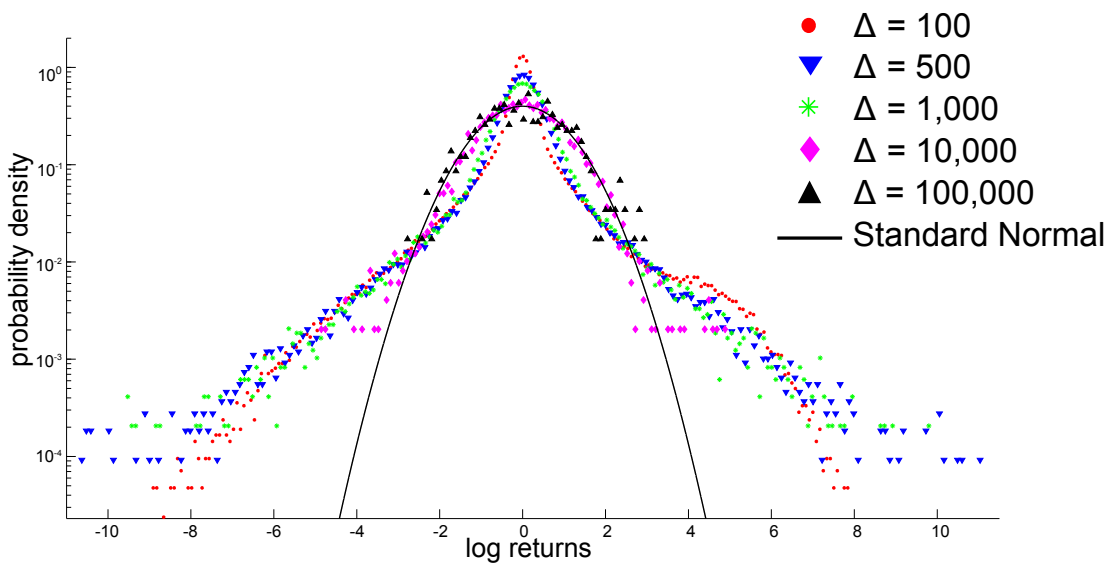

Figure 7.10: Graph of the distribution of normalised log returns $Z_{t,\Delta}$ calculated over different lags Δ for a long simulation ($T = 5 \cdot 10^7$) with Trader Set B and varying f. The solid black line shows a standard normal distribution. The vertical scale is logarithmic.

follows a discrete Euler approximation to GBM;

$$f_t = f_{t-1}(1 + \mu_f + \sigma_f \epsilon_t).$$

Its log returns therefore have a normal distribution. At large Δ, large events become rare and the consistent Gaussian influence of f on the fundamental traders dominates $Z_{t,\Delta}$. At large lags, any short term trends instigated by technical traders are not felt and the shape of the distribution is influenced principally by the fundamental traders.

To confirm that this is the reason for the aggregational Gaussianity, I have carried out the same analysis on log returns generated by the ABM with f set to a constant value for the entire simulation. Figure 7.11 shows the result. Even at large Δ, there is no agreement with a Gaussian distribution in this case. This is because there is no Gaussian influence on any traders and the log returns retain their fat tails. These results are similar to those found by Alfi et al in the analysis of their model [125].

This transition to Gaussianity is in line with what is found in empirical data, and this may indicate that there is some normally distributed variable influencing traders in the market. Many traders use models based on the Gaussian distribution such as the GBM model of stock prices which is the basis for the Black-Scholes-Merton equation discussed in Section 1.6.1. This in turn influences how they trade. There are many other influences on how people trade, such as the arrival of news, which may also produce a Gaussian distribution at large lags. This influence becomes dominant when looking at

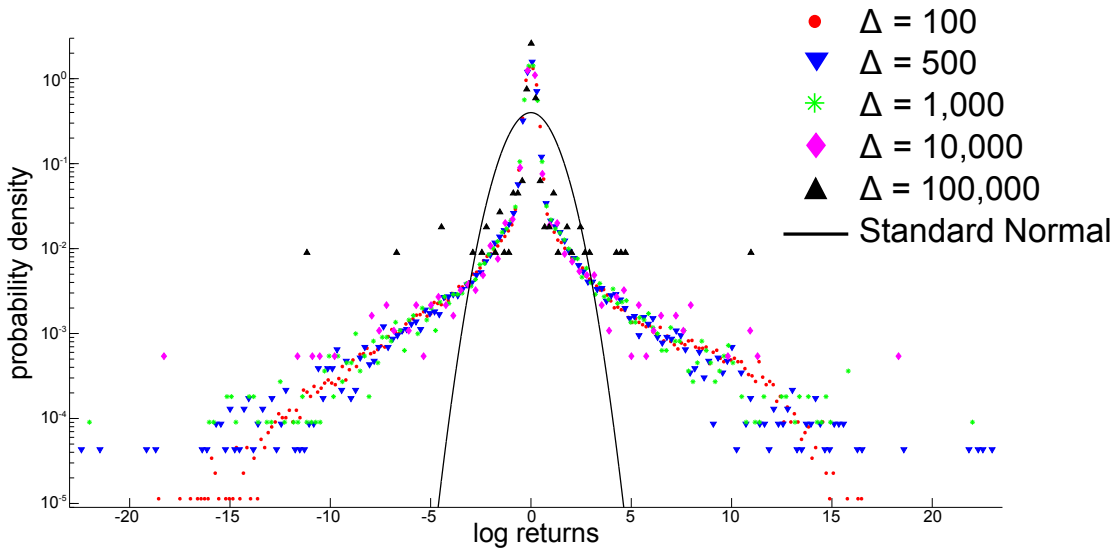

Figure 7.11: Graph of the distribution of normalised log returns $Z_{t,\Delta}$ calculated over different lags Δ for a long simulation ($T = 5 \cdot 10^7$) with Trader Set B and constant f. The solid black line shows a standard normal distribution. The vertical scale is logarithmic.

the distribution of log returns at lower resolution.

7.12 Chapter Summary

This chapter has outlined the main results obtained from the simple agent based model described in Chapter 6. As is the case with many ABMs, useful results are only obtained from this model in a limited area of the parameter space [44, 128]. Specifically, the number of traders is critical. The volatility clustering and non-Gaussian distribution do not feature in the generated log returns when there is a large number of traders. This indicates that these phenomena may be finite size effects. These stylised facts have been attributed to finite size effects in other ABMs [125, 161, 144].

Leptokurtic log returns are generated by the noise traders in the ABM. It has been shown that the varying number of active traders is the source of this feature in the results. This mimics the behaviour of real traders and offers an explanation for the leptokurtosis of empirical log returns.

Volatility clusters come from having some memory in the noise traders along with technical traders who analyse historical prices looking for patterns. Technical traders bring memory to the system as they detect trends and amplify them. If the long-memory noise traders are taken out of the ABM, the volatility clustering also disappears. Neither the technical traders alone nor the memory alone is enough to produce this feature. Both

of these are necessary, and the presence of technical traders necessitates the presence of fundamental traders to keep the price reasonably stable. It is also the fundamental traders who trigger the bursts of high volatility. Three essential ingredients have thus been identified for this model to produce this stylised fact of financial data. The memory of the noise traders, the inclusion of technical traders who trade in line with trends in the price, and the inclusion of fundamental traders who know the "fundamental value" of the stock and trade accordingly are all necessary components.

Transition of the distribution of the log returns to a Gaussian has also been identified as a statistical property of the log returns generated by the ABM. This is caused by the fundamental value and indicates that many real traders may also be under the influence of a GBM process.

Some of the most distinctive stylised facts of financial data have been produced by this model with just a few simple elements, not considering a limit order book or liquidity issues. However I have not yet examined the ABM's generated log returns for multifractal scaling properties. This will be pursued in the next chapter.

Chapter 8

Multifractality in the Model and some Extensions

8.1 Introduction

My motivation to build a new model of the market was to aid understanding of the stylised facts of financial data. I wanted to use the stylised facts as a benchmark for the fitness of the model. An examination of the model outputs for multifractality is therefore warranted.

In this chapter, I examine the log returns produced by my ABM for multifractality. First of all, some ABMs from the literature which have been shown to generate multifractal log returns are reviewed. Log returns generated by my new ABM are then tested for multifractality via MF-DFA. A couple of extensions to the model are also explored. This work can help to uncover the origin of multifractality in empirical data from the perspective of trader behaviour.

8.2 The Literature

I have found that not many agent-based models have had their generated log returns analysed for multifractality. However some have been found to produce time series with multifractal properties. A few of them are briefly reviewed here.

The ABM by Zhou and Sornette [162] based on the Ising model has been shown to produce multifractal time series. Each agent is connected to a number of others and these connections change in time to mimic human learning. Each agent makes trade decisions based on their expectation of their neighbours' decisions, external news and a random personal preference which changes in time. The price does not impact on traders'

decisions at all.

The model has two regimes. In the "boundedly rational" regime, agents become less likely to imitate others if they see that the news has been a good predictor and will instead trust the news and vice versa. In the "irrational" regime, the opposite is the case. Agents become more likely to imitate others when the news has been a good predictor. Agents trust that the crowd will come up with the best strategy.

The authors find that only the irrational regime produces the stylised facts of fat tails, aggregational Gaussianity and long memory in the absolute values of log returns [162]. They also find hallmarks of multiscaling in the relaxation of volatility in the log returns from a local peak, but do not discuss their origins.

Multifractality is also found in a version of the Cont-Bouchaud percolation model [149, 163, 128]. This model consists of an $L \times L$ lattice. Each site is occupied with probability p. For $p > p_c$ for some critical value p_c, infinite clusters of occupied sites appear which span the full width of the lattice. Sites are viewed as individual traders and clusters as groups of traders who all trade in the same direction. In this market a single asset is available for trade. At each time step, a cluster can buy with probability a, sell with probability a or stay inactive with probability $1 - 2a$. For $1/L^2 \ll a \ll 1/2$, the model is found to produce multifractal results.

This lattice model is not particularly helpful in identifying the source of multifractality in the real trade environment. It is difficult to identify the value of the parameter a with anything measurable in the actual marketplace. It could perhaps be related to traders' risk-aversion.

In the ABM by Thompson [77], agents submit either limit or market buy or sell orders to a continuous double auction order book[1]. Market orders are filled immediately at the best available price. Limit orders are queued and filled in the order of best-price-first. The price p of new limit orders are decided randomly according to

$$\begin{aligned} \text{sell:} \quad & p = b(t) + |\epsilon| \\ \text{buy:} \quad & p = a(t) - |\epsilon| \end{aligned}$$

where $b(t)$ is the highest bid price at time t and $a(t)$ is the lowest ask price at time t. The distribution of the random factor ϵ determines the multifractal properties of the resulting time series. When ϵ has heavy tails the price varies more wildly, there is volatility clustering in the log returns and a multifractal spectrum is found.

Thompson [77] concludes that the multifractality is a result of the double auction

[1]It is a double auction because buyers bid for the stock and sellers submit ask prices for the stock at the same time.

order book structure combined with informed agents who make decisions based on publicly available information. He also finds that the different strategies of technical and fundamental traders substantially affect the multifractal properties of the results.

The model by Thompson [77] is probably the most helpful of the three described here in explaining the origin of multifractality in empirical log returns. The double auction order book and public information are both realistic features of his model. The real world is of course much more complex and much work is still to be done in this area.

8.3 Multifractality in the ABM

The new ABM presented in Chapter 6 contains only a few different types of trader trading shares in a single asset and yet is capable of producing log returns with some realistic characteristics such as leptokurtosis and volatility clustering with a certain set of parameter values. Now I will examine the outputs of this model for signs of multifractal scaling. Some sample generated log returns are tested for multifractality via the method of MF-DFA. I will also examine log returns produced by the ABM with two different extensions.

8.3.1 The Original Model

The Trader Sets used in the model are restated in Table 8.1. When the model is simulated with Trader Set A, there are too many zeroes in the generated log return data to perform the MF-DFA analysis. The same problem arises as was encountered with the Euro Stoxx 50 data explained in Section 4.3.1. The MF-DFA procedure divides the data into segments ν of size s for varying s. When a segment ν is small enough to lie within an interval of constant value, the value $F(\nu)$ assigned by MF-DFA to that box is very small. Since the intervals of consecutive zeroes are even longer in the log returns produced by Trader Set A than in the Euro Stoxx 50 case, MF-DFA cannot be used. For a typical simulation with Trader Set A, the range of admissible segment sizes s covers less than one order of magnitude and so cannot give reliable information about any scaling which may be present.

MF-DFA can be used on the log returns generated by Trader Set B. Figure 8.1 shows the plots $\log(F_q)$ against $\log(s)$ along with their respective local slopes for a sample of log returns generated by Trader Set B. The time series used for this analysis have length 10000. For all values of q except $q = -10$, the slopes consistently decrease with increasing segment size s. Because the slopes decrease rather than oscillate about a constant value, we can conclude that multifractal scaling is not present in this data.

The analysis for a sample set of log return data generated by the ABM with Trader Set C is shown in Figure 8.2. There is no multifractal structure in the sample log returns examined here either. The slopes shown are all consistently decreasing except that for $q = -10$ which first increases and then decreases with s. The curvature in the local slopes shown in Figure 8.2(b) betray a lack of scaling.

The results of MF-DFA on a sample simulation of the ABM with Trader Set D are shown in Figure 8.3. This figure may reveal some scaling within the region $100 \leq s \leq 1000$ for $q < 10$. In this region, the slopes show little dependence on q, meaning that any scaling here may be mono- rather than multifractal. The multifractal spectrum for data produced by the ABM with Trader Set D often has a twist at the top, revealing non-monotonic dependence of the slope $h(q)$ on q. A twist in the top of the spectrum has previously been related to abrupt events in the data [101]. However the data produced by Trader Set D does not have any abrupt or extreme events. The twist may be connected to the monofractality (rather than multifractality) of the data. For exactly monofractal data, $h(q)$ is independent of q. In random data like those we're dealing with here, there may be some slight q dependence even for monofractal time series [82].

It is difficult to confirm the scaling properties since each simulation of the ABM gives a different result. The value $F(\nu, s)$ assigned by MF-DFA to each portion of the data is now a random variable, changing with each new simulation of the model. This also means that we cannot discount the possibility that the ABM may generate log returns with multifractal scaling during some simulation. However I have found that the model outputs are generally not multifractal.

For some random fractals, it may be reasonable to take an average of many realisations in order to unveil the scaling properties of the generating process [74]. However, for the structures under consideration here, the multifractality may well be due to temporal correlations. Averaging would destroy the correlations present in each separate model output. The averaging technique is therefore not suitable for studying the scaling of time series whose multifractal structure is due to correlations.

The result for Trader Set B is especially interesting. These log returns have been

model set-up	N_1	N_5	N_{21}	N_T	N_F
Trader Set A	4	4	8	2	2
Trader Set B	0	0	16	2	2
Trader Set C	100	0	0	0	0
Trader Set D	100	100	100	60	60

Table 8.1: The numbers of the different types of trader used in the model.

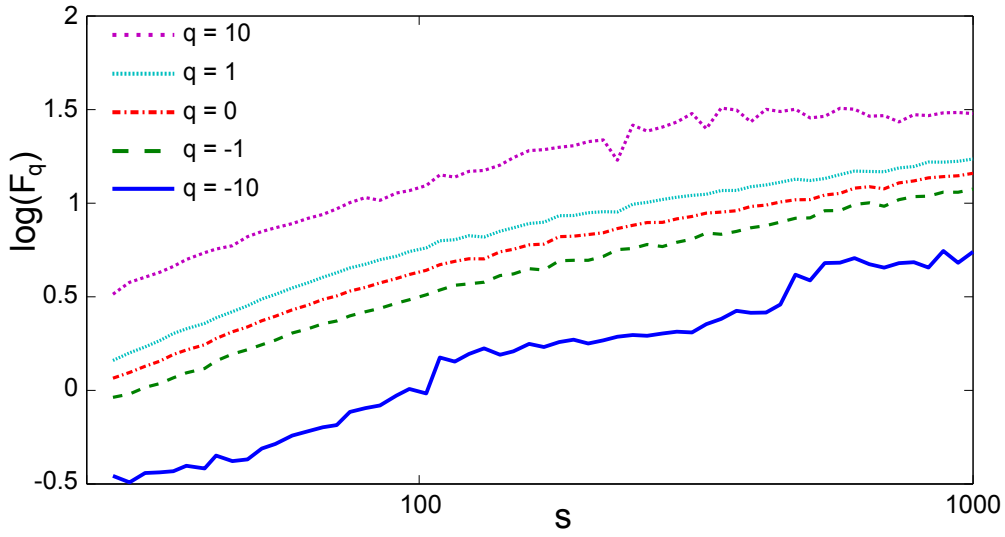

(a) Graph of $\log(F_q)$ versus $\log(s)$ for the values of q given on the graph.

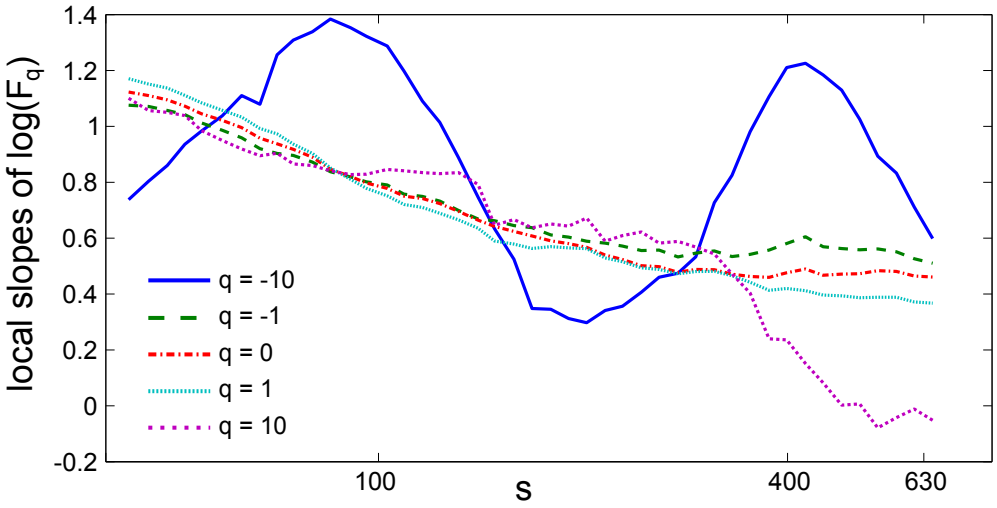

(b) Graph of the local slopes of $\log(F_q)$ calculated over a moving window of 15 points.

Figure 8.1: Results of the MF-DFA analysis carried out on data generated by the original ABM with Trader Set B. This data does not have any scaling.

shown to be characterised by fat tails, very short autocorrelation decay time as well as long memory in their volatility. As discussed in Section 4.3.2, a fat-tailed distribution and long memory are considered to be the two sources of multifractality in time series [82, 103, 88]. Despite these hallmarks being present, these log returns do not have multifractal scaling. It was shown in Section 7.5 that the distribution of log returns generated by Trader Set B have a rather abrupt truncation, unlike empirical data whose distribution has very long tails. It could be that although the log returns have a thin-peaked distribution, there are not enough extreme events to admit the property of multifractal scaling.

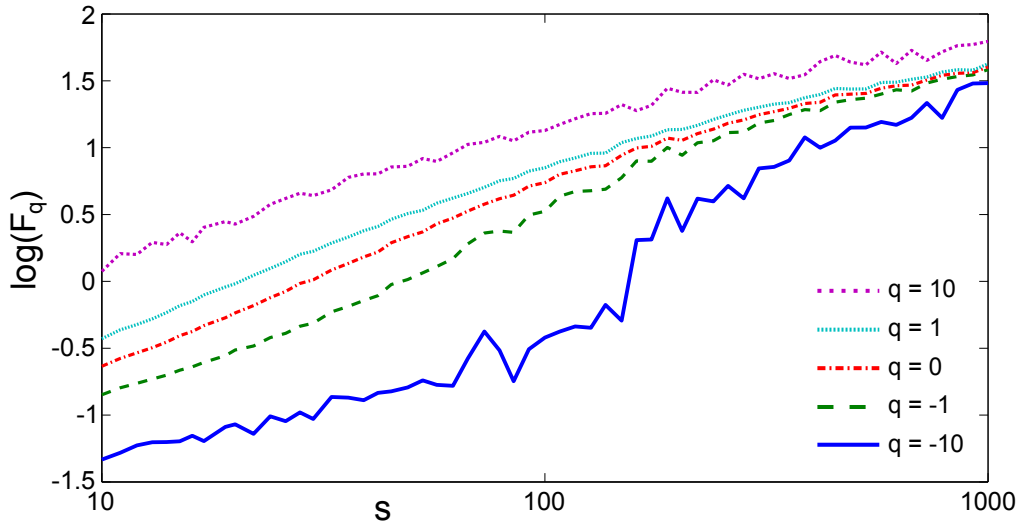

(a) Graph of $\log(F_q)$ versus $\log(s)$ for the values of q given on the graph.

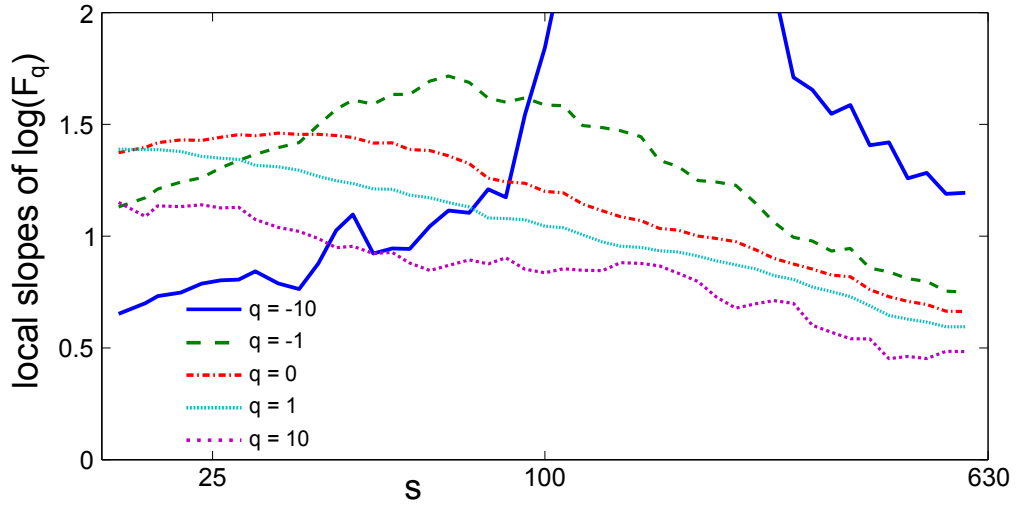

(b) Graph of the local slopes of $\log(F_q)$ calculated over a moving window of 15 points.

Figure 8.2: Results of the MF-DFA analysis carried out on data generated by the original ABM with Trader Set C. This data does not have any scaling.

In light of the fact that the original ABM as described in Chapter 6 does not generate time series with multifractal scaling, it seems reasonable to discuss next some options for extension of the model which may potentially lead to multifractal log return time series.

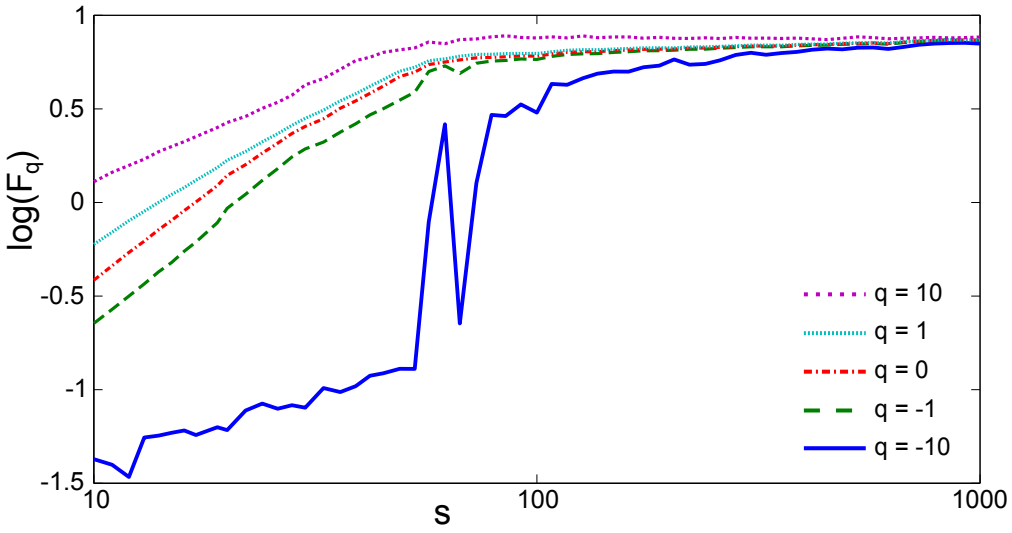

(a) Graph of $\log(F_q)$ versus $\log(s)$ for the values of q given on the graph.

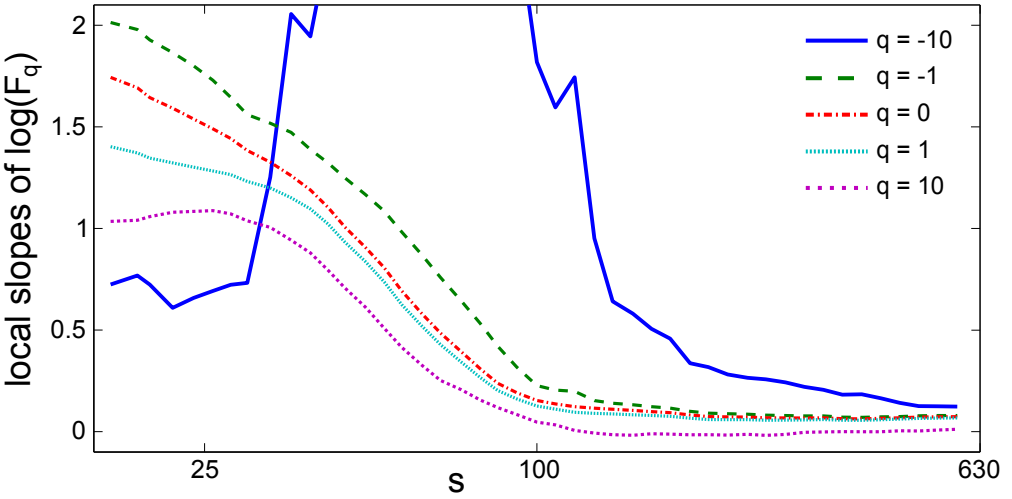

(b) Graph of the local slopes of $\log(F_q)$ calculated over a moving window of 15 points.

Figure 8.3: Results of the MF-DFA analysis carried out on data generated by the original ABM with Trader Set D.

8.3.2 First extension - heterogeneous investment horizons

One of the possible shortfalls of the ABM is that there is very little heterogeneity in the investment horizons of the traders. In the ABM, most traders trade on every iteration. Although some noise traders may not trade in a given time step, they can potentially all trade at the same time. And for the technical and fundamental traders the option to opt out of trading is very restricted. The technical traders don't trade if the MACD and its moving average are equal. The fundamental traders don't trade if the price and the fundamental value are equal. In the reality of the simulation, neither of these events ever happen and so all technical and fundamental traders are active in every time step.

We know that the reality of trading is very different. As emphasised by the Fractal Market Hypothesis [164], traders have a large number of different investment horizons and information has different effects on traders depending on each one's investment horizon. For example, the announcement of a new product by a company may be very significant to a short-term technical trader but is of little consequence to a long-term fundamental trader. Heterogeneous trading times are thought responsible for stylised facts of empirical data [53].

A basic way to bring this concept into the model is to give each type of agent a different time scale on which they are allowed to trade. The ABM can be adjusted so that the day traders trade on every iteration of the model, week traders every 5 iterations and month traders every 21 iterations (count each iteration as a day and there are no weekends or holidays in the model). Technical traders are generally short-term traders and so they will continue to trade on every iteration. Fundamental traders should have a longer investment horizon and so I allow them to trade only once every 100 iterations.

The results produced by the ABM with this change to trading horizons are shown in Figures 8.4 and 8.5 for Trader Sets A and B. In both cases the volatility clustering is lost. The spikes in the ACF for Trader Set B shown in Figure 8.5(b) occur every 21 steps because the month traders are trading only once every 21 days and they are dominant in this set. The log returns might look more realistic if each month trader picked a different day of the month on which to trade.

When these log return data are analysed with MF-DFA, the plots of $\log(F_q)$ versus $\log(s)$ seem to indicate some scaling for the region $100 \leq s \leq 1000$. The scaling results for Trader Set A are shown in Figure 8.6. The results for Trader Set B are in Figure 8.7. For both sets of these simulated log returns we encounter intervals of constant log returns with lengths up to 100. This explains the drop in $\log(F_q)$ for $q < 0$ at $s \approx 100$.

It is possible to produce part of the multifractal spectrum for the scaling region $100 \leq s \leq 1000$ for simulation results with both Trader Set A and B. These are shown in Figure 8.8 for 10 separate simulation results of the ABM for both Trader Set A and B.

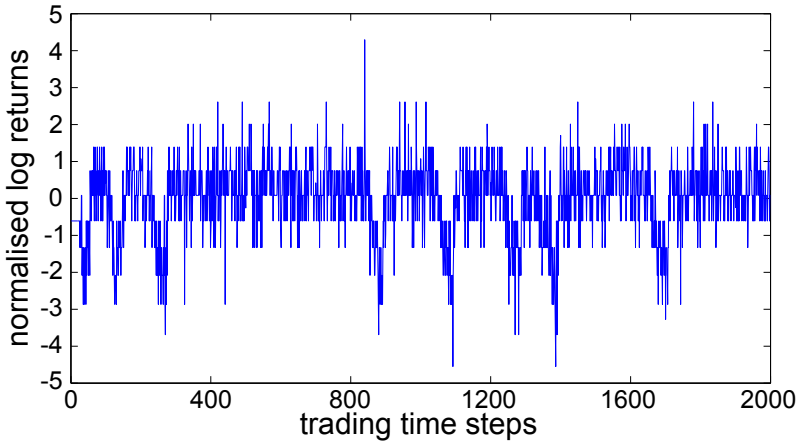

(a) Log returns

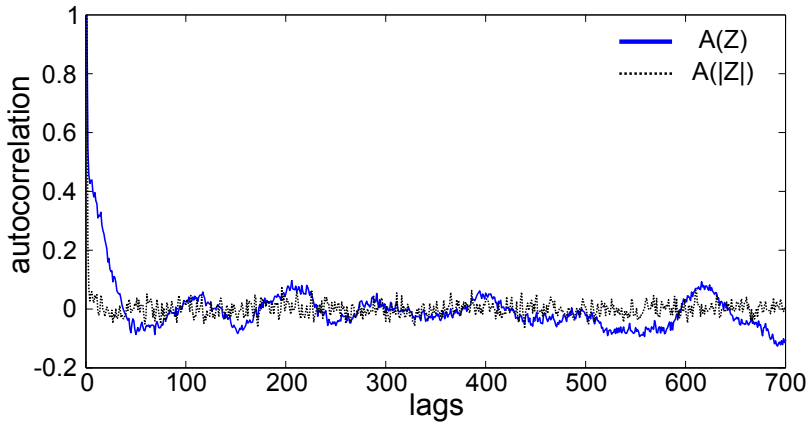

(b) ACF

Figure 8.4: (a) Log returns and (b) autocorrelation function generated by the ABM with heterogeneous trading times; Trader Set A.

There is a lack of extreme events in this data, meaning that the areas of high F, revealed by $q > 0$, are rare. This means that only the right side of the spectra could be generated with any accuracy. Those shown in Figure 8.8 for both Trader Set A and B are for $q < 0$ only. The right side is generated by $q < 0$ and reveals the scaling exponents for areas of small F, or log returns relatively close to the average, which are plentiful in these time series. Though the scaling is not found in the areas of large F, these log return time series can be described as multifractal. This type of situation was referred to in Section 3.4.3.

For each set of log returns generated by the model for both Trader Set A and B, the right side of the multifractal spectra are well-behaved. As prescribed by the MF-DFA method, the spectra all have their maxima at $f(\alpha(0)) = 1$. This value is the dimension of the underlying support of the multifractals, which are assumed to be straight lines by MF-DFA.

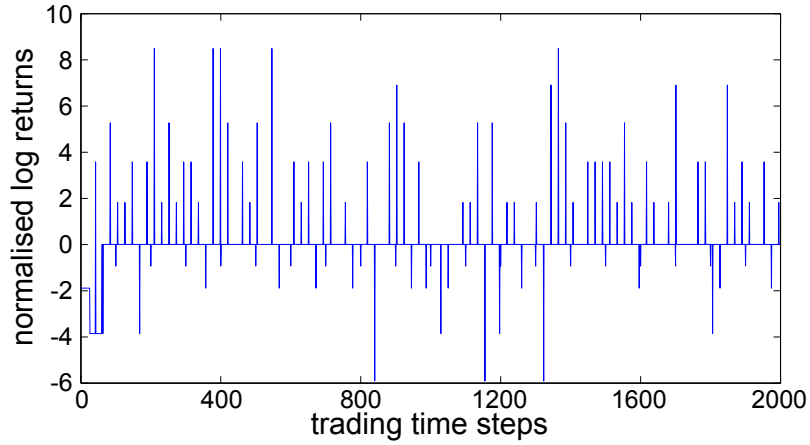

(a) Log returns

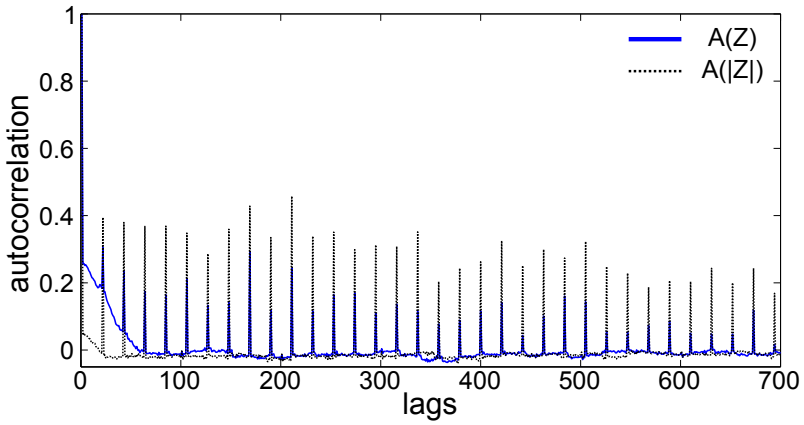

(b) ACF

Figure 8.5: (a) Log returns and (b) autocorrelation function generated by the ABM with heterogeneous trading times; Trader Set B.

Most of the spectra shown in Figure 8.8 have significant areas of $f(\alpha) < 0$ for large α. This is called the latent part and was also found in the spectrum for the Euro Stoxx 50 data in Section 4.3.1. This has been noted as a potential feature of random multifractals which is not found for deterministic multifractals [165]. The existence of a latent part betrays a breakdown in the scaling for areas of very small F which are revealed by $q \ll 0$.

The very negative $f(\alpha)$ can be traced back to how the generalised Hurst exponent $h(q)$ varies with q. From the equations in Step 11 in Section 3.4.1, I find that

$$f(\alpha) = q^2 \frac{dh(q)}{dq} + 1.$$

$f(\alpha) < 0$ therefore implies that

$$\frac{dh(q)}{dq} < -\frac{1}{q^2}. \tag{8.1}$$

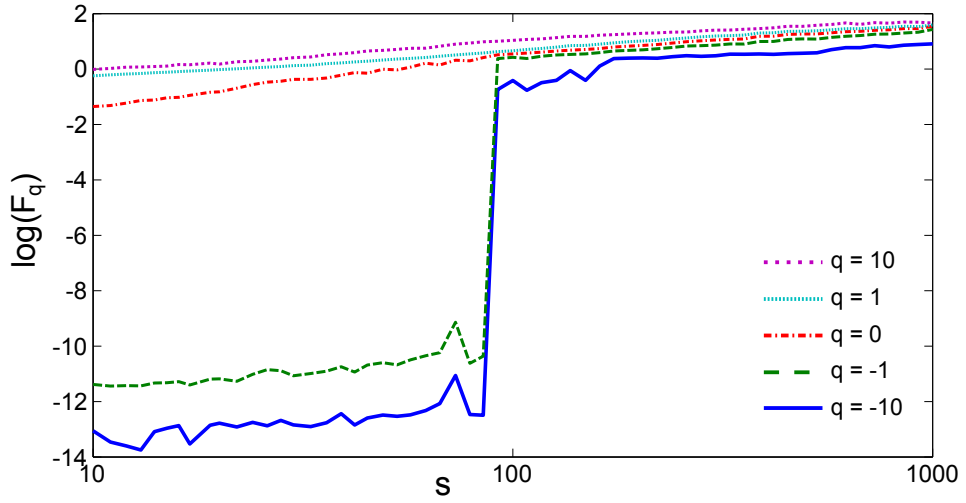

(a) Graph of $\log(F_q)$ versus s for the values of q given on the graph.

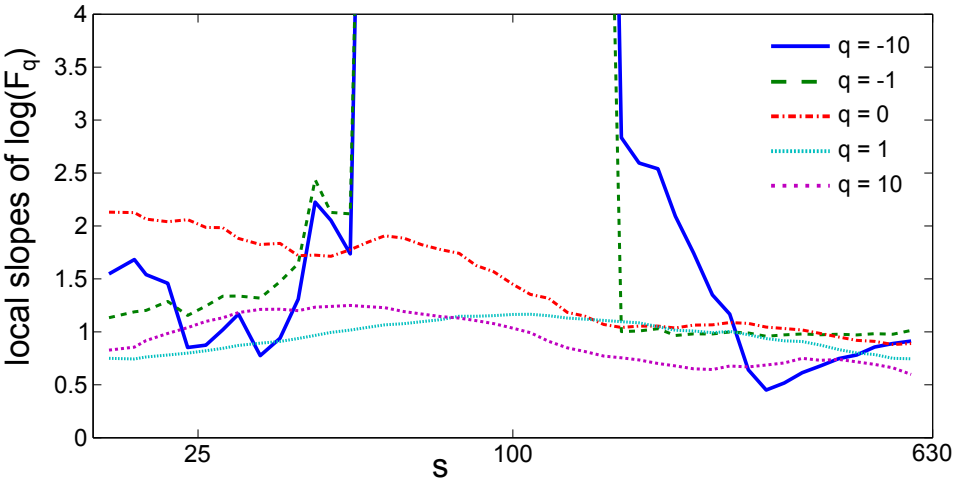

(b) Graph of the local slopes of $\log(F_q)$ calculated over a moving window of 15 points.

Figure 8.6: Results of the MF-DFA analysis carried out on data generated by the ABM with heterogeneous trading times; Trader Set A.

I have found that for the log returns produced by the ABM, the slopes $h(q)$ change much more sharply with q than for the empirical data examined in Chapter 4. It is intuitive for $h(q)$ to be sensitively dependent on q for small $|q|$ and much less so for large $|q|$. There is no point in using values of q for which $\frac{dh(q)}{dq} \approx 0$, as all the scaling is revealed by values of q closer to 0 for which $\frac{dh(q)}{dq} \lneq 0$. For the data generated by this version of the ABM, the inequality 8.1 holds for large negative q. Since for these time series only the right sides of the spectra are meaningful, I have not checked if the inequality holds for large positive q.

The shapes of the (right sides of the) spectra for this version of the ABM produced by Trader Set A more closely resemble those of the empirical DJIA and Euro Stoxx 50

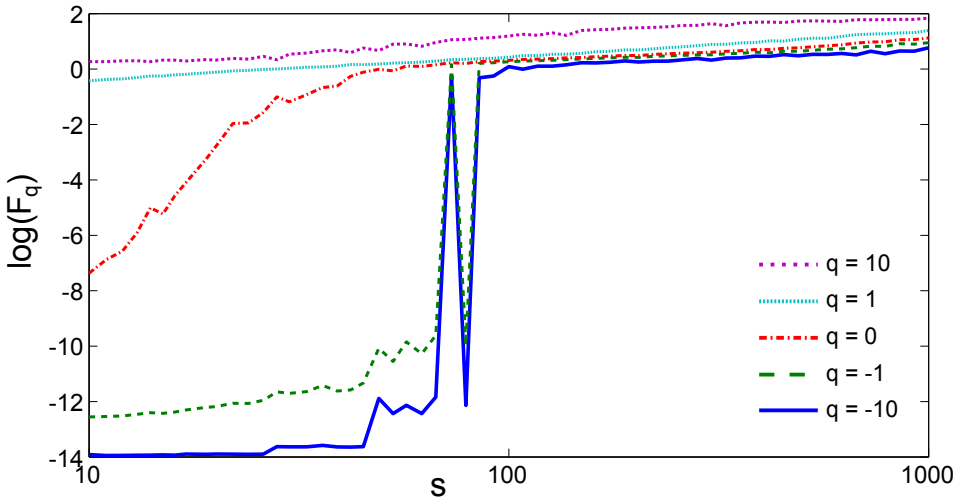

(a) Graph of $\log(F_q)$ versus s for the values of q given on the graph.

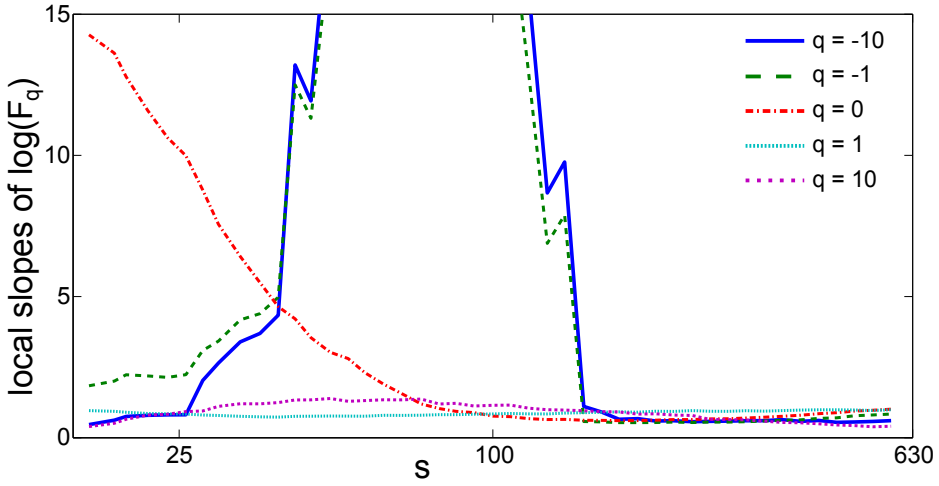

(b) Graph of the local slopes of $\log(F_q)$ calculated over a moving window of 15 points.

Figure 8.7: Results of the MF-DFA analysis carried out on data generated by the ABM with heterogeneous trading times; Trader Set B.

time series examined in Chapter 4 than those produced by Trader Set B. In the case with Trader Set A shown in Figure 8.8(a), $\alpha_{max} \approx 1.3$. (Here I have defined α_{max} by $f(\alpha_{max}) = 0$ where $f(\alpha)$ is decreasing.) This value is just slightly larger than the value of α_{max} found for DJIA and Euro Stoxx 50; see Table 4.1. However, for Trader Set B shown in Figure 8.8(b), the value is much larger; $\alpha_{max} \approx 2.2$. This larger value of α_{max} means that there is more variation in the slopes $h(q)$ of the $\log(F_q)$ versus $\log(s)$ plots which in turn is due to wide variation in the log returns. The log returns produced by this version of the ABM with Trader Set B have much higher kurtosis ($\kappa \approx 21$) than those produced by Trader Set A ($\kappa \approx 3$). This could explain the larger α_{max}. However this does not

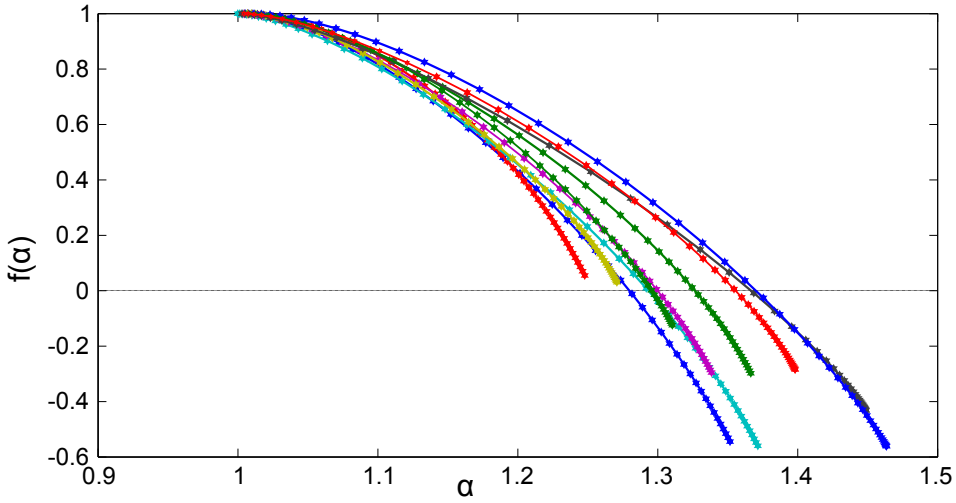

(a) Graph of $f(\alpha)$ versus α, $q < 0$, for 10 separate simulation results of the ABM with heterogeneous trading times; Trader Set A.

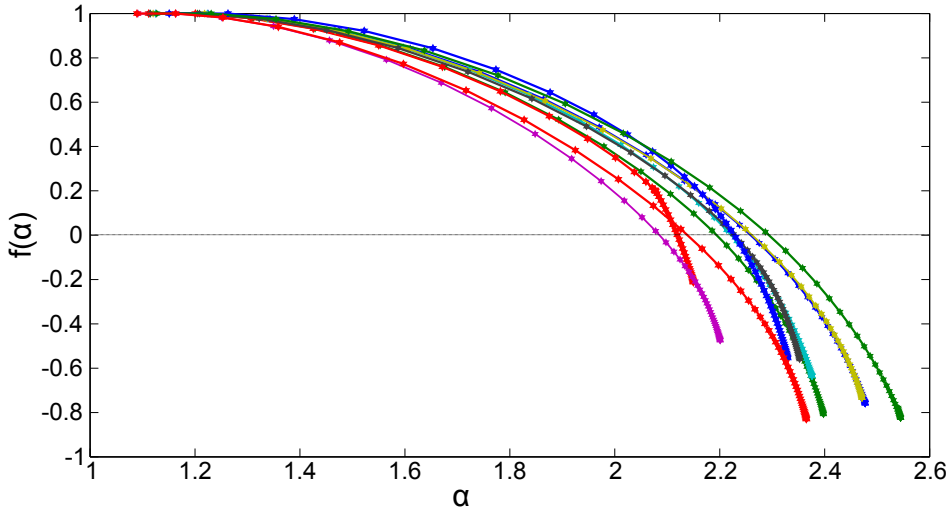

(b) Graph of $f(\alpha)$ versus α, $q < 0$, for 10 separate simulation results of the ABM with heterogeneous trading times; Trader Set B.

Figure 8.8: The right side of the multifractal spectra for 10 separate simulations of the ABM with heterogeneous trading times. There is some limited multifractal scaling in the log returns produced by this version of the model. The scaling does not follow through to areas of high F which are revealed by $q > 0$.

explain why α_{max} in this case is so much larger than α_{max} for the DJIA case which has similar kurtosis; see Table 2.1.

It is very interesting that this data displays some level of multifractal scaling. These log returns have been shown to be lacking other stylised facts of financial data such as fat tails and volatility clustering. It may be tempting to conclude from this result

that the generally accepted causes of multifractality in time series data of a fat-tailed distribution and temporal correlations [82] are not necessary for multifractal scaling to be present. However there may be some temporal correlations in these log returns which are not obviously apparent in the way volatility clustering is. The data would need further testing by means of shuffling as was done in Section 4.3.2 before any such conclusion could be drawn.

8.3.3 Second extension - heterogeneous beliefs

Another possible area for increased heterogeneity in the ABM involves the fundamental value. As it stands, the fundamental traders all agree on what the fundamental value of the stock is and so they all trade in the same direction at each iteration of the model. They sell if the price is higher than the fundamental value and buy if it is less.

Intuitively, it seems more realistic that different fundamental traders who analyse available information about a company and combine it with what they know about the economy in general may arrive at different conclusions about the correct fundamental value of the stock. There is a version of the Grand Canonical Minority Game in which each fundamental trader is given a different fundamental value with which to compare the price in order to make their trade decision [137]. This makes the stylised facts in that model more robust to any parameter changes.

Although those authors do not examine the output of their model for multifractality, this form of heterogeneity can be added to my ABM and its effect examined. Because this extension only affects the fundamental traders, results are shown in Figure 8.9 of a simulation run with Trader Set D in which there are many of this trader type. The price oscillates as the number of fundamental traders agreeing to buy or sell fluctuates. Volatility clustering and a leptokurtic distribution are not characteristics of these log returns.

The results of the MF-DFA analysis are shown in Figure 8.10 for various values of q. These plots reveal that there is scaling over one order of magnitude, $100 \leq s \leq 1000$. There is also some evidence of a crossover in this data. A crossover is a point where the slopes change on the graph of $\log(F_q)$ versus $\log(s)$. It can be seen in Figure 8.10 that the slopes of $\log(F_q)$ appear constant (except for $q = -10$) for $s < 100$ although different from the slopes for $s > 100$. This indicates a potential crossover point at $s = 100$. Multiscaling Multifractal Analysis [166], an extension to the MF-DFA method, has recently been recommended as a way to pick up information from any crossovers that might be in the data. However in this chapter I only consider the scaling for $s > 100$.

As is shown in Figure 8.9, there are very few log returns close to zero produced by this version of the ABM. Areas assigned a small value of F by MF-DFA will therefore

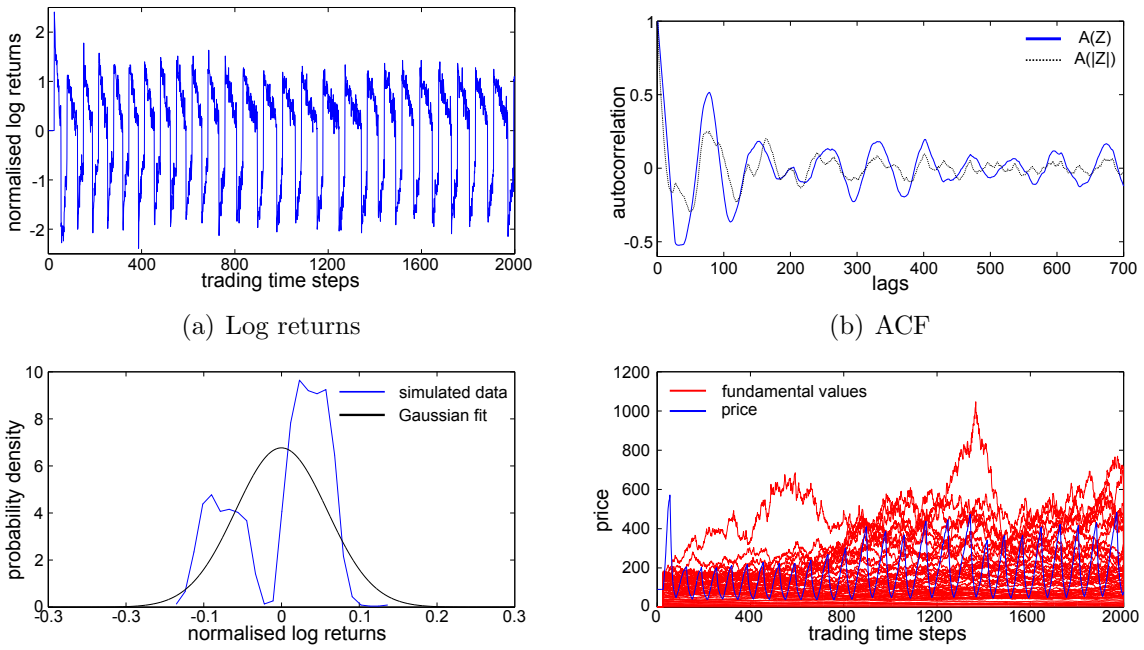

(a) Log returns

(b) ACF

(c) Distribution

(d) Price and fundamental values

Figure 8.9: An example of the time series generated by the model when each fundamental trader has his own fundamental value with which to compare the price; Trader Set D.

be rare in this data. It can therefore be expected that the right side of the multifractal spectrum may be poorly defined as this is the side which shows the scaling exponents for areas of small F in the time series. The spectra for 10 separate simulation results are shown in Figure 8.11. As predicted, the left side of the spectra are quite well defined whereas the right side is more likely to be stretched out. The stretch is due to the rarity of areas of small F in the time series. This is opposite to the situation encountered for all other spectra presented in this thesis where the lack of extreme events has led to an ill-defined left side.

Again as expected, all the spectra coincide at the point $f(\alpha(0)) = 1$. They have on average $\alpha_{min} \approx 0.9$ which is larger than the corresponding value for the empirical DJIA and Euro Stoxx 50 data reported in Table 4.1. (I define α_{min} by $f(\alpha_{min}) = 0$ where $f(\alpha)$ is increasing.) The value for α_{max} cannot be reliably calculated in this case.

Further analysis of the simulation results of my ABM and employing longer simulation lengths leads to an average $f(\alpha)$ spectrum as shown with error bars in Figure 8.12. This graph shows an $f(\alpha)$ which is the average of 20 $f(\alpha)$ spectra constructed for 20 separate simulations of the ABM. Each simulation had length 20,000. The error bars show the standard deviation in α and $f(\alpha)$ over those 20 separate results of the MF-DFA analysis. As expected, the right side of the spectrum ($q < 0$) is stretched out and the deviations

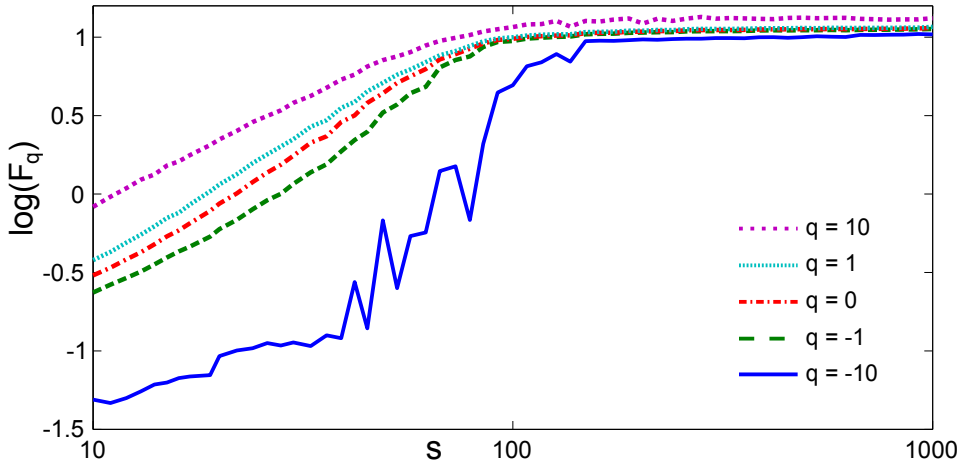

(a) Graph of $\log(F_q)$ versus s for the values of q given on the graph.

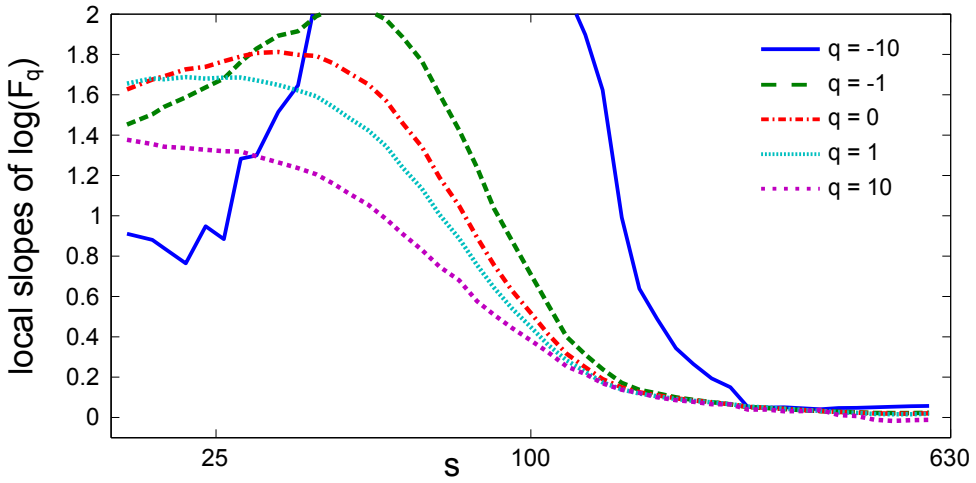

(b) Graph of the local slopes of $\log(F_q)$ calculated over a moving window of 15 points.

Figure 8.10: Results of the MF-DFA analysis carried out on data generated by the ABM with heterogeneous fundamental values; Trader Set D.

on that side are much larger than on the left. Even when averaging over more and longer simulations, the spectra show no evidence of converging. The areas of small F are too rare in the data for any scaling laws to become apparent among them. The twist in the top of the average $f(\alpha)$ spectrum comes from averaging over many spectra, some of which have unusual behaviour such as $f(\alpha) > 1$ for $q < 0$. This shows that the right sides of these spectra are completely unreliable to base any conclusions on about scaling in the small F areas of the log return data generated by this version of the ABM.

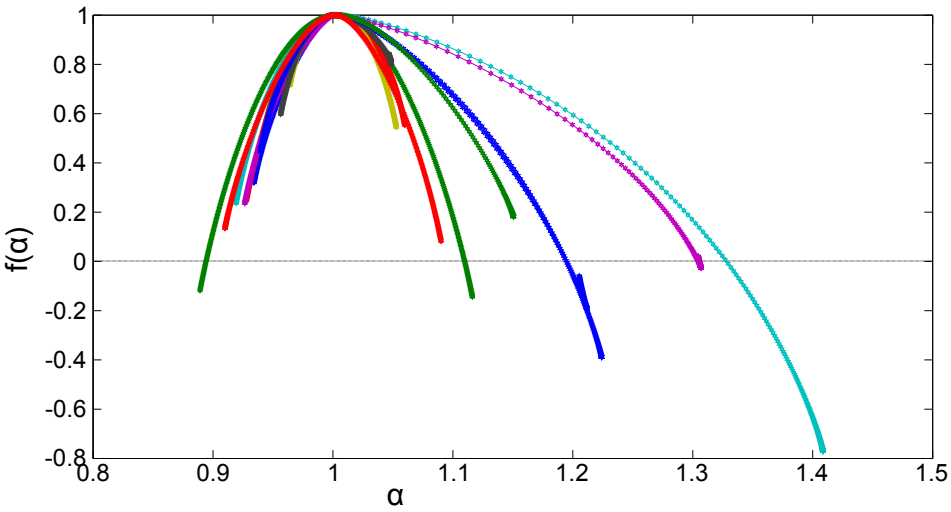

Figure 8.11: Graph of the multifractal spectrum, $f(\alpha)$ versus α, for 10 separate simulations of the ABM with heterogeneous fundamental values; Trader Set D. Since for this data there are few log returns close to zero, the right hand side of the spectra are more likely to be poorly defined. This is the side which describes scaling for areas of small F which are revealed by $q < 0$. The left side of the spectrum is well defined here in contrast to other spectra which have been presented in this thesis.

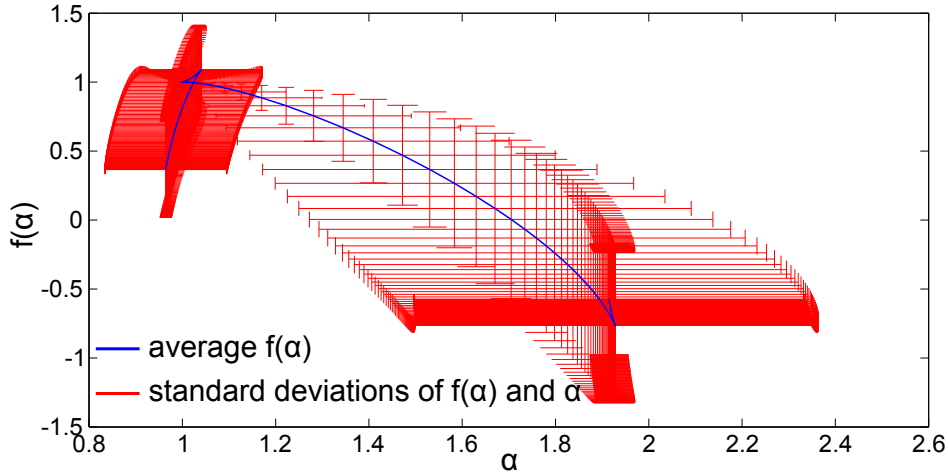

Figure 8.12: Graph of the average multifractal spectrum, $f(\alpha)$ versus α, for 20 separate simulations, each with length 20000, of the ABM with heterogeneous fundamental values; Trader Set D. The average spectrum is shown along with error bars which show the standard deviation in both α and $f(\alpha)$ over the 20 separate simulations.

8.4 Conclusions

In this chapter I have encountered some difficulty in unraveling the fractal structure of the log returns produced by the ABM. It is worth noting that statistical fractals such as these are notoriously difficult to work with. Diffusion Limited Aggregation [70, chapter 9] has been the paradigm problem for random fractals and much work has been done in this context [60, 74, 57, 56, 167, 168]. The study of random fractals is still lacking a rigorous mathematical basis.

The fact that the log returns produced by the original ABM are generally not multifractal shows that a leptokurtic distribution and volatility clusters are not enough to guarantee this type of scaling structure. Although multifractality in time series is ascribed to a combination of the distribution and the correlations [82], the leptokurtic distribution and nonlinear correlations in the outputs of the original ABM do not result in multifractality.

This analysis was conducted as an attempt to find the root cause of the multifractality which has been found in financial log returns. The two extensions to the ABM proposed in this chapter both offer more heterogeneity to how the traders behave. In both cases, we see some multifractal scaling in the resulting log returns. This allows us the conjecture that the multifractality found in empirical log returns is a consequence of the heterogeneity in the investment horizons and/or beliefs of traders in the market.

The log returns produced by both alternative versions of the ABM lack the essential traits of a leptokurtic distribution and volatility clustering. It can therefore be concluded that these traits are not necessary for multifractal scaling to be present. In fact these traits are neither necessary nor sufficient for multifractality.

8.5 Future Work

A smoothing technique such as grid-shifting [74] has the potential to allow for more conclusive results when working with statistical multifractals. MF-DFA divides the data into $2N_s$ segments to ensure all the data is included in at least one box. Grid-shifting involves dividing the data into as many as sN_s segments at each scale s. The segments all have different placements within the data and the variance $F_q(\nu, s)$ is found over all these segments at each scale s. This results in significant smoothing of the data and is helpful for dealing with random nature of statistical fractals. It may help with the specific problem of negative $f(\alpha)$ which has been encountered in this chapter. However that work is beyond the scope of this thesis.

There is also potential for future work in the extension of the ABM. A possible area

for extension lies with the technical traders. Heterogeneity could be introduced to their trading strategies. All of the technical traders in the current ABM use the MACD technical analysis. There must be many other types of strategies which are used in real trading. Giving some technical traders different types of analysis is an option for further investigation.

Another area where heterogeneity could be included in the ABM is in the the probability of buying for the noise traders, P_t. It may be enlightening to allow the parameter u to vary during the simulation. u controls the steepness of P_t. As was described in Chapter 7, u can be thought of as the herding strength between the noise traders. When u is low, the function P_t is quite flat and there is room for disagreement on which direction to trade. When it is higher, P_t changes more steeply and so for a given proportional price change R_t, the noise traders are more likely to agree on how to respond. Larger values lead to high correlation in the log returns because everyone agrees on which direction to trade. However allowing u to vary while maintaining $u^- < u < u^+$ for suitable upper and lower limits u^+ and u^- might give interesting results. For $u < 0$, the noise traders would become contrarians, selling after a positive price move and buying after a negative price move.

8.6 Chapter Summary

This chapter first gave a brief overview of some ABMs which have been found to produce log returns with multifractal properties. I then used MF-DFA to analyse the log returns generated by my ABM. I found that the log returns generally do not have multifractal scaling. This is interesting since the log returns do display other features of empirical data such as a leptokurtic distribution and volatility clustering. I then explored a couple of extensions to the model which bring more heterogeneity to the traders. Some multifractal scaling has been found in the log returns produced by these versions of the ABM which feature heterogeneous trading time horizons or heterogeneous fundamental values. This is surprising since the log returns produced by these alternative versions of the ABM do not display the classical stylised facts of volatility clustering and fat tails. This chapter has shown than leptokurtosis and volatility clustering are neither necessary nor sufficient for the presence of a multifractal structure. The results of the analysis conducted in this chapter also leads me to suggest that it is the heterogeneity in the trading horizons and beliefs of traders which leads to the multifractality found in empirical log returns.

Chapter 9

Summary and Conclusions

9.1 Summary of Work

This thesis has been concerned with the properties of financial log returns. In the first chapter, the basic mechanism of the financial market was described. I then discussed the study of financial data. It is important to select appropriate units when studying any type of time series. Log returns are the focus of the financial literature. They are studied because they are insensitive to the changes in scale which occur over time.

Chapter 1 also outlined a literature review of some of the most influential models which have been used to describe financial data over the last century, beginning with Bachelier's random walk model of 1900 [7]. Being the first known work of mathematics to be applied to finance, his thesis can be viewed as the genesis of financial mathematics.

This new field of financial mathematics laid mostly dormant until the 1960's when the concept of Brownian motion was developed into geometric Brownian motion. This in turn led to the famous Black-Scholes-Merton option-pricing formulae published in 1973 [15]. Myron Scholes and Robert Merton directly accredited Bachelier for his role in the research of option pricing in their Nobel prize acceptance speech [17, 18].

The Gaussian models were later found to be inadequate because they are not able to reproduce the statistical properties of empirical data which came to be discovered. This finding motivated the development of the Stable Paretian Hypothesis [21, 22] which asserted that the price changes were in fact Lévy-distributed rather than Gaussian-distributed. This could account for the fat tails of the distribution of log returns.

Another groundbreaking work came in 1982 with Engle [33] and the introduction of the ARCH models. For the first time, a financial model could reproduce the volatility clusters which had been identified by Mandelbrot back in 1963.

The Efficient Market Hypothesis [26, 39] was then described. It states that in an efficient market, prices perfectly reflect all available information. This has been the

subject of much debate and further research over the years [169].

In Chapter 2, the stylised facts of financial data were described and illustrated. Empirical log returns are universally found to be linearly uncorrelated, to have a leptokurtic distribution with negative skew, and to feature volatility clustering. Also as the lag of the log returns increases, their distribution is better fit by a Gaussian. This phenomenon is known as aggregational Gaussianity. Samples of empirical daily log returns from the DJIA and minutely log returns from the Euro Stoxx 50 were examined in detail and shown to display these features.

The concept of multifractality was introduced in Chapter 3. The classical examples of a fractal and multifractal, the von Koch curve and the Binomial measure, were described. The relation between multifractality and finance was also developed. It was explained that much financial data has been found to have a multifractal structure and the method of MF-DFA was outlined. Some financial models which have incorporated multifractality were reviewed. Mandelbrot's MMAR [76] was the first of these.

Chapter 4 went on to present a comprehensive study of the two empirical data sets, DJIA and Euro Stoxx 50 log returns, using MF-DFA. The results show that the temporal correlations are the dominant source of the multifractal scaling in both data sets. I also showed that the extreme events in the Euro Stoxx 50 minutely data seem to belong to a separate scaling regime or may not scale at all. They are inimical to the scaling of the full time series. This chapter also highlighted the need for more statistical tools to make the task of judging whether or not a time series has multifractal scaling more objective and standardised.

A new approach to financial modelling was then expounded in Chapter 5. This was Agent-Based Modelling. Where other models have been concerned with the reproduction of time series with characteristics similar to those of empirical data, ABMs are principally used to explain the sources of these characteristics or of noteworthy events in the financial world such as Black Monday. This chapter contained a literature review of some of the most influential ABMs in the field of finance.

Chapter 6 then went on to present a new ABM. This new model was motivated by the desire to have a model as simple as possible which also could produce the crucial stylised facts of empirical data. With a simple model it should be possible to determine the source of the stylised facts. The main features of this new model are the noise traders who are more likely to trade after there has been a large price move, the technical traders who use MACD analysis to inform their trades and the fundamental traders who know the fundamental value of the stock. This ABM can also be viewed as an iterative map of coupled equations and these are also given at the end of Chapter 6.

The properties of the model outputs were then outlined in Chapter 7. With the

appropriate number of each type of trader active in the ABM, it was found to produce time series which have fat tails, volatility clustering and aggregational Gaussianity as well as other interesting features. This has been helpful in identifying some of the reasons for these stylised facts which are seen in empirical financial log returns.

Since ABMs have the mandate to identify the sources of the stylised facts, it was then appropriate to test my model of Chapter 6 for multifractality. This was done in Chapter 8. Since no multifractality was found in the outputs of the ABM, two alterations to the model were proposed. With extra heterogeneity incorporated into the agents' trading time horizon, the resulting log returns have some limited multifractal scaling. Heterogeneity in the fundamental values produces log returns without fat tails or volatility clustering but also leads to some limited multifractal scaling. This shows that a thin-peaked distribution and volatility clusters are neither necessary nor sufficient for the property of multifractality. This work also suggests that increased heterogeneity in trader beliefs and investment horizons leads to the multifractality found in empirical data.

9.2 Main Contributions of the Thesis to Research

Chapter 4 contains a number of contributions to research in the area of multifractals. First, MF-DFA was carried out on two data sets which have not previously been studied in this way to my knowledge. The result of MF-DFA on the Euro Stoxx 50 data is an important addition to the literature as it shows that the presence of multifractal scaling in financial data must not be assumed. The linearity of the plots of the log of the scaling function $\log(F_q(s))$ against $\log(s)$ is not certain. This alerts us to the need for stricter testing of data before it is accepted as having multifractal scaling. The metric $\Delta\alpha$ is not comprehensive enough as a measure of the level of multifractal scaling. The linearity of the log-log plots is crucial and further testing methods are required to remove the subjectivity from this judgment.

This is also related to the results found for the shuffled data sets. Where other researchers have found multifractal scaling in shuffled time series, the more comprehensive analysis which I have carried out shows that there is no multifractal scaling in the shuffled DJIA log returns. The multifractal scaling in the shuffled Euro Stoxx 50 log returns is greatly reduced. This result comes directly from the careful examination of the log-log plots and their local slopes.

The most significant result is the finding of the negative effect of the most extreme events on the scaling in the Euro Stoxx 50 minutely data. The reduction of just 42 points in the data has a major impact on the scaling results and the shape of the $f(\alpha)$ spectrum.

A major contribution to research by this thesis is the new ABM described in Chapter 6.

The noise traders in this ABM are unique in their trading rules as far as I am aware. Some of the model concepts, such as the inclusion of technical and fundamental traders, are based on other ABMs [144, 48, 44].

The results of the model outlined in Chapter 7 show that the trading mechanism of the noise traders is responsible for the leptokurtic log returns which are generated. The fact that more of them trade after a large price move and less trade following a small price move is crucial to the emergence of this stylised fact. The bursts of high volatility are triggered by the fundamental value crossing over the price, affecting the way that fundamental traders trade. The distribution of log returns becomes more Gaussian at longer time scales as a result of the fundamental value following a discrete Euler approximation to a GBM process.

Chapter 8 has shown that the log returns produced by the ABM are not multifractal. This shows that nonlinear correlations and a leptokurtic distribution are not a sufficient guarantee of the presence of multifractal scaling. However introducing heterogeneity to the trading horizons or to the fundamental values used by the traders leads to some limited multifractal scaling. Since the log returns produced by these versions of the model do not have fat tails or volatility clustering, this shows that these stylised facts are not necessary for such scaling to occur either.

9.3 Conclusions

Some of the main conclusions of the research presented in this thesis are encapsulated in the following points:

- The daily DJIA and minutely Euro Stoxx 50 log returns which I have examined in Chapter 2 have the expected statistical properties of financial data such as fat tails, volatility clustering, asymmetry and lack of linear correlation.
- The DJIA log returns studied in Chapter 2 display aggregational Gaussianity.
- Multifractality is not necessarily a feature of financial data, as has been shown for the Euro Stoxx 50 log returns examined in Chapter 4.
- Extreme events are inimical to the multifractal scaling (if it is accepted that such scaling is present) in the Euro Stoxx 50 minutely log returns examined in Chapter 4.
- The spectrum width $\Delta\alpha$ is not a suitable indicator of the multifractality of a time series.

- There is a need for more rigorous tests to remove any subjectivity from the assertion of multifractality in time series, as outlined in Chapter 4.
- The new ABM presented in Chapter 6 indicates that the fluctuation of the number of active traders in response to the size of the previous price change leads to log returns which are distributed leptokurtically.
- Noise traders whose activity level fluctuates and who have some memory, technical traders and fundamental traders are all necessary to generate volatility clusters in the log returns of this ABM.
- Traders influenced by a GBM process result in a transition to Gaussianity of the log returns at long time scales in this ABM.
- Time series with fat tails and volatility clustering (such as those generated by this ABM) may not be multifractal, as shown in Chapter 8.
- Time series without fat tails or volatility clustering (such as those produced by a version of this ABM with heterogeneous investment times or heterogeneous fundamental values, presented in Chapter 8) may have some multifractal scaling.
- The multifractality of log returns produced by versions of the ABM with heterogeneous investment times and beliefs hint that these may be the cause of multifractaltiy in empirical data.

The study of the financial market will never be complete. It is an evolving adaptive system which changes as more financial products are added to the market, technology advances, trading methods are updated and the rules which govern financial institutions are adjusted. Also, as soon as practitioners get their hands on the most recent research, they immediately begin to exploit whatever new information they have. This may give a short-term advantage but this quickly diminishes as others in the market catch up with the new developments. The value of the short-term advantage gained may be tremendous in financial terms and this will continue to propagate the demand for new models.

Appendices

Appendix A

Derivation of $f(\alpha)$ for the Binomial Measure

Let us examine the Binomial measure for some stage of iteration n assuming without loss of generality that $p_0 > p_1$. As has already been shown, in the leftmost box $\mu \sim s^\alpha$, where $\alpha = -\log_2 p_0$. A similar scaling ansatz can be defined in all parts of the measure. In general, if $B_s(x)$ is a ball of radius s centred at x, then the measure contained in this ball, $\mu(B_s(x))$, scales as

$$\mu(B_s(x)) \underset{s\to 0}{\sim} s^\alpha. \tag{A.1}$$

And so the local Hölder exponent α is defined

$$\alpha(x) = \lim_{s\to 0} \frac{\log(\mu(B_s(x)))}{\log(s)}. \tag{A.2}$$

If the limit is removed, this becomes the coarse Hölder exponent which applies to a particular stage of iteration n. At this stage, the leftmost segment has measure p_0^n and the rightmost section has measure p_1^n. The sections in between have varying amounts of measure.

The measure in any box can be found if its location is known. If the number of boxes to the left of any box are counted and this number is converted to binary form, this gives a binary location code of length n for the box [74]. The number of 0's and 1's in the location code correspond to the number of $p_0's$ and p_1's which make up the measure of that box. Any other box with the same number of 0's and 1's in its location code will also have the same amount of measure. So the measure $\mu(d_1 d_2 ... d_n), d_i \in \{0, 1\}$, can be completely determined by the binary representation $d_1 d_2 ... d_n$:

$$\mu(d_1 d_2 ... d_n) = p_0^{n_0} p_1^{n_1}$$

where n_0 and n_1 are respectively the number of 0's and 1's in the binary location code.

For the coarse exponent,

$$\begin{aligned}\alpha &= \frac{\log \mu(B_s(x))}{\log s} \\ &= \frac{\log p_0^{n_0} p_1^{n_1}}{\log 1/2^n} \\ &= \frac{n_0}{n} a_0 + \frac{n_1}{n} a_1\end{aligned}$$

where $a_0 = -\log_2 p_0$, $a_1 = -\log_2 p_1$. $\frac{n_0}{n}$ is simply the proportion of 0's in the binary location code for the particular box we're interested in, so this can be slightly simplified to

$$\alpha = \frac{n_0}{n}(a_0 - a_1) + a_1$$

It is easy to see that a_0 and a_1 are respectively the maximum and minimum possible values for α when $p_0 > p_1$ as we have assumed. We rename them α_{max} and α_{min}. Letting $z = \frac{n_0}{n}$, we obtain

$$\alpha = z(\alpha_{max} - \alpha_{min}) + \alpha_{min}. \tag{A.3}$$

This relates the Hölder exponent α of a box simply to the proportion of 0's in its binary location code.

The number of boxes $N(\alpha)$ sharing the same α value will increase as $s \to 0$. At resolution $s = 2^{-n}, N(\alpha) = \binom{n}{zn}$.

Proceeding via Sterling's approximation for large n, $n! \approx \left(\frac{n}{e}\right)^n \sqrt{2\pi n}$,

$$\begin{aligned}N(\alpha) &= \frac{n!}{zn!(n-zn)!} \\ &\underset{n\to\infty}{\approx} \frac{\sqrt{n}}{\sqrt{z} z^n \sqrt{2\pi(n-zn)} \left(\frac{n-zn}{e}\right)^{n-zn}} \\ &= \frac{\sqrt{2\pi n}\left(\frac{n}{e}\right)^n}{\sqrt{2\pi zn}\left(\frac{zn}{e}\right)^{zn}\sqrt{n-zn}\left(\frac{n-nz}{e}\right)^{n-zn}} \\ &\approx \frac{\sqrt{n} n^n}{\sqrt{zn}(zn)^{zn}\sqrt{n-zn}(n-zn)^{n-zn}} \qquad \text{(A.4)} \\ &= \frac{\left(z^{z+\frac{1}{2n}}(1-z)^{1-z}\right)^{-n} n^{n-z(n+1)}}{\sqrt{n(1-z)}} \\ &\approx \frac{\left(z^z(1-z)^{1-z}\right)^{-n}}{\sqrt{n(1-z)}} \qquad \text{(A.5)}\end{aligned}$$

where A.4 is obtained by approximating $2\pi \approx e \approx 1$ compared to n as $n \to \infty$ and A.5

is from the approximation $\sqrt{z} \approx 1$ [74].

The expression A.5 can be written as

$$N(\alpha) \approx \lim_{s \to 0} (2^{-n})^{-f(z)} \sim s^{-f(z)} \tag{A.6}$$

where $f(z) = -\log_2(z^z(1-z)^{1-z})$. This function can be expressed in terms of α via equation A.3 as

$$\begin{aligned} f(\alpha) = &- \left(\frac{\alpha_{max} - \alpha}{\alpha_{max} - \alpha_{min}} \right) \log_2 \left(\frac{\alpha_{max} - \alpha}{\alpha_{max} - \alpha_{min}} \right) \\ &- \left(\frac{\alpha - \alpha_{min}}{\alpha_{max} - \alpha_{min}} \right) \log_2 \left(\frac{\alpha - \alpha_{min}}{\alpha_{max} - \alpha_{min}} \right). \end{aligned} \tag{A.7}$$

Appendix B

Finding the quenched average, F_0

To find F_0, it is necessary to take the limit of F_q as $q \to 0$ [74]. Let us represent $F(v,s)$ by F for brevity.

$$F_0 = \lim_{q\to 0}\left(\frac{1}{2N_s}\sum_{v=1}^{2N_s}(F^2)^{q/2}\right)^{\frac{1}{q}}$$
$$\ln(F_0) = \lim_{q\to 0}\frac{1}{q}\ln\left(\frac{1}{2N_s}\sum_{v=1}^{2N_s}F^q\right)$$

Let

$$f(q) = \ln\left(\frac{1}{2N_s}\sum_{v=1}^{2N_s}F^q\right) \qquad \Longrightarrow f'(q) = \frac{1}{\sum_{v=1}^{2N_s}F^q}\sum_{v=1}^{2N_s}(F^q\ln F)$$
$$g(q) = q \qquad \Longrightarrow g'(q) = 1$$

Proceeding by l'Hôpitals' Rule yields

$$\ln(F_0) = \lim_{q\to 0}\frac{\sum_{v=1}^{2N_s}F^q\ln F}{\sum_{v=1}^{2N_s}F^q}$$
$$= \frac{\sum_{v=1}^{2N_s}\ln F}{2N_s}$$
$$\Rightarrow F_0 = exp\left[\frac{1}{2N_s}\sum_{v=1}^{2N_s}\ln F\right].$$

Appendix C

MF-DFA of data with various detrending orders

This appendix reports on results for performing MF-DFA on DJIA and Euro Stoxx 50 data for different detrending orders $n = 2, 3$. The graphs shown here can be compared with Figures 4.1 and 4.3, which are found using order 1 polynomials. I have concluded that using order 1 polynomials leads to the best results.

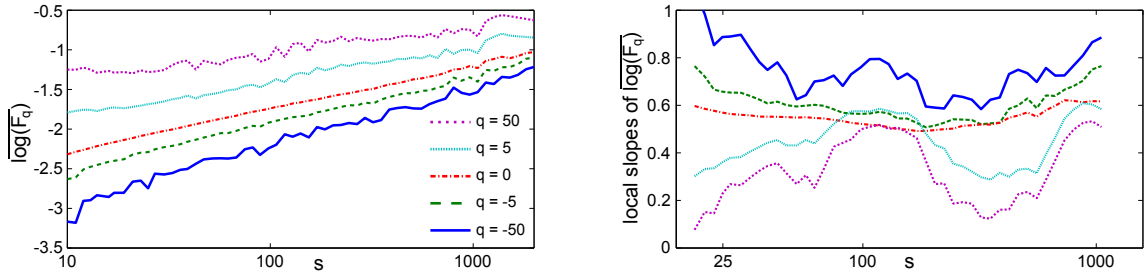

(a) Plots of $\log(\overline{F_q})$ versus $\log(s)$.

(b) Local slopes of $\log(\overline{F_q})$.

Figure C.1: DJIA data; MF-DFA carried out using order 2 polynomials:
(a) Graph of the log of the average scaling function, $\overline{\log(F_q)}$, versus the log of the scale, $\log(s)$, for selected values of q as shown on the graph.
(b) Graph of the local slopes of the lines in (a) calculated over 15 points for the same values of q.

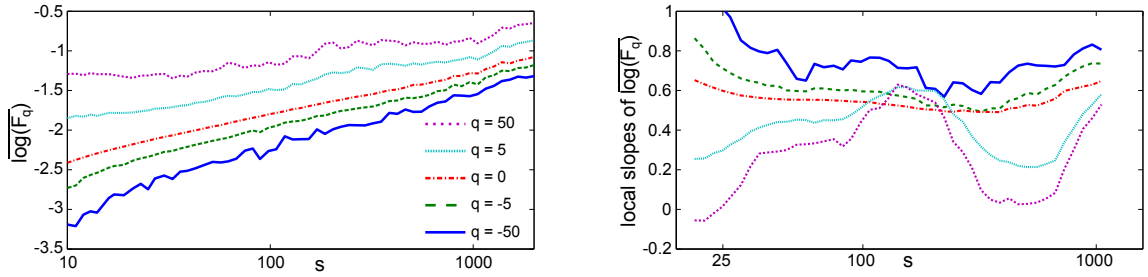

(a) Plots of $\log(\overline{F_q})$ versus $\log(s)$.

(b) Local slopes of $\log(\overline{F_q})$.

Figure C.2: DJIA data; MF-DFA carried out using order 3 polynomials:
(a) Graph of the log of the average scaling function, $\overline{\log(F_q)}$, versus the log of the scale, $\log(s)$, for selected values of q as shown on the graph.
(b) Graph of the local slopes of the lines in (a) calculated over 15 points for the same values of q.

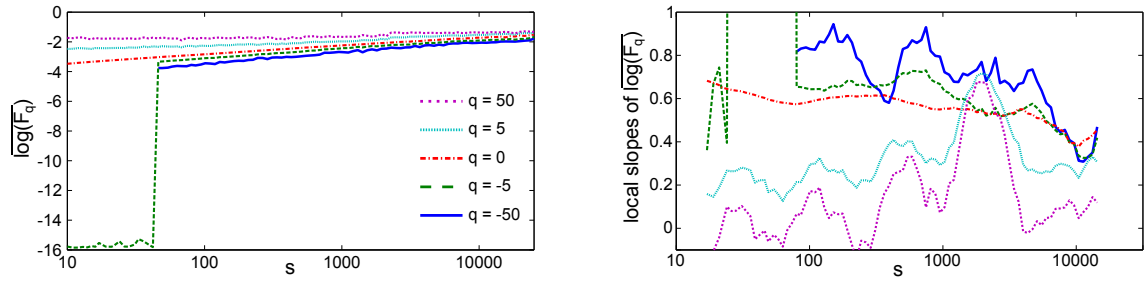

(a) Plots of $\log(\overline{F_q})$ versus $\log(s)$.

(b) Local slopes of $\log(\overline{F_q})$.

Figure C.3: Euro Stoxx 50 data; MF-DFA carried out using order 2 polynomials:
(a) Graph of the log of the average scaling function, $\overline{\log(F_q)}$, versus the log of the scale, $\log(s)$, for selected values of q as shown on the graph.
(b) Graph of the local slopes of the lines in (a) calculated over 15 points for the same values of q.

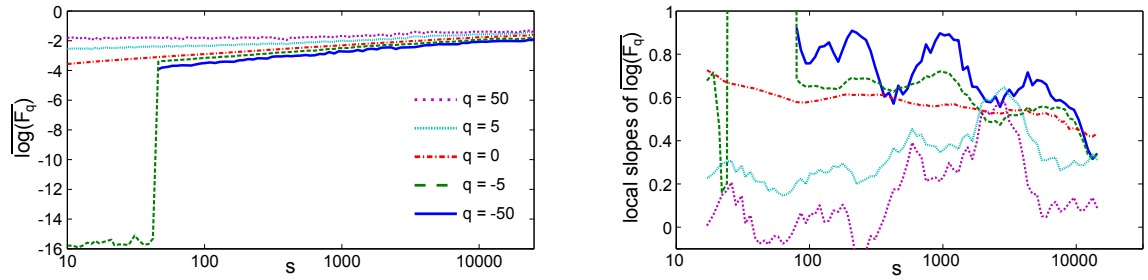

(a) Plots of $\log(\overline{F_q})$ versus $\log(s)$.

(b) Local slopes of $\log(\overline{F_q})$.

Figure C.4: Euro Stoxx 50 data; MF-DFA carried out using order 3 polynomials:
(a) Graph of the log of the average scaling function, $\overline{\log(F_q)}$, versus the log of the scale, $\log(s)$, for selected values of q as shown on the graph.
(b) Graph of the local slopes of the lines in (a) calculated over 15 points for the same values of q.

Appendix D

Higher order detrending for the shuffled data

I have found that using higher oder detrending $n = 2, 3$ does not affect the results for the shuffled DJIA and Euro Stoxx 50 data. Here I report results of the analysis conducted with detrending orders 2 and 3 for comparison with those conduced with order 1 as shown in the main text in Figures 4.9 and 4.10.

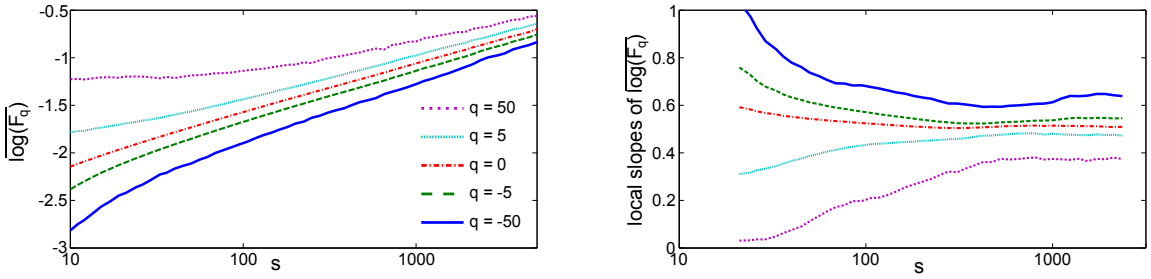

(a) Plots of $\log(\overline{F_q})$ versus $\log(s)$.

(b) Local slopes of $\log(\overline{F_q})$.

Figure D.1: Shuffled DJIA data; MF-DFA carried out using order 2 polynomials:
(a) Graph of the log of the average scaling function, $\overline{\log(F_q)}$, versus the log of the scale, $\log(s)$, for selected values of q as shown on the graph.
(b) Graph of the local slopes of the lines in (a) calculated over 15 points for the same values of q.

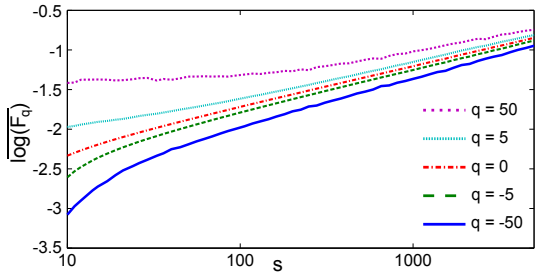

(a) Plots of $\log(\overline{F_q})$ versus $\log(s)$.

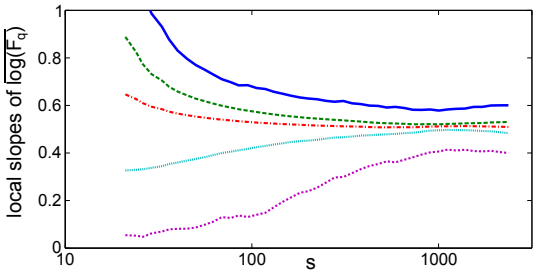

(b) Local slopes of $\log(\overline{F_q})$.

Figure D.2: Shuffled DJIA data; MF-DFA carried out using order 3 polynomials:
(a) Graph of the log of the average scaling function, $\overline{\log(F_q)}$, versus the log of the scale, $\log(s)$, for selected values of q as shown on the graph.
(b) Graph of the local slopes of the lines in (a) calculated over 15 points for the same values of q.

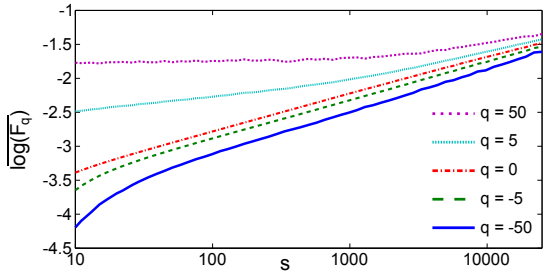

(a) Plots of $\log(\overline{F_q})$ versus $\log(s)$.

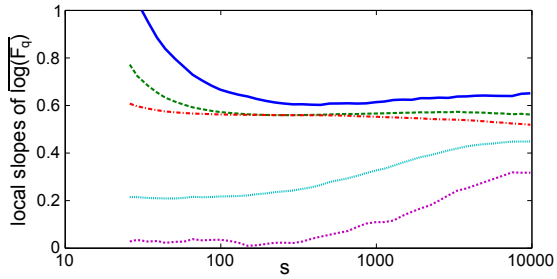

(b) Local slopes of $\log(\overline{F_q})$.

Figure D.3: Shuffled Euro Stoxx 50 data; MF-DFA carried out using order 2 polynomials:
(a) Graph of the log of the average scaling function, $\overline{\log(F_q)}$, versus the log of the scale, $\log(s)$, for selected values of q as shown on the graph.
(b) Graph of the local slopes of the lines in (a) calculated over 15 points for the same values of q.

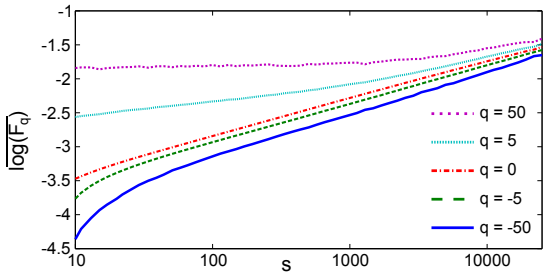

(a) Plots of $\log(\overline{F_q})$ versus $\log(s)$.

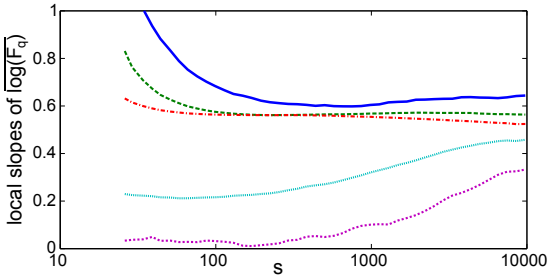

(b) Local slopes of $\log(\overline{F_q})$.

Figure D.4: Shuffled Euro Stoxx 50 data; MF-DFA carried out using order 3 polynomials:
(a) Graph of the log of the average scaling function, $\overline{\log(F_q)}$, versus the log of the scale, $\log(s)$, for selected values of q as shown on the graph.
(b) Graph of the local slopes of the lines in (a) calculated over 15 points for the same values of q.

Bibliography

[1] Yanhui Liu, Parameswaran Gopikrishnan, Cizeau, Meyer, Peng, and H. Eugene Stanley. Statistical properties of the volatility of price fluctuations. *Physical Review E*, 60(2):1390–1400, 1999.

[2] Jean-Philippe Bouchaud. Power-laws in economics and finance: some ideas from physics. Science & Finance (CFM) working paper archive 500023, Science & Finance, Capital Fund Management, 2000.

[3] H Eugene Stanley and Rosario N Mantegna. *An introduction to econophysics*. Cambridge University Press, Cambridge, 2000.

[4] H.E. Stanley, V. Afanasyev, L.A.N. Amaral, S.V. Buldyrev, A.L. Goldberger, S. Havlin, H. Leschhorn, P. Maass, R.N. Mantegna, C.-K. Peng, P.A. Prince, M.A. Salinger, M.H.R. Stanley, and G.M. Viswanathan. Anomalous fluctuations in the dynamics of complex systems: from DNA and physiology to econophysics. *Physica A: Statistical Mechanics and its Applications*, 224(12):302–321, 1996.

[5] C.G. De Vries and K.U. Leuven. Stylized facts of nominal exchange rate returns. Papers 94-002, Purdue University, Krannert School of Management-Center for International Business Education and Research (CIBER), 1994.

[6] Kenneth R French and Richard Roll. Stock return variances: The arrival of information and the reaction of traders. *Journal of financial economics*, 17(1):5–26, 1986.

[7] L. Bachelier. Théorie de la spéculation. *Annales scientifiques de l'École Normale Supérieure, Sér. 3*, 3:21–86, 1900. Translated into English in P. Cootner *The Random Character of the Stock Market*. MIT Press, Cambridge MA (1964).

[8] Franck Jovanovic. Bachelier: Not the forgotten forerunner he has been depicted as. An analysis of the dissemination of Louis Bachelier's work in economics. *The European Journal of the History of Economic Thought*, 19(3):431–451, 2012.

[9] Robert Brown. A brief account of microscopical observations made in the months of June, July and August, 1827, on the particles contained in the pollen of plants; and on the general existence of active molecules in organic and inorganic bodies. *The Philosophical Magazine, or Annals of Chemistry, Mathematics, Astronomy, Natural History and General Science*, 4(21):161–173, 1828.

[10] Wolfgang Paul and Jörg Baschnagel. *Stochastic Processes; from physics to finance*. Springer, 1999.

[11] P. A. Samuelson. Rational theory of warrant pricing. *Industrial Management Review*, 6(2):13, 1965.

[12] John C. Hull. *Options, Futures and Other Derivatives*. Pearson Prentice Hall, New Jersey, sixth edition, 2006.

[13] Kai Lai Chung and Ruth J Williams. *Introduction to stochastic integration*, volume 2. Springer New York, 1990.

[14] Bernt Øksendal. *Stochastic differential equations*. Springer Berlin Heidelberg, 2003.

[15] Fischer Black and Myron Scholes. The pricing of options and corporate liabilities. *Journal of Political Economy*, 81(3):637–654, 1973.

[16] P. Richmond, J. Mimkes, and S. Hutzler. *Econophysics and Physical Economics*. Oxford University Press, Oxford, 2013.

[17] Myron S. Scholes. Derivatives in a dynamic environment. *The American Economic Review*, 88(3):350–370, 1998.

[18] Robert C. Merton. Applications of option-pricing theory: Twenty-five years later. *The American Economic Review*, 88(3):323–349, 1998.

[19] Rama Cont. Empirical properties of asset returns: stylized facts and statistical issues. *Quantitative Finance*, 1:223–236, 2001.

[20] Benoît B. Mandelbrot. Selected topics in mathematics, physics, and finance originating in fractal geometry. In Miroslav M. Novak, editor, *Thinking in Patterns: Fractals and Related Phenomena in Nature*. World Scientific, 2004.

[21] Benoît B. Mandelbrot. The variation of certain speculative prices. *The Journal of Business*, 36:394, 1963.

[22] Eugene F. Fama. Mandelbrot and the Stable Paretian Hypothesis. *The Journal of Business*, 36(4):420–429, 1963.

[23] Benoît B. Mandelbrot. Fractals and scaling in finance: discontinuity, concentration, risk: selecta volume E (with foreword by RE Gomory, and contributions by PH Cootner et al.), 1997.

[24] John W Lamperti. *Probability: A survey of the mathematical theory*, volume 770. John Wiley & Sons Inc, New York, 2011.

[25] William J Adams. *The life and times of the central limit theorem.* American Mathematical Society, 1974.

[26] Eugene F. Fama. The behavior of stock-market prices. *The Journal of Business*, 38(1):34–105, 1965.

[27] Antonios Antypas, Phoebe Koundouri, and Nikolaos Kourogenis. Aggregational Gaussianity and barely infinite variance in financial returns. *Journal of Empirical Finance*, 20:102–108, 2013.

[28] Vedat Akgiray and G. Geoffrey Booth. The stable-law model of stock returns. *Journal of Business & Economic Statistics*, 6(1):51–57, 1988.

[29] Peter K. Clark. A subordinated stochastic process model with finite variance for speculative prices. *Econometrica*, 41(1):135–155, 1973.

[30] Thomas W Epps and Mary Lee Epps. The stochastic dependence of security price changes and transaction volumes: Implications for the mixture-of-distributions hypothesis. *Econometrica: Journal of the Econometric Society*, pages 305–321, 1976.

[31] George E Tauchen and Mark Pitts. The price variability-volume relationship on speculative markets. *Econometrica: Journal of the Econometric Society*, pages 485–505, 1983.

[32] Austin Gerig, Javier Vicente, and Miguel A Fuentes. Model for non-Gaussian intraday stock returns. *Physical Review E*, 80(6):065102, 2009.

[33] Robert F Engle. Autoregressive conditional heteroscedasticity with estimates of the variance of United Kingdom inflation. *Econometrica: Journal of the Econometric Society*, pages 987–1007, 1982.

[34] Zhuanxin Ding, Clive W.J. Granger, and Robert F. Engle. A long memory property of stock market returns and a new model. *Journal of Empirical Finance*, 1(1):83–106, 1993.

[35] Timo Teräsvirta. An introduction to univariate GARCH models. In *Handbook of Financial Time Series*, pages 17–42. Springer Berlin Heidelberg, 2009.

[36] Tim Bollerslev. Generalized autoregressive conditional hetroskedasticity. *Journal of Econometrics*, 31:307–327, 1986.

[37] Robert F. Engle, editor. *ARCH: Selected Readings*. Oxford University Press, Oxford, 1995.

[38] Luc Bauwens, Sébastien Laurent, and Jeroen V. K. Rombouts. Multivariate GARCH models: a survey. *Journal of Applied Econometrics*, 21:79–109, 2006.

[39] Paul A Samuelson. Proof that properly anticipated prices fluctuate randomly. *Industrial management review*, 6(2):41–49, 1965.

[40] John Muth. Rational expectations and the theory of price movements. *Econometrica*, 29(3):315–335, 1961.

[41] John M. Keynes. *The general theory of employment, interest and money*. The Easton Press, Norwalk, Connecticut, 1936.

[42] J Doyne Farmer. Toward agent-based models for investment. In *AIMR Conference Proceedings*, volume 2001, pages 61–71. CFA Institute, 2001.

[43] Robert Shiller. Investor behaviour in the October 1987 stock market crash: survey evidence. *NBER working papers*, (2446), 1987.

[44] M Cristelli, L Pietronero, and A Zaccaria. Critical overview of agent-based models for economics. Technical Report arXiv:1101.1847, Jan 2011. Proceedings of the School of Physics.

[45] Stephen J Brown. The efficient markets hypothesis: The demise of the demon of chance? *Accounting & Finance*, 51(1):79–95, 2011.

[46] Charles M Macal and Michael J North. Agent-based modeling and simulation: ABMS examples. In *Proceedings of the 40th Conference on Winter Simulation*, pages 101–112. Winter Simulation Conference, 2008.

[47] Eric Bonabeau. Agent-based modeling: methods and techniques for simulating human systems. *Proceedings of the National Academy of Science USA*, 99:7280–7287, 2002.

[48] Michele Marchesi and Thomas Lux. Volatility clustering in financial markets: A microsimulation of interacting agents. *International Journal of Theoretical and Applied Finance*, 3(4):675–702, 2000.

[49] Mawuli Segnon and Thomas Lux. Multifractal models in finance: Their origin, properties, and applications. Technical Report 1860, Kiel Working Paper, 2013.

[50] David A. Dickey and Wayne A. Fuller. Distribution of the estimators for autoregressive time series with a unit root. *Journal of the American Statistical Association*, 74(366a):427–431, 1979.

[51] D. A. Dickey, W. R. Bell, and R. B. Miller. Unit roots in time series models: tests and implications. *American Statistician*, 40:12–26, 1986.

[52] Richard B. Olsen, Ulrich A. Mller, Michel M. Dacorogna, Olivier V. Pictet, Rakhal R. Dav, and Dominique M. Guillaume. From the bird's eye to the microscope: A survey of new stylized facts of the intra-daily foreign exchange markets. *Finance and Stochastics*, 1(2):95–129, 1997.

[53] Blake LeBaron. Time scales, agents, and empirical finance. *Medium Econometrische Toepassingen (MET)*, 14(2), 2006.

[54] Peter D Ekman. Intraday patterns in the S&P 500 index futures market. *Journal of Futures Markets*, 12(4):365–381, 1992.

[55] Thomas C Halsey, Paul Meakin, and Itamar Procaccia. Scaling structure of the surface layer of diffusion-limited aggregates. *Physical review letters*, 56:854–857, 1986.

[56] W.G. Hanan and D.M. Heffernan. Multifractal analysis of the branch structure of diffusion-limited aggregates. *Physical review. E, Statistical, nonlinear, and soft matter physics*, 85(2-1):021407, 2012.

[57] W.G. Hanan and D.M. Heffernan. Global structure and finite-size effects in the $f(\alpha)$ of diffusion-limited aggregates. *Physical Review E*, 77(1):011405, 2008.

[58] H. Eugene Stanley and Paul Meakin. Multifractal phenomena in physics and chemistry. *Nature*, 335(6189):405–409, 1988.

[59] A. Cummings, G. O'Sullivan, W.G. Hanan, and D.M. Heffernan. Multifractal analysis of selected rare-earth elements. *Journal of Physics B: Atomic, Molecular and Optical Physics*, 34(13):2547, 2001.

[60] W.G. Hanan, D.M. Heffernan, and J.C. Earnshaw. Left-sided multifractality of the harmonic measure on 2-d cluster-cluster aggregates. *Chaos, Solitons & Fractals*, 9(6):875 – 880, 1998.

[61] Benoît B. Mandelbrot. Intermittent turbulence in self-similar cascades: divergence of high moments and dimension of the carrier. *Journal of Fluid Mechanics*, 62:331–358, 1974.

[62] Plamen Ch Ivanov, Luís A Nunes Amaral, Ary L Goldberger, Shlomo Havlin, Michael G Rosenblum, Zbigniew R Struzik, and H Eugene Stanley. Multifractality in human heartbeat dynamics. *Nature*, 399(6735):461–465, 1999.

[63] Yi Zheng, Jianbo Gao, Justin C Sanchez, Jose C Principe, and Michael S Okun. Multiplicative multifractal modeling and discrimination of human neuronal activity. *Physics Letters A*, 344(2):253–264, 2005.

[64] E. A. Ihlen. Introduction to multifractal detrended fluctuation analysis in Matlab. *Frontiers in Fractal Physiology*, 3:141, 2012.

[65] A. Feldmann, A. C. Gilbert, and W. Willinger. Data networks as cascades: investigating the multifractal nature of internet WAN traffic. *SIGCOMM Computer Communication Review*, 28(4):42–55, October 1998.

[66] N. Sala. Fractal geometry in the arts: an overview across the different cultures. In Miroslav M. Novak, editor, *Thinking in Patterns: Fractals and Related Phenomena in Nature*. World Scientific, 2004.

[67] John Bendler. Fractals in science. *Journal of Statistical Physics*, 81(3-4):857–860, 1995.

[68] Sangit Chatterjee and Mustafa R Yilmaz. Chaos, fractals and statistics. *Statistical Science*, 7(1):49–12, 1992.

[69] Yakov Pesin and Vaughn Climenhaga. *Lectures on Fractal Geometry and Dynamical Systems*. American Mathematical Society, 2009.

[70] Heinz-Otto Peitgen, Hartmut Jürgens, and Dietmar Saupe. *Chaos and fractals: new frontiers of science*. Springer New York, 2004.

[71] Robert C. Hilborn. *Chaos and Nonlinear Dynamics: An introduction for scientists and engineers*. Oxford University Press, Oxford, second edition, 2000.

[72] Edward Ott. *Chaos in dynamical systems*. Cambridge University Press, Cambridge, 2002.

[73] Tamas Tel. Fractals, multifractals, and thermodynamics. *Z. Naturforsch, 43a*, 1154, 1988.

[74] William Hanan. *Fractal Properties of 2-D Aggregation Phenomena*. PhD thesis, National University of Ireland, Maynooth, 2006.

[75] Benoît B. Mandelbrot. How long is the coast of Britain? *Science*, 156:636–638, 1967.

[76] Benoît B Mandelbrot, Adlai J Fisher, and Laurent E Calvet. A multifractal model of asset returns. *Cowles Foundation for Economic Research Working Paper*, 1997.

[77] James R. Thompson. *Analysis of Market Returns Using Multifractal Time Series and Agent-Based Simulation*. PhD thesis, North Carolina State University, 2013.

[78] Thomas C Halsey, Mogens H Jensen, Leo P Kadanoff, Itamar Procaccia, and Boris I Shraiman. Fractal measures and their singularities: the characterization of strange sets. *Physical Review A*, 33(2):1141, 1986.

[79] Peter Grassberger. Generalized dimensions of strange attractors. *Physics Letters A*, 97(6):227–230, 1983.

[80] Jean-François Muzy, Emmanuel Bacry, and Alain Arneodo. Wavelets and multifractal formalism for singular signals: Application to turbulence data. *Physical Review Letters*, 67:3515–3518, 1991.

[81] Jean-François Muzy, Emmanuel Bacry, and Alain Arneodo. The multifractal formalism revisited with wavelets. *International Journal of Bifurcation and Chaos*, 4(02):245–302, 1994.

[82] Jan W. Kantelhardt, Stephan A. Zschiegner, Eva Koscielny-Bunde, Shlomo Havlin, Armin Bunde, and H.Eugene Stanley. Multifractal detrended fluctuation analysis of nonstationary time series. *Physica A: Statistical Mechanics and its Applications*, 316(14):87–114, 2002.

[83] Paweł Oświęcimka, Jarosław Kwapień, and Stanisław Drożdż. Wavelet versus Detrended Fluctuation Analysis of multifractal structures. *Physical Review E*, 74(1):016103, 2006.

[84] P. Oświęcimka, J. Kwapień, S. Drożdż, and R. Rak. Investigating multifractality of stock market fluctuations using wavelet and detrending fluctuation methods. *Acta Physica Polonica B*, 36(8):2447–2457, 2005.

[85] Aicko Y. Schumann and Jan W. Kantelhardt. Multifractal moving average analysis and test of multifractal model with tuned correlations. *Physica A: Statistical Mechanics and its Applications*, 390(14):2637–2654, 2011.

[86] C-K Peng, Sergey V Buldyrev, Shlomo Havlin, M Simons, H Eugene Stanley, and Ary L Goldberger. Mosaic organization of DNA nucleotides. *Physical Review E*, 49(2):1685, 1994.

[87] Jan W Kantelhardt, Eva Koscielny-Bunde, Henio HA Rego, Shlomo Havlin, and Armin Bunde. Detecting long-range correlations with detrended fluctuation analysis. *Physica A: Statistical Mechanics and its Applications*, 295(3):441–454, 2001.

[88] Elena Green, William Hanan, and Daniel Heffernan. The origins of multifractality in financial time series and the effect of extreme events. *The European Physical Journal B*, 87(6):129, 2014.

[89] Robert A Wood, Thomas H McInish, and J Keith Ord. An investigation of transactions data for NYSE stocks. *The Journal of Finance*, 40(3):723–739, 1985.

[90] Zhou Yu, Leung Yee, and Yu Zu-Guo. Relationships of exponents in multifractal detrended fluctuation analysis and conventional multifractal analysis. *Chinese Physics B*, 20(9):090507, 2011.

[91] Petr Jizba and Jan Korbel. Methods and techniques for multifractal spectrum estimation in financial time series. URL: http://www.lorentzcenter.nl, 2013.

[92] Laurent Calvet and Adlai Fisher. Multifractality in asset returns: theory and evidence. *Review of Economics and Statistics*, 84(3):381–406, 2002.

[93] Laurent Calvet and Adlai Fisher. Forecasting multifractal volatility. *Journal of Econometrics*, 105(1):27–58, 2001.

[94] Laurent Calvet and Adlai Fisher. How to forecast long-run volatility: regime switching and the estimation of multifractal processes. *Journal of Financial Econometrics*, 2(1):49–83, 2004.

[95] Jean-François Muzy, Jean Delour, and Emmanuel Bacry. Modelling fluctuations of financial time series: from cascade process to stochastic volatility model. *The European Physical Journal B*, 17(3):537–548, 2000.

[96] E. Bacry, J. Delour, and J. F. Muzy. Multifractal random walk. *Physical Review E*, 64(2):026103, July 2001.

[97] Benoît Pochart, Jean-Philippe Bouchaud, et al. The skewed multifractal random walk with applications to option smiles. *Quantitative finance*, 2(4):303–314, 2002.

[98] AI Saichev and VA Filimonov. On the spectrum of multifractal diffusion process. *Journal of Experimental and Theoretical Physics*, 105(5):1085–1093, 2007.

[99] Vladimir Filimonov and Didier Sornette. Self-excited multifractal dynamics. *Europhysics Letters*, 94(4):46003, 2011.

[100] Benoît B. Mandelbrot and R. Hudson. *On the (mis)behaviour of markets, a fractal view of risk, ruin and reward*. Profile Books, London, 2005.

[101] Ł. Czarnecki and D. Grech. Multifractal dynamics of stock markets. *Acta Physica Polonica, A*, 117(4):623–629, 2010.

[102] Antonio Turiel and Conrad J. Pérez-Vicente. Multifractal geometry in stock market time series. *Physica A: Statistical Mechanics and its Applications*, 322(0):629–649, 2003.

[103] Wei-Xing Zhou. The components of empirical multifractality in financial returns. *Europhysics Letters*, 88(2):28004, 2009.

[104] V Romanov, V Slepov, M Badrina, and A Federyakov. Multifractal analysis and multiagent simulation for market crash prediction. *Computational Finance and Its Applications III*, pages 256–266, 2008.

[105] Kaushik Matia, Yosef Ashkenazy, and H Eugene Stanley. Multifractal properties of price fluctuations of stocks and commodities. *Europhysics Letters*, 61(3):422, 2003.

[106] P. Suárez-García and D. Gómez-Ullate. Multifractality and long memory of a financial index. *Physica A: Statistical Mechanics and its Applications*, 394(0):226–234, 2014.

[107] Jean-Philippe Bouchaud, M. Potters, and M. Meyer. Apparent multifractality in financial time series. *European Physical Journal B*, 13(3):595–599, 2000.

[108] Thomas Lux. Detecting multifractal properties in asset returns: The failure of the "scaling estimator". *International Journal of Modern Physics C*, 15(04):481–491, 2004.

[109] Wei-Xing Zhou. Finite-size effect and the components of multifractality in financial volatility. *Chaos, Solitons & Fractals*, 45(2):147–155, 2012.

[110] Jan W Kantelhardt. Fractal and multifractal time series. In *Mathematics of Complexity and Dynamical Systems*, pages 463–487. Springer New York, 2011.

[111] Benoît B Mandelbrot. Multifractal measures, especially for the geophysicist. In *Fractals in geophysics*, pages 5–42. Springer Birkhäuser Basel, 1989.

[112] Charles Meneveau and KR Sreenivasan. The multifractal nature of turbulent energy dissipation. *Journal of Fluid Mechanics*, 224(429-484):180, 1991.

[113] Gabjin Oh, Cheoljun Eom, Shlomo Havlin, Woo-Sung Jung, Fengzhong Wang, H Eugene Stanley, and Seunghwan Kim. Effect of Asian currency crisis on multifractal spectra. *The European Physical Journal B*, 85:214, 2012.

[114] Sunil Kumar and Nivedita Deo. Multifractal properties of the Indian financial market. *Physica A: Statistical Mechanics and its Applications*, 388(8):1593–1602, 2009.

[115] J Kwapień, S Drożdż, et al. Components of multifractality in high-frequency stock returns. *Physica A: Statistical Mechanics and its Applications*, 350(2):466–474, 2005.

[116] Y. Wang, C. Wu, and Z. Pan. Multifractal detrending moving average analysis on the US dollar exchange rates. *Physica A: Statistical Mechanics and its Applications*, 390(20):3512–3523, 2011.

[117] Didier Sornette. Critical market crashes. *Physics Reports*, 378(1):1–98, 2003.

[118] Victor S. L'vov, Anna Pomyalov, and Itamar Procaccia. Outliers, extreme events, and multiscaling. *Physical Review E*, 63(5):056118, 2001.

[119] Didier Sornette. Dragon-kings, black swans and the prediction of crises. *International Journal of terraspace science and engineering*, 2(1), 2009.

[120] Jozef Barunik, Tomaso Aste, Tiziana Di Matteo, and Ruipeng Liu. Understanding the source of multifractality in financial markets. *Physica A: Statistical Mechanics and its Applications*, 391(17):4234–4251, 2012.

[121] Saâd Benbachir and Marwane El Alaoui. A multifractal detrended fluctuation analysis of the Moroccan stock exchange. *International Research Journal of Finance and Economics*, (78):6–17, 2011.

[122] P. Norouzzadeh and B. Rahmani. A multifractal detrended fluctuation description of Iranian rial-US dollar exchange rate. *Physica A: Statistical Mechanics and its Applications*, 367(0):328–336, 2006.

[123] H. Chen and C. Wu. Forecasting volatility in Shanghai and Shenzhen markets based on multifractal analysis. *Physica A: Statistical Mechanics and its Applications*, 390(16):2926–2935, 2011.

[124] J Doyne Farmer and Duncan Foley. The economy needs agent-based modelling. *Nature*, 460(7256):685–686, 2009.

[125] V. Alfi, M. Cristelli, L. Pietronero, and A. Zaccaria. Minimal agent based model for financial markets II. Statistical properties of the linear and multiplicative dynamics. *European Physical Journal B*, 67:399–417, 2009.

[126] Rama Cont. Volatility clustering in financial markets: Empirical facts and agent-based models. In Gilles Teyssiére and Alan P. Kirman, editors, *Long Memory in Economics*, pages 289–309. Springer Berlin Heidelberg, 2007.

[127] Blake LeBaron. Agent-based computational finance: Suggested readings and early research. *Journal of Economic Dynamics & Control*, 24:679–702, 2000.

[128] E Samanidou, E Zschischang, D Stauffer, and T Lux. Agent-based models of financial markets. *Reports on Progress in Physics*, 70(3):409, 2007.

[129] Martin Gardner. Mathematical games; the fantastic combinations of John Conway's new solitaire game "life". *Scientific American*, 223(4):120–123, 1970.

[130] Conway's Game of Life; A community for Conway's Game of Life and related cellular automata. URL: http://www.conwaylife.com, September 2013.

[131] Eric Weisstein. Eric Weisstein's treasure trove of The Game of Life. URL:http://www.ericweisstein.com/encyclopedias/life/InfiniteGrowth.html, September 2013.

[132] Jason Summers. Jason's life page. URL: http://entropymine.com/jason/life/, September 2013.

[133] W Brian Arthur. Inductive reasoning and bounded rationality (The El Farol problem). *The American Economic Review*, 84(2):406–411, 1994.

[134] ER Grannan and GH Swindle. Contrarians and volatility clustering. *Complex Systems*, 8(2):75–90, 1994.

[135] D. Challet and Y.-C. Zhang. Emergence of cooperation and organization in an evolutionary game. *Physica A: Statistical Mechanics and its Applications*, 246(34):407–418, 1997.

[136] D. Challet, M. Marsili, and Y.-C. Zhang. Stylized facts of financial markets and market crashes in minority games. *Physica A: Statistical Mechanics and its Applications*, 294(3):514–524, 2001.

[137] Fernando F. Ferreira, Viviane M. de Oliveira, Antnio F. Crepaldi, and Paulo R.A. Campos. Agent-based model with heterogeneous fundamental prices. *Physica A: Statistical Mechanics and its Applications*, 357(34):534–542, 2005.

[138] Damien Challet, Matteo Marsili, and Yi-Cheng Zhang. Modeling market mechanism with minority game. *Physica A: Statistical Mechanics and its Applications*, 276(1):284–315, 2000.

[139] Irene Giardina, Jean-Philippe Bouchaud, and Marc Mézard. Microscopic models for long ranged volatility correlations. *Physica A: Statistical Mechanics and its Applications*, 299(1):28–39, 2001.

[140] Neil F. Johnson, Michael Hart, Pak Ming Hui, and Dafang Zheng. Trader dynamics in a model market. *International Journal of Theoretical and Applied Finance*, 3(3):443–450, 2000.

[141] Paul Jefferies, M. L. Hart, Pak Ming Hui, and Neil F. Johnson. From market games to real-world markets. *The European Physical Journal B*, 20(4):493–501, 2001.

[142] Jean-Philippe Bouchaud, Irene Giardina, and Marc Mezard. On a universal mechanism for long-range volatility correlations. *Quantitative Finance*, 1(2):212–216, 2001.

[143] W.F Brian Arthur. *Asset pricing under endogenous expectations in an artificial stock market*. PhD thesis, Brunel University, London, 1996.

[144] V. Alfi, M. Cristelli, L. Pietronero, and A. Zaccaria. Minimal agent based model for financial markets I: Origin and self-organization of stylized facts. *The European Physical Journal B*, 67:385–397, February 2009.

[145] Alan Kirman. Ants, rationality and recruitment. *The Quarterly Journal of Economics*, 108(1):137–156, 1993.

[146] Torben G Andersen and Tim Bollerslev. Heterogeneous information arrivals and return volatility dynamics: Uncovering the long-run in high frequency returns. *The Journal of Finance*, 52(3):975–1005, 1997.

[147] I. Giardina and J.-P. Bouchaud. Bubbles, crashes and intermittency in agent based market models. *The European Physical Journal B*, 31(3):421–437, 2003.

[148] Ling-Yun He. Is price behavior scaling and multiscaling in a dealer market? Perspectives from multi-agent based experiments. *Computational Economics*, 36(3):263–282, 2010.

[149] Rama Cont and Jean-Philipe Bouchaud. Herd behavior and aggregate fluctuations in financial markets. *Macroeconomic dynamics*, 4(2):170–196, 2000.

[150] Stefan Thurner, J Doyne Farmer, and John Geanakoplos. Leverage causes fat tails and clustered volatility. *Quantitative Finance*, 12(5):695–707, 2012.

[151] Michele Tumminello, Fabrizio Lillo, Jyrki Piilo, and Rosario N Mantegna. Identification of clusters of investors from their real trading activity in a financial market. *New Journal of Physics*, 14(1):013041, 2012.

[152] Didier Sornette and Jorgen Vitting Andersen. A non-linear super-exponential rational model of speculative financial bubbles. *International Journal of Modern Physics C*, 13(2):171–187, 2002.

[153] J. P. Royston. A simple method for evaluating the Shapiro-Francia W' test of non-normality. *Journal of the Royal Statistical Society. Series D (The Statistician)*, 32(3):297–300, 1983.

[154] Randolph Westerfield. The distribution of common stock price changes: An application of transactions time and subordinated stochastic models. *The Journal of Financial and Quantitative Analysis*, 12(5):743–765, 1977.

[155] A Ronald Gallant, Peter Eric Rossi, and George Tauchen. Stock prices and volume. *Review of Financial studies*, 5(2):199–242, 1992.

[156] Jonathan M. Karpoff. The relation between price changes and trading volume: A survey. *The Journal of Financial and Quantitative Analysis*, 22(1):109–126, 1987.

[157] Marcus Davidsson. Volume, volatility and momentum in financial markets. *International Research Journal of Applied Finance*, 5(3):211–223, 2014.

[158] Zeyu Zheng, Zhi Qiao, Joel N Tenenbaum, H Eugene Stanley, and Baowen Li. Predicting market instability: New dynamics between volume and volatility. *arXiv preprint arXiv:1403.5193*, 2014.

[159] Jianbo Gao, Jing Hu, Wen-Wen Tung, Yinhe Cao, N Sarshar, and Vwani P Roychowdhury. Assessment of long-range correlation in time series: how to avoid pitfalls. *Physical Review E*, 73(1):016117, 2006.

[160] Giovani L Vasconcelos. A guided walk down Wall Street: an introduction to econophysics. *Brazilian Journal of Physics*, 34(3B):1039–1065, 2004.

[161] Damien Challet and Matteo Marsili. Criticality and market efficiency in a simple realistic model of the stock market. *Physical Review E*, 68(3):036132, 2003.

[162] W-X Zhou and Didier Sornette. Self-organizing Ising model of financial markets. *The European Physical Journal B*, 55(2):175–181, 2007.

[163] Filippo Castiglione and Dietrich Stauffer. Multi-scaling in the Cont–Bouchaud microscopic stock market model. *Physica A: Statistical Mechanics and its Applications*, 300(34):531–538, 2001.

[164] Edgar E Peters. *Fractal Market Analysis: Applying Chaos Theory to Investment and Economics*. John Wiley & Sons Inc, New York, 1994.

[165] Wei-Xing Zhou, Hai-Feng Liu, and Zun-Hong Yu. Anomalous features arising from random multifractals. *Fractals*, 9(03):317–328, 2001.

[166] J Gierałtowski, JJ Żebrowski, and R Baranowski. Multiscale multifractal analysis of heart rate variability recordings with a large number of occurrences of arrhythmia. *Physical Review E*, 85(2):021915, 2012.

[167] Jysoo Lee and H Eugene Stanley. Phase transition in the multifractal spectrum of diffusion-limited aggregation. *Physical review letters*, 61(26):2945, 1988.

[168] Benoît B. Mandelbrot. New anomalous multiplicative multifractals: Left sided $f(\alpha)$ and the modelling of DLA. *Physica A: Statistical Mechanics and its Applications*, 168(1):95 – 111, 1990.

[169] Andrew W. Lo. Efficient markets hypothesis. *The new palgrave: A dictionary of economics*, 2:782–794, 2007.